STUDIES ON PRODUCTION AND APPLICATION OF BACTERIAL CELLULOSE

Ph.D. THESIS

by

SWATI DUBEY

DEPARTMENT OF BIOTECHNOLOGY
INDIAN INSTITUTE OF TECHNOLOGY ROORKEE
ROORKEE- 247 667 (INDIA)
DECEMBER, 2017

STUDIES ON PRODUCTION AND APPLICATION OF BACTERIAL CELLULOSE

A THESIS

Submitted in partial fulfilment of the requirements for the award of the degree

of

DOCTOR OF PHILOSOPHY

in

BIOTECHNOLOGY

by

SWATI DUBEY

DEPARTMENT OF BIOTECHNOLOGY
INDIAN INSTITUTE OF TECHNOLOGY ROORKEE
ROORKEE- 247 667 (INDIA)
DECEMBER, 2017

INDAIN INSTITUTE OF TECHNOLOGY ROORKEE ROORKEE

CANDIDATE'S DECLARATION

I hereby certify that the work which is being presented in the thesis entitled **"STUDIES ON PRODUCTION AND APPLICATION OF BACTERIAL CELLULOSE"** in partial fulfilment of the requirements for the award of the Degree of Doctor of Philosophy and submitted in the Department of Biotechnology of the Indian Institute of Technology Roorkee, Roorkee is an authentic record of my own work carried out during a period from December, 2011 to December, 2017 under the supervision of Dr. R. P. Singh, Professor, Department of Biotechnology, Indian Institute of Technology Roorkee, Roorkee, India.

The matter presented in this thesis has not been submitted by me for the award of any other degree of this or any other institute.

(**SWATI DUBEY**)

This is to certify that the above statement made by the candidate is correct to the best of my knowledge.

(R P Singh)
Supervisor

Dated:

DEDICATED TO

My loving parents
(Mr. Shiv Kumar Dubey & Mrs. Jayanti Dubey)

Bacterial cellulose (BC) or Bacterial Nanocellulose (BNC), a polymer formed by linear coupling of glucopyranose units using microbial processes, has primed a great deal of attention worldwide due to its unique physico-structural properties. It is identical in chemical composition to plant cellulose, however, its physico-structural features such as ultra-fine nanofibrous network, mechanical strength, ability to be molded in any shape, and extra purity (*i.e.* devoid of pectin, lignin, hemicellulose and other metabolic products); bestow BNC with plenteous advantages over plant cellulose and make it a potential precursor for breakthrough technologies in several vital arenas leading to cutting edge products like optoelectronic materials, acoustic membranes, ultrafiltration membranes, supercapacitors, fuel cell, polymer matrices reinforcement, cosmetics, wound dressing materials, surgical implants, tissue engineering scaffolds, drug delivery systems and other biomedical devices.

Despite its multidimensional applicability, the widespread usage of this promising polymer hinge on the practical considerations such as the scale-up capability and production costs, as if comparing with other popular commercial organic products, BNC is still expensive, therefore, its use is limited. Consequently, the reduction of production costs and scaling up the production process are technological prerequisites for BNC to be adopted at wider scale. One of the ways to make the production process economically feasible is to search for low- or no-cost, abundant and easily available carbon sources (as during BNC production, the culture medium itself represents approximately 30 % of the total cost) and to design a simple, less labor intensive cultivation strategy for higher productivity of BNC.

Moreover, the low conversion yield of BNC, in terms of high input of raw materials, is another major economic constraint to the commercialization of BNC at a "low" cost. In addition, there are very few microorganisms proficient in producing BNC up to an extent where its industrial use is possible. Only a few bacteria of the genus *Komagataeibacter* (preferably *Komagataeibacter xylinus*: the most referenced and used strain worldwide) were found to produce significant amount of BNC. Since, BNC synthesis has been strictly linked to the bacterial cell metabolism; the strain type and the culture conditions have a crucial influence on BNC production, in particular regarding factors such as carbon and nitrogen sources, metabolic stimulants, temperature and pH.

In this context, the present work was undertaken with a view to search for a potential cellulose producing strain(s) and to optimize the metabolic status of the selected strain(s) towards

enhanced cellulose synthesis by ameliorating the physiological dynamics to achieve a high conversion yield of BNC along with developing inexpensive culture media using low- or no-cost feedstocks to make the production process cost effective, followed by designing a simple and less labor intensive production process strategy to scale-up the production process for higher productivity of BNC. This may thus enable wider applicability of this value product and open up new avenues to deliver multifarious products to the market at competitive price.

The thesis has been divided into six chapters. Chapter 1 and 2 includes the introduction and detailed literature review of the bacterial nanocellulose with respect to its properties, production, purification and applications.

Chapter 3 embodies isolation of cellulose producing bacterial strain(s) and reprogramming of culture parameters for enhanced cellulose production. A total of 46 bacterial strains were isolated from different natural sources based on their colony size, shape and morphology. Amongst these, 4 bacterial isolates were found positive for cellulose production. All of these strains were isolated from black rotten grapes (*Vitis vinifera*) and no cellulose producers were obtained from other natural sources. Out of these 4 strains, isolate SGP37 was competent to produce notable amounts of BNC (5.61 ± 0.11 g L^{-1}, after 16 days of cultivation), hence selected as the most potent BNC producer for further studies. The isolate was identified as a strain of *Komagataeibacter europaeus* (formerly *Gluconacetobacter europaeus*). The strain was kinetically analyzed to evaluate BNC production under different physiological conditions. The stagnant cultivation of the strain in HS medium resulted into the production of 5.61 g L^{-1} cellulose after 2 weeks of fermentation, with conversion yield of 0.36 g cellulose/g sugar, at initial production rate of 0.95 g L^{-1} d^{-1}. Amelioration of physiological dynamics of the strain by devising preeminent culture conditions, enhanced the production rate of cellulose by ~1.65 fold (1.55 g L^{-1} d^{-1}) and attained 9.98 g L^{-1} cellulose with initial sugar consumption of 12.08 g L^{-1}, resulting into a very high conversion yield (0.82 g cellulose/g sugar) ever reported.

Chapter 4 focuses on the development of inexpensive production media and designing the production process for low-cost and scaled-up production of bacterial nanocellulose. Sweet lime pulp waste (SLPW) and banana peel waste (BPW) were utilized as a low- or no-cost feedstock for the production of bacterial nanocellulose (BNC) alone and in amalgamation with other nutritional supplements by the isolate *K. europaeus* SGP37 under static batch and static intermittent fed-batch cultivation. The highest yield (26.2 ± 1.50 g L^{-1}) was obtained in the hot water extract of SLPW supplemented with the components of HS medium, which got further boosted to 38 ± 0.85 g L^{-1} as

the cultivation strategy was shifted from static batch to static intermittent fed-batch. BNC obtained from various SLPW and BPW medium was similar or even superior to that obtained with standard HS medium in terms of its physicochemical properties. The production yields of BNC thus obtained are significantly higher and fit well in terms of industrial scale production.

Chapter 5 depicts the effect of various purification approaches on purity and physicochemical properties of BNC. The study was carried out to evaluate the impact of various treatment approaches onto the purity and physicochemical properties of BNC in order to find out precisely a process that can remove the bacteria from BNC pellicle but, at the same time, prevents the polymorphic transformation of cellulose I to cellulose II. The BNC pellicles were purified using 0.5 M NaOH, 0.5 M KOH, 10% SDS, 0.5 M NaOCl and 0.5 M H_2O_2 separately and the purity of the membranes was monitored using solid-state ^{13}C-NMR. Only the BNC treated with NaOH and KOH had shown the pure fingerprints of cellulose while the other treated samples were found to be contaminated by proteins which may be due to the presence of bacterial smidgens left after purification. Atomic force Microscopy (AFM) and Field Emission Scanning Electron Microscopy (FE-SEM) analyses also revealed the presence of bacterial cells and some other cloudy aggregations in all the BNC membranes except the BNC purified using NaOH and KOH. However, the BNC membrane purified using KOH method was more crystalline and thermally stable than the membrane purified using NaOH. Together, these results suggested that the KOH treatment of the pellicle was effectively able to remove the bacterial cells and other contaminants from the BNC membrane and at the same time was able to maintain the physicochemical properties of BNC.

Chapter 6 focuses on the preparation of 3-D microporous-nanofibrous BNC scaffolds and evaluation of their potential for bone tissue engineering. Microporous-nanofibrous BNC scaffolds (mBNC) were prepared using freeze-dry method and thoroughly characterized in terms of their morphology, chemical structure, crystallinity and biodegradability which were then followed by culturing C3H10T1/2 mesenchymal stem cells on these scaffolds to assess the cell attachment, proliferation, infiltration and osteoblastic differentiation for effective regeneration of bone tissue. The prepared scaffolds revealed a highly porous microarchitecture compared to native BNC membrane. The *in vitro* biocompatibility of the mBNC scaffolds was analyzed based on the adhesion, growth and proliferation of C3H10T1/2 mesenchymal stem cells. Results indicated strong cell adhesion with extended morphology of the cells on the surface as well as inside the pores of mBNC scaffold. The scaffold exhibited very good biocompatibility with hardly any

detectable cell death and the cells continued to proliferate with respect to time. Cell ingress into mBNC scaffolds was observed by DAPI stained cell nuclei in scaffold cross sections and found that C3H10T1/2 cells had infiltrated and homogeneously distributed throughout the entire depth of scaffold; indicating the potential of mBNC scaffold for tissue in-growth. Alizarin red staining (ARS) and energy-dispersive X-ray spectroscopy (EDS) analysis revealed osteogenic differentiation of C3H10T1/2 on the scaffolds, which demonstrate the potential of mBNC scaffolds for bone tissue engineering applications.

Today, I really don't have words what to say. "Bhagwan Ji, THANK YOU for everything."

The completion of my Ph.D. has been a long journey. It's true that "Life is what happens" when you are completing your thesis. Life doesn't stand still, nor wait until you are finished and have time to manage it. I always dreamed to be a scientist, thus, my Ph.D. has always been my priority, but as most know, there are several priorities in a person's life at any one time. Unfortunately due to life's challenges and the changes that followed, my thesis could not always be the number one priority. At any rate, I have finished, but not alone. Today, when I am intended to attain the biggest milestone of my life in the form of this thesis, it will be simple to name all those people who helped me to get this done, but it will be tough to thank them appropriately. I am obliged to God for blessing me the company of such nice people around me.

At this felicitous moment, first and foremost, I would like to record my sincere gratitude and regards to my supervisor Prof. R. P. Singh, Department of Biotechnology, IIT Roorkee, for giving me the opportunity to work under his guidance and showing confidence in my abilities despite all odds. I still remember that phone call and will never forget that date, when I came to know that I can join his laboratory for carrying out my doctoral work. Words cannot express how grateful I feel to be his student. This feat was possible only because of his unconditional support, constant motivation and timely discussions. He has always made himself available at every stage of this research despite his busy schedule. His straightforward criticisms combined with heart-warming support have given me a great confidence as a researcher. I am very much gratified to him for developing the scientific temperament in me and providing me a healthy, professional and free working atmosphere, as a result, research life became rewarding for me. Above all and the most needed, he provided me the unflinching support in various ways which can't be described in words. Thank you Sir Thanks a lot!

With profound indebtedness, I owe my sincere thanks and deep regards to Prof. P. Roy, Head, Department of Biotechnology, IIT Roorkee, to provide me the space in his laboratory, otherwise this thesis would not have been completed.

I extend my sincere thanks to my research committee members, Prof. V. Pruthi (Chairman DRC), Prof. R. Prasad (Chairman SRC), Prof. P. Roy (Internal expert) and Prof. U. P. Singh (External expert) for their valuable advice and critical comments on my research work time to time. I also express my gratitude to all the faculty members of Department of Biotechnology, IIT Roorkee for their support and help.

I wish to express my sincere thanks to Dr. Neeraj Sinha, CBMR Lucknow, for providing the research facility to carry out NMR studies. As well as, I am very much thankful to his student Dr. Rajkumar Sharma for helping me in the same.

I am sincerely thankful to Institute Instrumentation Center, IIT Roorkee for the instrumentation facilities to carry out the analytical work of my thesis.

Words are inadequate to express my heartfelt thanks to Ms. Rutusmita Mishra not only for helping in my research work with all her sincerity but also for the those late night stays in the lab despite being extremely sleepy, those lifts on cycle in the chilling winter and those laughter moments when I felt low. Don't get angry Ms. Ritu Varshney; I can never forget your support also. I would not have got those stunning images without your help. Heartily thanks to Somesh, Neeladri, Sandeep and Parul for the unasked support and making the comfortable time in the lab.

I would also like to acknowledge the immense support and love provided by my labmates Dr. Samta Saroj, Dr. Pragati Agarwal, Jyoti, Mukta, Shobhit, Aditi, Namrata and Pooja. I have created a bond with them that I will never forget. I am thankful to each one of them for making this journey memorable.

In recognition of all the support and help, I would also like to thank all the office staff of the department in particular, Jain Sir, Saini Sir, Mr. Walthare, Mrs. Shashi Prabha, Mr. Rajesh Paul and Pradeep Bhaiya.

I would like to avail this felicitous opportunity to express my deep respect and profound gratitude to Ma'am, Mrs. Pratima Singh for her kind affection and encouraging thoughts to achieve this destination. I never felt homesick since beginning only because of her incessant loving and caring nature.

Last, but not least, I would like to dedicate this thesis to my family and especially to my father for all of the sacrifices that you've made on my behalf. Your prayer for me was what sustained me thus far.

Dated: Dec 21, 2017 ***(Swati Dubey)***

TABLE OF CONTENTS

CHAPTER 4. Development of inexpensive production media and designing the production process for low-cost & scaled-up production of bacterial nanocellulose

CHAPTER 5. Effect of various purification approaches on purity and physicochemical properties of BNC

CHAPTER 6. Preparation of 3-D microporous-nanofibrous BNC scaffolds and evaluation of their potential for bone tissue engineering

CHAPTER 1

Introduction

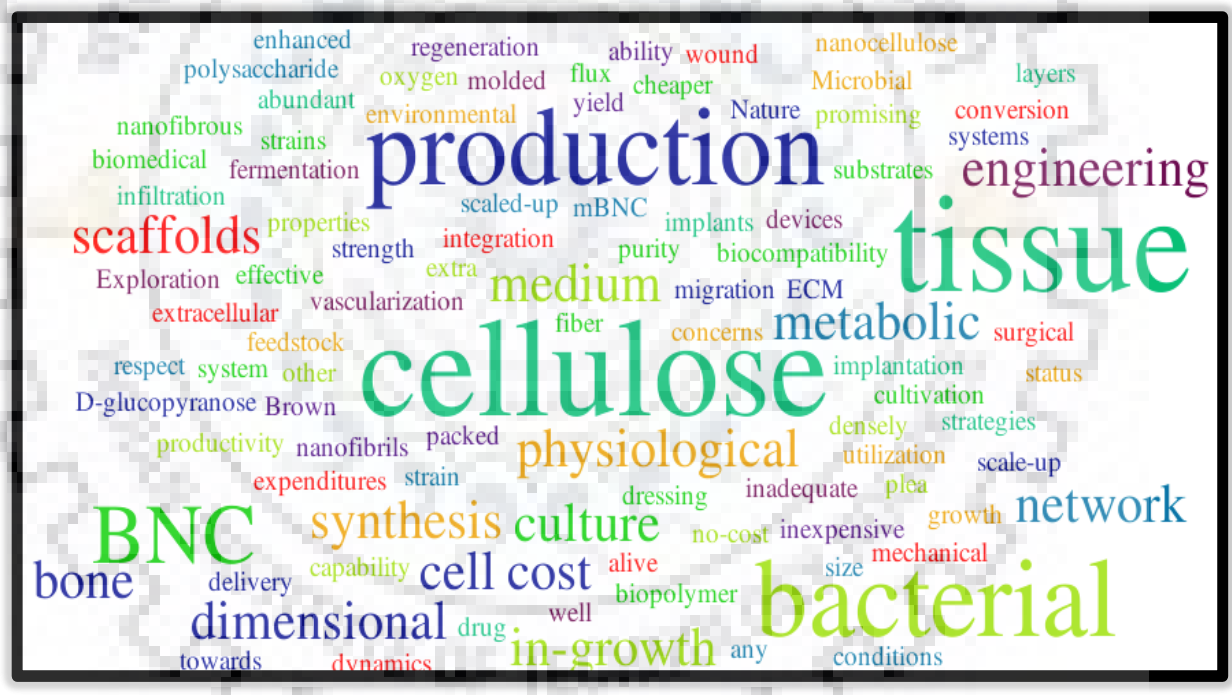

Introduction

In today's era, various groups are engaged worldwide to produce cellulose by employing processes that reduce both environmental impact and production cost. Traditionally, cellulose is being extracted from plants but the rising industrial demand for cellulose derived products has enforced extreme stress on the ecological steadiness of the plant world instigating global environmental concerns. Therefore, a great deal of attention is primed worldwide on the production of cellulose by alternative sources such as bacterial system to reduce the environmental backlashes to minimum.

Some bacteria are able to produce an extracellular form of cellulose termed bacterial cellulose (BC) or bacterial nanocellulose (BNC) that functions by positioning the bacterial cells at the surface of the culture medium to meet high oxygen plea with an incessant supply of nutrients through diffusion. It comprises parallel chains of β-1, 4-D-glucopyranose molecules stabilized by intermolecular hydrogen bridges, which is identical in chemical composition to plant cellulose. However, its physico-structural features such as ultra-fine nanofibrous network, mechanical strength, ability to be molded in any shape and extra purity (*i.e.* devoid of pectin, lignin, hemicellulose and other metabolic products); bestow BNC with plenteous advantages over plant cellulose and make it a potential precursor for breakthrough technologies in several vital arenas like biomedicine, food, paper, textile, cosmetics, and materials industry, leading to cutting edge products like optoelectronic materials, acoustic membranes, proton-conducting membranes, ultrafiltration membranes, supercapacitors, fuel cell, polymer matrices reinforcement, cosmetics, wound dressing materials, surgical implants, tissue engineering scaffolds, drug delivery systems and other biomedical devices.

Despite all of its impressive properties and remarkable potential for a wide range of applications, the widespread usage of this promising polymer is limited due to the scale-up capability and production expenditures which confine its use as an alternative to plant cellulose.

Consequently, the reduction of production costs and scaling up the production process are technological prerequisites for BNC to be adopted at wider scale. These include efforts (i) to explore alternative media formulations which are cheaper, abundant and readily available (as during BNC production, the culture medium itself represents approximately 30 % of the total cost), (ii) development of novel, simple, less labor intensive cultivation strategies for higher productivity, (iii) designing more efficient reactors for fermentation, (iv) search for novel, genetically stable,

high yielding cellulose producing bacterial strains and (v) to optimize the metabolic status of the strain(s) towards enhanced cellulose synthesis by ameliorating the physiological dynamics to achieve a high conversion yield.

Further, in terms of its application, as mentioned earlier, BNC possesses a natural refined 3-D nanofibrils network which has a shape analogous to that of natural ECM (extra cellular matrix) as well as exhibits excellent biocompatibility, ultrahigh mechanical strength and high water holding ability which makes it an excellent biomaterial to be used as a scaffold for bone tissue engineering. However, the major downside of this biomaterial is the lack of cell infiltration which is caused by the inadequate pore size ensuing from tightly packed BNC fiber layers. Hence, the vascularization of the scaffold and the supply of nutrients and removal of wastes are restricted, thereby hinders tissue in-growth. It has been documented that the pore size and structure is an essential parameter in the development of scaffolds for tissue engineering, as well as the pores must be interconnected and large enough to allow cell growth and migration, nutrient flow, vascularization, new tissue formation and remodeling so as to facilitate host tissue integration upon implantation. In this context, creation of pores suitable for cell growth and migration would be pertinent for effective 3- dimensional tissue in-growth which would lead into efficient regeneration of bone.

Keeping all these points in view, the present work is undertaken with the aim to search for the potential cellulose producing bacterial strain(s) and to optimize the metabolic status of the selected strain(s) towards enhanced cellulose synthesis to achieve high conversion yield of BNC, followed by developing an inexpensive culture medium and designing the production process strategy for cost effective and scaled-up production of bacterial nanocellulose, which was further employed as an scaffold for bone tissue engineering. Thus, the major objectives of the study are:

1. Exploration, isolation and screening of cellulose producing bacterial strain(s) from different natural sources

2. Reprogramming of physiological conditions to direct metabolic flux towards enhanced cellulose synthesis for the selected strain(s)

3. Designing the production process and utilization of low- or no-cost substrates as feedstock for scaled-up & cost effective production of bacterial nanocellulose

4. Evaluating the effect of various purification approaches on physicochemical properties of bacterial nanocellulose

5. Fabrication and physico-structural characterization of 3-dimensional microporous-nanofibrous BNC (mBNC) scaffolds

6. *In vitro* evaluation of mBNC scaffolds for bone tissue engineering

Details of the investigations on the above defined aspects have been enumerated in the following chapters of the present work.

CHAPTER 2

Review of Literature

"*In terms of the massive quantity of natural polymer biosynthesis, Nature is alive and well with respect to cellulose*" – [R. M. Brown, 1996]

Cellulose is one of the oldest and most abundant naturally occurring renewable biopolymer on the earth. Being the primary component of the plant cell wall, it forms the major part of plants and trees. According to a worldwide estimate, 10^{14} tons of cellulose is produced every year, accentuating the economic importance of this polymer [Jozala *et al*., 2016]. Despite of being so extensively used and explored for over millenary of years, there is still much to be probed about its production and applications.

2.1 HISTORICAL BACKGROUND

The scientific and technical understanding of cellulose started relatively late. In 1838, the French agricultural chemist Anselme Payen (1795-1871) first used the term "Cellulose" when he discovered a fibrous residual material after purification of various plant tissues with an acid-ammonia treatment, followed by extraction in water, alcohol and ether. He deduced the molecular formula as $C_6H_{10}O_5$ by elemental analysis and recognized the isomerism of its structure with starch (C: 44.4 % and H: 6.2 %) consisted of glucose residues, and was coined as cellulose [Payen, 1838].

2.2 STRUCTURE

Cellulose is an unbranched homo-polymer consists of D-glucopyranose units bridged by β(1-4)-glycosidic bond with a syndiotactic configuration [Helbert *et al*., 1996]. The repeat unit is comprised of two anhydroglucose molecules, comprehending the molecular formula $(C_6H_{10}O_5)n$; n=10,000-20,000, depending on its source [Samir *et al*., 2005; Cacicedo *et al*., 2016]. Because of the high intensity of hydroxyl groups along the skeleton, extended networks of hydrogen bonds are formed between the poly-glucan chains as shown in Fig 2.1. Driven by this hydrogen bonding force, 30-100 poly-glucan chains got aggregated to form elementary fibrils which then got amassed to form microfibrils and then to macrofibrils to make cellulose fiber (Fig. 2.1).

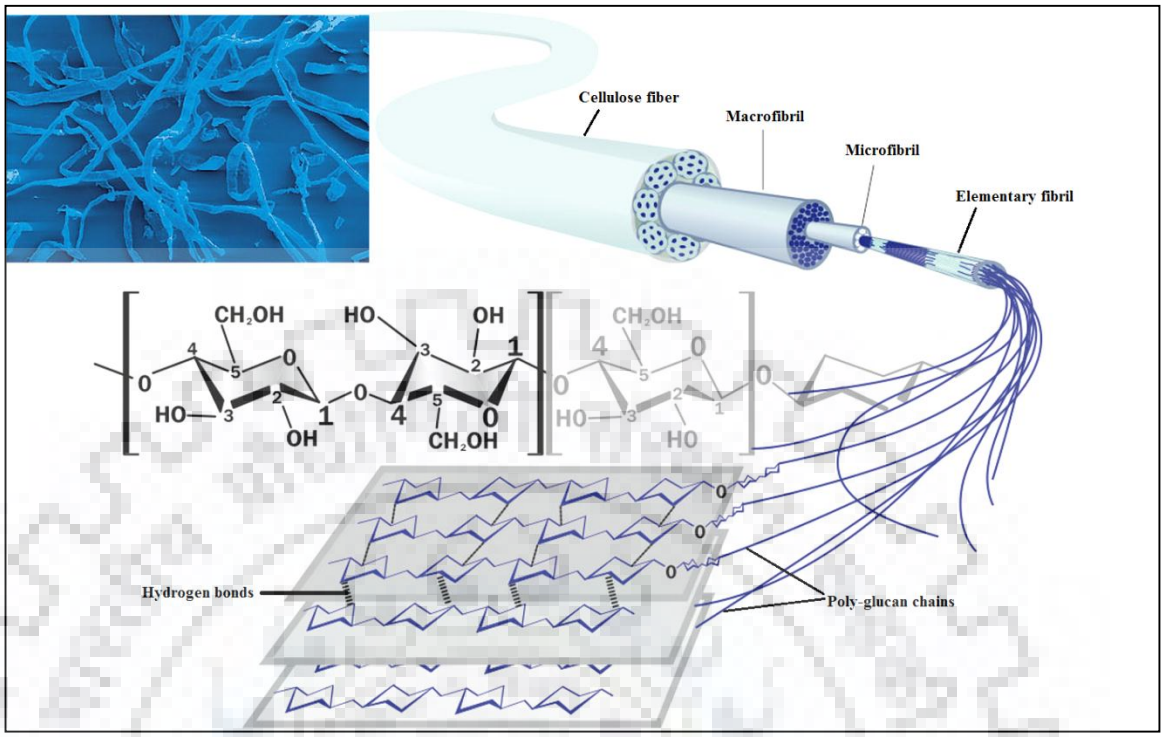

Fig. 2.1 Fibrillar and molecular structure of cellulose [Modified from http://www.jrs.eu/jrs_en/innovative-functionality/functions-jrs-products/]

Further, six different crystalline forms of cellulose are known- I (Iα and Iβ), II, III, IV, VI [Samir *et al*., 2005]. However, with the emergence of X-ray diffraction, it was observed that most of the native cellulose belongs crystallographically to Cellulose I. Cellulose I has been identified to exist as two types: Iα and Iβ form [Attala and VanderHart, 1984; Samir *et al*., 2005]. Both of these forms are similar in chain conformation, with the principal difference being the manner in which the chains are staggered longitudinally. This gives triclinic crystallographic symmetry to the Iα form and monoclinic symmetry to Iβ form, as shown in Fig. 2.2.

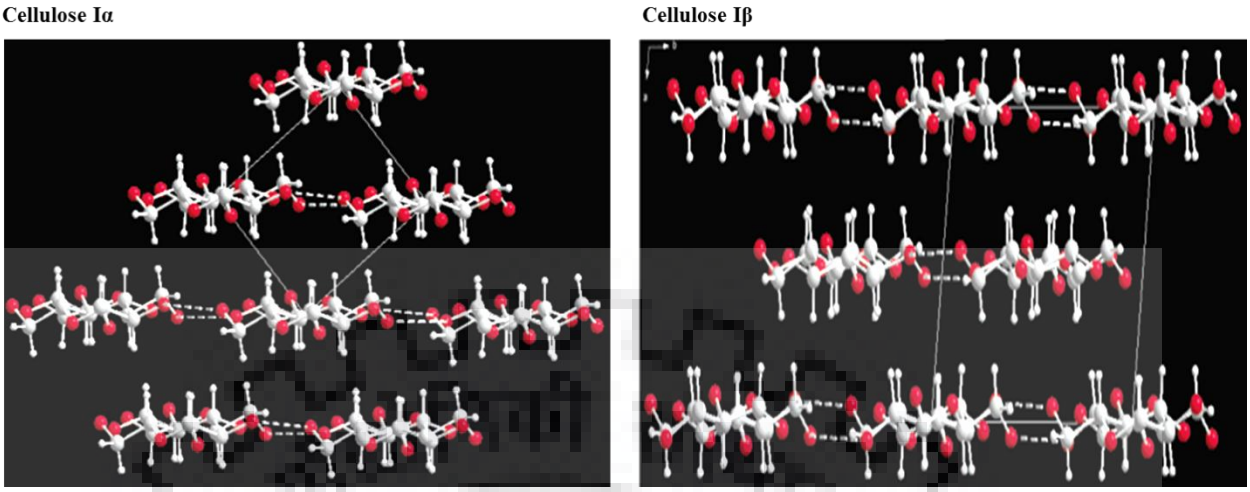

Fig. 2.2 Projections of the crystal structures of Cellulose Iα and Cellulose Iβ (C, O, and H atoms are represented as white large balls, red balls and white small balls, respectively; covalent and hydrogen bonds are denoted as full and dashed sticks, respectively) [Wada *et al*., 2004]

2.3 SOURCES

Although plants and trees are the major contributor of cellulose, two other less commonly followed sources are also included *i.e.* (i) *in vitro* enzymatic synthesis outsetting from cellobiosyl fluoride and (ii) chemical synthesis using glucose by ring-opening polymerization of benzylated and pivaloylated derivatives [Kobayashi *et al*., 1992; Nakatsubo *et al*., 1996]. Beside this, cellulose is also produced by some groups of microorganisms like fungi (*Saprolegnia*, *Dictyostelium discoideum*), algae (*Vallonia*) and bacteria (*Agrobacterium*, *Aerobacter*, *Acetobacter*: reclassified as *Komagataeibacter*, *Achromobacter*, *Azotobacter*, *Pseudomonas*, *Rhizobium*, *Sarcina*) [Chawla *et al*., 2009; Jozala *et al*., 2016]. Of these, however, only a few bacteria of the genus *Komagataeibacter* (preferably *Komagataeibacter xylinus*: the most referenced and used strain worldwide) were known to be capable of producing cellulose in commercially viable quantities [Cacicedo *et al*., 2016; Dubey *et al*., 2017]; and hence, the produced cellulose is termed as 'Bacterial Cellulose'.

2.4 BACTERIAL CELLULOSE OR BACTERIAL NANOCELLULOSE

2.4.1 Historical perspective

Brown, (1886) was the first who discovered bacterial cellulose when he detected an organism in the 'mother of vinegar' producing an extremely strong membrane at the surface of the culture medium. In his original paper, Brown described his observations as, *"A pure cultivation of the "vinegar plant" when commencing to grow in a liquid favorable to its free development, is usually first noticed as a jelly-like translucent mass on the surface of the culture fluid;"* This jelly-like translucent membrane was found to be chemically identical with cotton cellulose by Barsha and Hibbert (1934), in a series of experiments involving methylation, acetylation, acetolysis and hydrolysis.

2.4.2 Biosynthesis

It is still an open quest of biologists as, why bacteria produce cellulose. Some plausible theories have been put forward in this regard: (i) one considers that the aerobic bacteria produce cellulose pellicle to uphold their position in proximity to the surface of culture medium to get the necessary oxygen for their metabolism where oxygen concentration is the highest, (ii) another states that the bacteria produce cellulose to protect themselves from ultraviolet light, and (iii) some contemplate that the bacteria confined themselves in the cellulose pellicle to guard themselves from adversaries and heavy-metal ions, whereas nutrients can be supplied simply by diffusion [Schramm and Hestrin, 1954; Iguchi *et al*., 2000].

The synthesis of BC is a synchronized process which involves various enzymes and protein complexes. The process includes the uptake of the carbon source (*e.g.* glucose, fructose etc.) from external environment into the cell and then the biosynthesis of BC takes place in four enzymatic steps: (i) phosphorylation of glucose to glucose-6-phosphate by glucokinase, (ii) phosphoglucomutase catalyzed isomerization of glucose-6-phosphate to glucose-1-phosphate, (iii) conversion of glucose-1-phosphate to uridine diphosphate glucose (UDP-glucose) by UDP-glucose pyrophosphorylase, and then (iv) synthesis of cellulose from UDP-glucose by cellulose synthase [Ross *et al*., 1991; Lin *et al*., 2013; Rajwade *et al*., 2015; Reiniati *et al*., 2017b].

The nascent chains of cellulose are then extruded through the cell membrane by complex terminals (CTs). A single cell of *Komagataeibacter* spp. carries about 50 and 80 complex

terminals (pores) for extruding these cellulose chains from their cell membrane. Through these complex terminals, the bacteria extrude these nascent chains that aggregate to form subfibrils. The subfibrils are then auto assembled into nanofibrils (3–4 nm thick) which in turn are united to form a ribbon with 40–60 nm width [Cacicedo *et al*., 2016]. These ribbons then aggregate together and form a 3-D network structure in the form of a gelatinous film at the surface of the culture broth as shown in Fig. 2.3.

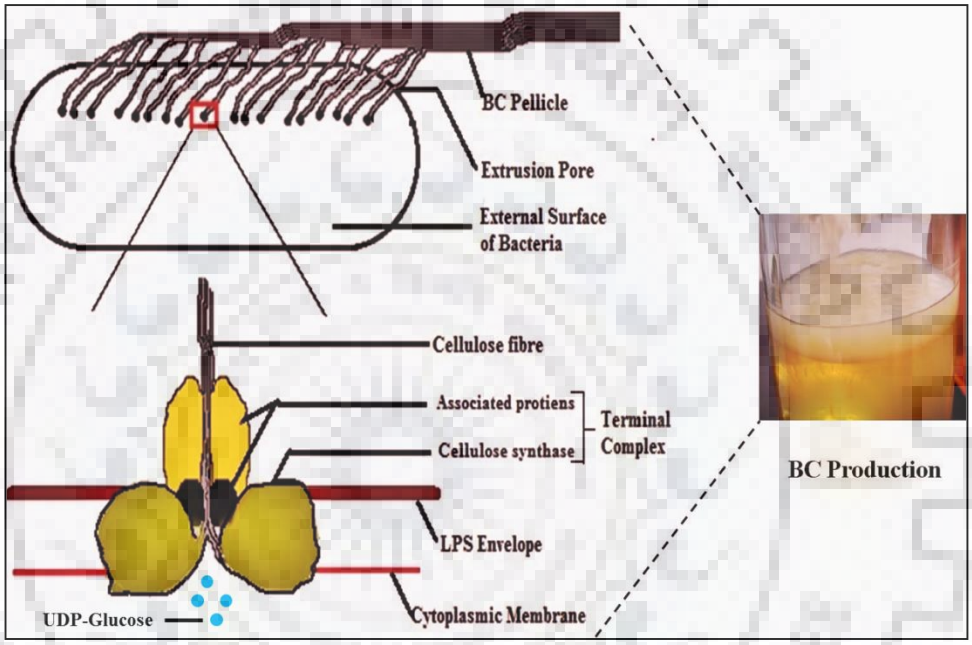

Fig. 2.3 Schematic representation of bacterial cellulose synthesis [Dubey *et al*., 2015]

2.4.3 Properties and differences from plant cellulose

The cellulose produced by bacteria is identical to that produced by plants in terms of its molecular formula but possesses different physicochemical properties which make it superior over plant cellulose [Cacicedo *et al*., 2016; Jozala *et al*., 2016]. Plant cellulose is produced as a lignocellulosic material where cellulose molecules are strongly associated with other substances such as lignin, pectin and hemicelluloses; as well as the cellulose content in plants hinge on the natural sources being used, for instance, the cotton contains around 90% of the cellulose while in wood the cellulose content is reduced to about 50% [Cacicedo *et al*., 2016]. Hence, the purification and isolation of cellulose from plants is a difficult task and it becomes more difficult if it is intended to be used in the sensitive areas such as in biomedicine where the fine molecular tuning is vital. Cellulose purification from plants involves complex procedures such as mechanical

treatment followed by pre-treatments based on the use of harsh chemical and/or enzymatic processes which consumes very high energy approximately 1000 kWh/Ton; apart from this, environmental issues required to be attended due to the toxicity of byproducts discarded during purification process [Cacicedo *et al*., 2016]. However, bacterial cellulose is produced in a highly pure form which reduces the efforts of purification and makes the purification process simpler, economic and eco-friendly [Shi *et al*., 2014; Cacicedo *et al*., 2016].

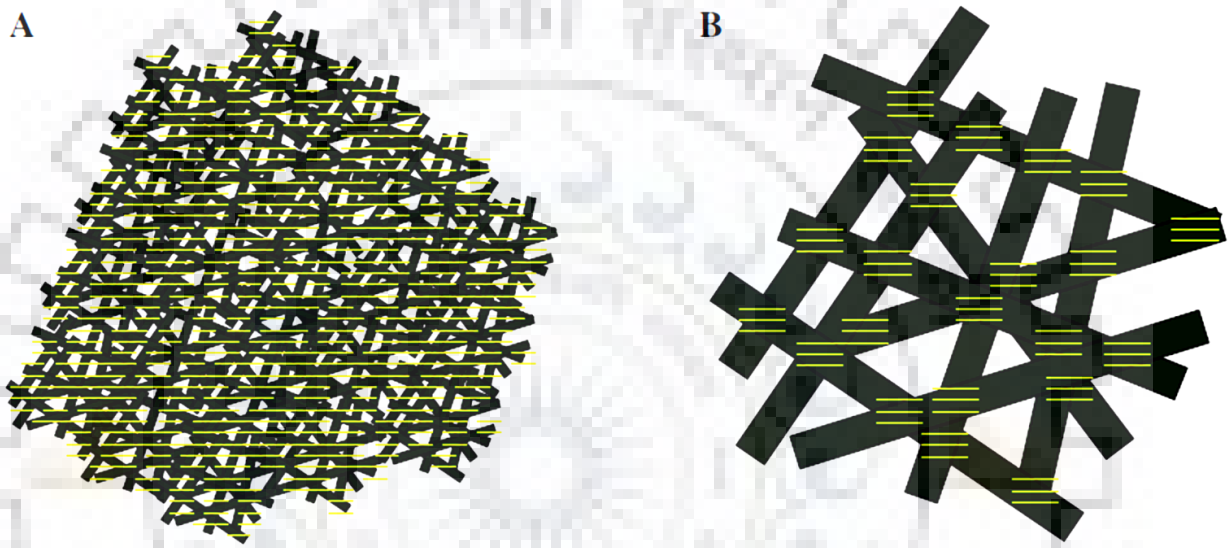

Fig. 2.4 Schematic elucidating extensive hydrogen bonding in (a) bacterial cellulose (nano-size network) as compared to (b) plant cellulose (micro-size network) [Soykeabkaew *et al*., 2009]

Since, cellulose synthesized by bacterial processes is of nano-size; as a result hydrogen bonding between the cellulose fibrils is greater than that of plant cellulose (Fig. 2.4) and makes it superior over plant cellulose in terms of physicochemical properties. Due to its nano-fibrillar structure and extended H-bonding network, it displays a very high mechanical strength, crystallinity, thermal stability, moldability and water holding capacity [Cacicedo *et al*., 2016]. Table 2.1 below briefly shows the distinguishing features of bacterial cellulose as compared to plant cellulose.

Table 2.1 Comparison of plant and bacterial-derived cellulose [Modified from Reiniati *et al*., 2017b]

Parameter	Plant cellulose	Bacterial cellulose
Production time	Months to years, depending on plant species	Days, reliant on bacterial species
Growth conditions	Soil type, nutrients, climate conditions and prone to insect pest infestation	Pure sugars and/or sugars/carbon from agro-industrial wastes, fermentation conditions such as pH, temperature, aeration
Composition	Cellulose associated with lignin, pectin and hemicelluloses	Devoid of these contaminants and pure cellulose can be obtained after removal of bacterial cells
Energy requirements	Harvesting and transportation of logs, wood chipping, pulp processing	Sterilization of nutrients and equipment used to produce cellulose
Purification	Several steps, involving different physical, mechanical and chemical processes	Alkali treatment
Properties	Fiber width (20-40 μm), Crystallinity (50-60 %), Degree of polymerization (13, 000-14, 000), Water content (50-60 %)	Fiber width (40-80 nm), Crystallinity (60-90 %), Degree of polymerization (2, 000–6, 000), Water content (98 %)
Process commercialization	Commercial process is established	Produced industrially and vended as food product called 'natade-coco'. Several scale-up amenities produce BNC membranes for biomedical applications. More improved process is needed to facilitate its high yield at lower cost in shorter time.

Further, the nanofibrillar branching network of BC which account for its unique physicochemical properties, is influenced by the proliferation rate of bacterial cells (which in turned be governed by the physiological conditions like culture media, pH, temperature, oxygen tension among others) and the approaches used for its purification [Gea *et al*., 2011; Gu and Catchmark, 2012] which makes a point of investigation at this aspect in BNC research.

2.4.4 BNC Production

Because of all the above mentioned properties, BNC has primed a great deal of attentiveness worldwide and has gained multidimensional applicability in several vital arenas, from bioprocesses to biomedicine, paper, cosmetic, food, electronics, etc. [Shi *et al*., 2014; Mohite and Patil, 2014a;

Dubey *et al*., 2015; Keskin *et al*., 2017; Picheth *et al*., 2017]. However, the main challenge is to introduce BNC into the market with an economical price and production as if comparing with other popular commercial organic merchandises, BNC is quiet expensive [Kiziltas *et al*., 2015; Mohammadkazemi *et al*., 2015]. Therefore, various efforts are being made around the world to devise strategies for effective and inexpensive production of BNC. These include (i) exploration of alternative media formulations which are cheaper, abundant and readily available (as during BNC production, the culture medium itself counts approximately 30 % of the total cost), (ii) development of novel, simple, less labor intensive cultivation strategies for higher productivity, (iii) designing more efficient reactors for fermentation, (iv) search for novel, genetically stable, high yielding cellulose producing bacterial strains and (v) to optimize the metabolic status of the strain(s) towards enhanced cellulose synthesis by ameliorating the physiological dynamics to achieve a high conversion yield. The following sections will provide a detailed description of these efforts.

2.4.4.1 BNC producing strains

BNC is produced by a diverse group of bacteria, such as those belongs to the genera *Acetobacter* (*Gluconacetobacter*), *Achromobacter*, *Aerobacter*, *Azotobacter*, *Agrobacterium*, *Alcaligenes*, *Escherichia*, *Pseudomonas*, *Rhizobium*, *Salmonella and Sarcina* [Parola, 1970; Deinema and Zevenhuizen, 1971; Napoli *et al*., 1975; Zogaj *et al*., 2001; Shoda and Sugano, 2005; Chawla *et al*., 2009; Jozala *et al*., 2016]. Among them, the most efficient producers of cellulose are the bacteria belonging to the genus *Komagataeibacter* [Chawla *et al*., 2009; Cacicedo *et al*., 2016], which is recently created by reclassifying the *Gluconacetobacter* genus on the basis of chemotaxonomic characteristics and 16S rRNA sequence phylogeny [Yamada, 2014]. The *Komagataeibacter* species is defined as Gram-negative, non-photosynthetic, strictly aerobic, living primarily in decomposing fruits and vegetables; and are able to metabolize common carbon sources such as glucose, fructose, sucrose, glycerol, mannitol and other organic substrates into cellulose within a period of a few days [Seto *et al*., 2006; Nguyen *et al*., 2008; Carreira *et al*., 2011; Trovatti *et al*., 2011]. Various bacterial cellulose producing strains and their yields are depicted in Table 2.2.

Table 2.2 Carbon sources, inducers and bacterial strains used for the production of bacterial nanocellulose

Bacterial strain	Carbon Source	Supplement/Inducer	Culture time	Yield (g L^{-1})	Reference
Gluconacetobacter xylinus IFO 13772	Glucose (2%)	Lignosulfonate (1%)	7 days	11.44	Keshk and Sameshima, 2006a
Gluconacetobacter xylinus IFO 13773	Glucose (2%)	Lignosulfonate (1%)	7 days	16.22	Keshk and Sameshima, 2006a
Coculture of *Gluconacetobacter xylinus* st-60-12 and *Lactobacillus mali* st-20	Sucrose (4%)	-	5 days	4.4	Seto *et al.*, 2006
Acetobacter xylinum NUST4.1	Glucose (1.8%), Sucrose (2.1%)	Sodium alginate (0.04%)	5 days	6.0	Zhou *et al.*, 2007
Gluconacetobacter xylinus strain (K3)	Mannitol (2%)	Green tea (0.3%)	7 days	3.34	Nguyen *et al.*, 2008
Gluconacetobacter xylinus ATCC 53524	Sucrose (2%)	-	4 days	3.83	Mikkelsen *et al.*, 2009
Acetobacter sp. V6	Glycerol (3%)	-	7 days	4.98	Jung *et al.*, 2010
Gluconacetobacter sacchari	Glycerol (2%)	-	4 days	2.07	Carreira *et al.*, 2011
Gluconacetobacter sacchari	Glucose (1%), Galactose (1%)	-	4 days	2.60	Carreira *et al.*, 2011
Gluconacetobacter sacchari	Glucose (2%)	-	4 days	2.7	Trovatti *et al.*, 2011
Gluconacetobacter sacchari	Fructose (2%)	-	4 days	2.0	Trovatti *et al.*, 2011
Gluconacetobacter sp. F6	Glucose (1%)	Ethanol (0.4%)	6 days	4.50	Jahan *et al.*, 2012
Gluconacetobacter medellensis	Glucose (2%)	-	14 days	4.50	Castro *et al.*, 2012
Gluconacetobacter hansenii	Glucose (5%)	Ethanol (2%)	7 days	2.87	Li *et al.*, 2012

Table 2.2 continued..

Gluconacetobacter hansenii	Glucose (5%)	Ethanol (2%), Sodium citrate (2%)	7 days	3.07	Li *et al*., 2012
Gluconacetobacter xylinus BCRC 12334	Glucose (2%)	Thin stillage	7 days	10.38	Wu and Liu, 2012
Gluconacetobacter persimmonis GH-2	Fructose (1%), Sucrose (1%)	-	14 days	8.79	Hungund *et al*., 2013
Rhodococcus sp. MI 2	Sucrose (1.5%)	-	14 days	7.40	Tanskul *et al*., 2013
Gluconoacetobacter intermedius NT	Glucose (2%)	-	10	8.5	Tyagi and Suresh, 2013
Gluconacetobacter hansenii PJK (KCTC 10505BP)	Glucose (1%)	Glucuronic acid-based oligosaccharide (2%)	10 days	12.74	Ul-Islam *et al*., 2013
Gluconacetobacter xylinus IFO 13693	Glucose (2%)	Vitamin C (0.5%)	7 days	16.0	Keshk, 2014
Gluconacetobacter xylinus IFO 13773	Glucose (2%)	Vitamin C (0.5%	7 days	19.3	Keshk, 2014
Gluconacetobacter xylinus ATCC 10245	Mannitol (2.5%)	Sodium alginate (0.04%)	6 days	8.25	Atwa *et al*., 2015
Komagataeibacter sucrofermentans DSM 15973	Crude glycerol (1.8%)	Sunflower meal (SFM) hydrolysate	15 days	13.3	Tsouko *et al*., 2015
Gluconacetobacter xylinus BCRC 12334	Glucose (2%)	Acetate buffered (100 mM)	8 days	2.46	Kuo *et al*. 2016
Komagataeibacter europaeus SGP37	Fructose (2%)	Ethanol (0.2%)	16 days	9.98	Dubey *et al*., 2017

2.4.4.2 Culture medium

BNC production has conventionally been made using defined culture medium named HS medium honoring Hestrin and Schramm who developed the media in 1954, which consisted of glucose, yeast extract, peptone, disodium hydrogen phosphate, citric acid and adjusted to pH 6 [Hestrin and Schramm, 1954]. However, changes in the carbon source, nitrogen source, pH and

inducers starting from this culture medium were used by various researchers to modify the BNC productivity. For instance, *K. xylinum* (the most widely used strain around the world) was grown in production medium using several carbon sources such as glucose, fructose, sucrose, maltose, glycerol, mannitol, etc. [Jung *et al*., 2010; Trovatti *et al*., 2011; Tanskul *et al*., 2013; Atwa *et al*., 2015] (Table 2.2). Moreover, to stimulate the metabolism in the microorganism and/or to reduce the formation of metabolic by-products, several metabolic inducers were added to the BNC production medium by various researchers [Li *et al*., 2012; Keshk, 2014; Kuo *et al*. 2016]. Table 2.2 shows some of inducers used for the BNC production.

Further, with the advancement in the field of biotechnology towards green, sustainable and economic production, different agro-industrial residues are being used for the production of various microbial products [Joshi and Khare, 2013; Kumar *et al*., 2017; Rane *et al*., 2017]; for instance, bioethanol production through simultaneous saccharification and fermentation of corncob and soybean cake [Zhang *et al*., 2010], production of xylanase by solid state fermentation utilizing deoiled *Jatropha curcas* seed cake [Joshi and Khare, 2011; Sadaf and Khare, 2014], production of poly(3-Hydroxybutyric Acid) from orange peel and rapeseed cake [Sukan *et al*., 2014], among others. It not only makes the production process economic but also has an eco-friendly effect by wiping out these wastes from the environment. In order to make the production process economically feasible, several agro-industrial wastes have been explored for the production of BNC also, and listed in Table 2.3.

Table 2.3 Various agro-industrial wastes used for BNC production

Agro-industrial waste	Bacterial strain	Reference
Sugar cane molasses	*Acetobacter xylinum* IFO 13772	Keshk and Sameshima, 2006b
Beet molasses	*Gluconacetobacter xylinus* ATCC 10245	Keshk *et al*., 2006
Konjac powder	*Acetobacter aceti* subsp. *xylinus* ATCC 23770	Hong and Qiu, 2008
Processed rice bark	*Acetobacter xylinum* ATCC 23769	Goelzer *et al*., 2009
Saccharified food wastes	*Acetobacter xylinum* KJ1	Li *et al*., 2011
Grape skins	*Gluconacetobacter sacchari*	Carreira *et al*., 2011
Cheese whey	*Gluconacetobacter sacchari*	Carreira *et al*., 2011
Sulfite pulping liquor	*Gluconacetobacter sacchari*	Carreira *et al*., 2011
Mandarin fruit dregs	*Gluconacetobacter intermedius* CIs26	Yang *et al*., 2013
Wheat straw	*Gluconacetobacter xylinus* ATCC 23770	Chen *et al*., 2013
Dry olive mill residue	*Gluconacetobacter sacchari*	Gomes *et al*., 2013
Waste fiber sludge	*Gluconacetobacter xylinus* ATCC 23770	Cavka *et al*., 2013
Wastewater from rice wine distillery	*Gluconacetobacter* xylinus BCRC 12334	Wu and Liu, 2013
Waste beer yeast	*Gluconacetobacter hansenii* CGMCC	Lin *et al*., 2014
Pineapple and watermelon peels	*Komagataeibacter hansenii* MCMB-967	Kumbhar *et al*., 2015
Waste water of candied jujube processing industry	*Gluconacetobacter xylinum* CGMCC 2955	Li *et al*., 2015
Corncob acid hydrolysate	*Gluconacetobacter xylinus* CH001	Huang *et al*., 2015a
Hot water extracted wood sugars	*Acetobacter xylinus* ATCC 23769	Kiziltas *et al*., 2015
Carob and haricot bean extracts	*Gluconacetobacter xylinus* (ATCC 700178	Bilgi *et al*., 2016
Wastewater after lipid fermentation	*Gluconacetobacter xylinus* CH001	Huang *et al*., 2016
Agricultural corn stalk	*Acetobacter xylinum* ATCC 23767	Cheng *et al*., 2017
Cashew tree residues	*Komagataeibacter rhaeticus*	Pacheco *et al*., 2017

2.4.4.3 Cultivation strategies

BNC has conventionally been produced by static and agitated culture methods. However, commonly static cultivation has been used for BNC production by forming pellicles at the surface of the culture medium [Krystynowicz *et al*., 2002; Hsieh *et al*., 2016] and once the pellicle reaches to a certain thickness, the growth of bacterial cells as well as BNC production slows down as the pellicle limits the access of oxygen to the lower part (liquid zone) of the pellicle and nutrients to the upper part (aerobic zone) of the pellicle, results into a low productivity of BNC. Conversely, in agitated culture, the bacterial cells have better contact with circulating air that results into better growth rate and consequently enhanced BNC production. However, BNC production in agitated culture is often accompanied by a considerable increase in the viscosity of the culture medium, which further impedes the diffusion of air into the culture medium. In addition, although the agitated culture led into a superior growth rate to that achieved in static culture and results in a bacterial doubling time of 4–6 h (as opposed to 8–10 h in static culture), it can cause the undesirable growth of cellulose$^-$ mutants in some bacterial strains [Krystynowicz *et al*., 2002], which become more enriched than the wild-type strain because of their faster growth, thus lowers BNC productivity. However, the study conducted by Nguyen *et al*. (2010) do not support this theory and demonstrated that different nutrient conditions rather than agitation affect the growth of spontaneous mutants in *G. xylinus* strain isolated from Kombucha. Another disadvantage of agitated culture is that BNC is obtained in the form of granules rather than pellicles as produced in static cultures which affects its physicochemical properties.

Therefore, it is necessary to develop the strategies and reactors for the production of BNC which lead into the higher productivity in lesser culture time and does not allow transformation of cellulose$^+$ strains into cellulose$^-$ strains. There are some reports in the literature where different reactors have been used for BNC production and have been discussed in the subsequent section.

2.4.4.4 Bioreactors

To meet commercial scale production, several attempts have been made for designing the suitable bioreactor for BNC production by various researchers, as summarized below.

2.4.4.4.1 Rotating disk reactor

In rotating disk reactor, half of the surface of the disk remains submerged in the culture broth, while the other half is exposed to the air. During continuous rotation, both surfaces of the

disk alternate between the culture medium and air; thus the bacteria take nutrients from the culture medium and oxygen from the atmosphere during the submerged and air-exposed periods, respectively [Ul-Islam *et al*., 2017]. BNC production in this type of reactor is influenced by different variables such as the volume of the culture medium, rotation speed and the number of disks used. Krystynowicz *et al*. (2002) observed that maximum BNC production was achieved when the ratio of the surface area to the medium volume (S/V) and rotation speed were 0.71 cm^{-1} and 4 rpm, respectively.

2.4.4.4.2 Rotary biofilm contactor

The rotary biofilm contactor possesses a series of circular disks fixed on a horizontal tube. The mounted disks are continuously rotated and alternate between exposure to the culture broth and the air. This type of reactor is advantageous because the microbes do not face shear stress (which can cause conversion of $cellulose^+$ strains into $cellulose^-$ strains) and can easily take up oxygen from the air. *Gluconacetobacter sp*. has been used in such a reactor and was found to produce up to 5.52 g L^{-1} of BNC when eight disks were used [Kim *et al*., 2007].

2.4.4.4.3 Bioreactor equipped with spin filter

Jung *et al*. (2005) had developed this bioreactor which was equipped with a turbine impeller composed of six flat blades and a spin filter consisting of a cylinder surrounded by a stainless steel mesh. The stainless steel bottom was attached to the agitator shaft. BNC production was carried out using *G. hansenii PJK* and a maximum of 4.57 g L^{-1} of BNC was produced after 140 h of culture in a periodic perfusion culture which was significantly higher than the overall yield from a conventional jar fermenter [Jung *et al*., 2005; Ul-Islam *et al*., 2017].

2.4.4.4.4 Bioreactor with a silicone membrane

This bioreactor is a static reactor where BNC pellicles form on both the surface of an oxygen-permeable synthetic membrane as well as on the air-liquid interface of the culture broth. Yoshino *et al*. (1996) had designed this bioreactor which contained an oxygen permeable silicone membrane surface in the bottom of the fermentation vessel. By doing this, the rate of cellulose production got doubled since BNC pellicles can be formed on the air-liquid interface of the culture medium as well as on the oxygen-permeable silicone membrane. They had also observed that the

rate of cellulose production on the silicone membrane strongly influenced by the degree of roughness of the membrane surface. The BNC production rate was about five times higher on a smooth silicone membrane than on an irregular surfaced membrane [Yoshino *et al*., 1996].

2.4.4.4.5 Aerosol bioreactor

Hornung *et al*. (2007) had developed this bioreactor which generates an aerosol spray of the glucose (or the other carbon source used) and ensures its uniform dissemination to the bacteria living in the air-liquid interface. BNC produced in the aerosol bioreactor exhibited greater mechanical strength than the conventionally produced BNC from a static flask/beaker or box/tray culture.

2.4.5 BNC: Recovery and purification

BNC harvested after fermentation contains impurities like bacterial cells and the culture medium components; thus needed to be purified to get pure cellulose. The most commonly used process of its purification is the treatment of BNC pellicle with alkali (such as NaOH or KOH) at 60–100 °C for 1–3 h [Chawla *et al*., 2009; Sulaeva *et al*., 2015]. The pellicle can also be purified using aqueous solution of SDS (Sodium dodecyl sulfate) followed by washing with NaOH and subsequent neutralization with acetic acid or by repeated washing with distilled water (DW) [Sakairi *et al*., 1998; Chawla *et al*., 2009]. Peroxide at concentrations of about 0.05–10% is used in some cases to whiten the BNC films [Sulaeva *et al*., 2015]. The medical application of BNC entails special procedure of purification to eliminate bacterial cells and toxins which can be the reason of pyrogenic reactions. The most effective protocol in this regard is the gentle processing of BNC pellicle between absorbent sheets to exorcize approximately 80 % of the liquid followed by leaving the membrane in 3% NaOH for overnight. This procedure is repeated 3 times and after that the pellicle is incubated in 3% HCl solution, pressed and thoroughly washed with DW which was then followed by sterilization using autoclave [Chawla *et al*., 2009].

Although alkali treatment of the BNC pellicle almost completely lyses the bacterial cells, but sometimes, a fraction of cell debris remains embedded in the BNC fibers which can be removed by (1) using more stringent NaOH treatment (2) adding repeated DW wash cycles, and/or (3) subjecting BNC to the ultrasound treatment [Reiniati *et al*., 2017b]. Removal of all the impurities from BNC pellicle also increases its mechanical properties. For instance, BNC

membranes treated with 2.5% NaOH solution was rated twice on Young's modulus compared to the untreated ones [Gea *et al*., 2011], conversely, a NaOH solution exceeding 6% causes distortion and shrinkage. Alkali treatment using concentrated NaOH solutions causes damage to BNC fibers, alters their mechanical characteristics [McKenna *et al*., 2009] and may transform cellulose I to cellulose II if treated for longer period of time [Shibazaki *et al*., 1997].

2.4.6 Bacterial Nanocellulose: Functional aspects

Since BNC exhibits several unique properties such as ultra-fine nanofibrous network, mechanical strength, ability to be molded in any shape and extra purity (*i.e.* devoid of pectin, lignin, hemicellulose and other metabolic products); which bestow it with plenteous advantages over plant cellulose and make it a potential precursor for breakthrough technologies in several vital arenas leading to frontline products like optoelectronic materials, acoustic membranes, ultrafiltration membranes, supercapacitors, fuel cell, polymer matrices reinforcement, cosmetics, immobilization matrix, wound dressing materials, surgical implants, tissue engineering scaffolds, drug delivery systems and other biomedical devices [Akduman *et al*., 2013; Barud *et al*., 2013; Lin *et al*., 2013; Wang *et al*., 2013; Shi *et al*., 2014; Mohite and Patil, 2014a; Dubey *et al*., 2015; Rajwade *et al*., 2015; Cacicedo *et al*., 2016; Jozala *et al*., 2016; Baldikova *et al*., 2017; Picheth *et al*., 2017]. Various applications of the bacterial nanocellulose are summarized in Table 2.4 and a detailed emphasis on biomedical based applications of BNC is given in the subsequent section.

Table 2.4 Various applications of bacterial nanocellulose [Modified from Lin *et al*., 2013; Rajwade *et al*., 2015; Jozala *et al*., 2016]

Category	Applications
Aerogels	Sound and heat insulation, Gas sorption, Ultralight, Flexible, and Fire-Resistant Carbon
Biosensors	Hydrogen peroxide bionsensor, Formaldehyde sensors, Humidity sensors
Biomedicine	Drug carrier, Artificial blood vessels, Tissue scaffolds, Nasal septal perforation, Wound dressing, Artificial skin
Cosmetics	Stabilizer of emulsions like creams, tonics, conditioners, nail polishes
Electronics	Flexible displays, Electronic paper displays, Diaphragms for microphones and stereo headphones, Photocatalyst, Flexible luminescent membranes, Supercapacitors
Energy	Membrane fuel cell (palladium)
Filtration material	Dialysis membrane, ultra-filtration membranes
Food	Dessert 'nata de-coco', As a thickening, gelling, stabilizing, emulsifying and binding agent
Immobilization matrices	Immobilization of denitrifying bacteria, Urease immobilization, Glucoamylase immobilization, Yeast immobilization for ethanol fermentation
Mining and refinery	Collection of leaking oil by Sponges, toxins absorbing materials
Paper	High quality papers, Flame retardant papers
Packaging	Casing for Bacteriostatic sausage, Active food packaging
Reinforcing agent	Reinforcement for fine structures, such as fibers, polymer foams and the composite matrices

2.4.7 Bacterial Nanocellulose and Biomedical area

The physicochemical properties described earlier plus the excellent biocompatibility of this biomaterial has opened the window of several applications for human health as described in the following sections and represented in Fig. 2.5

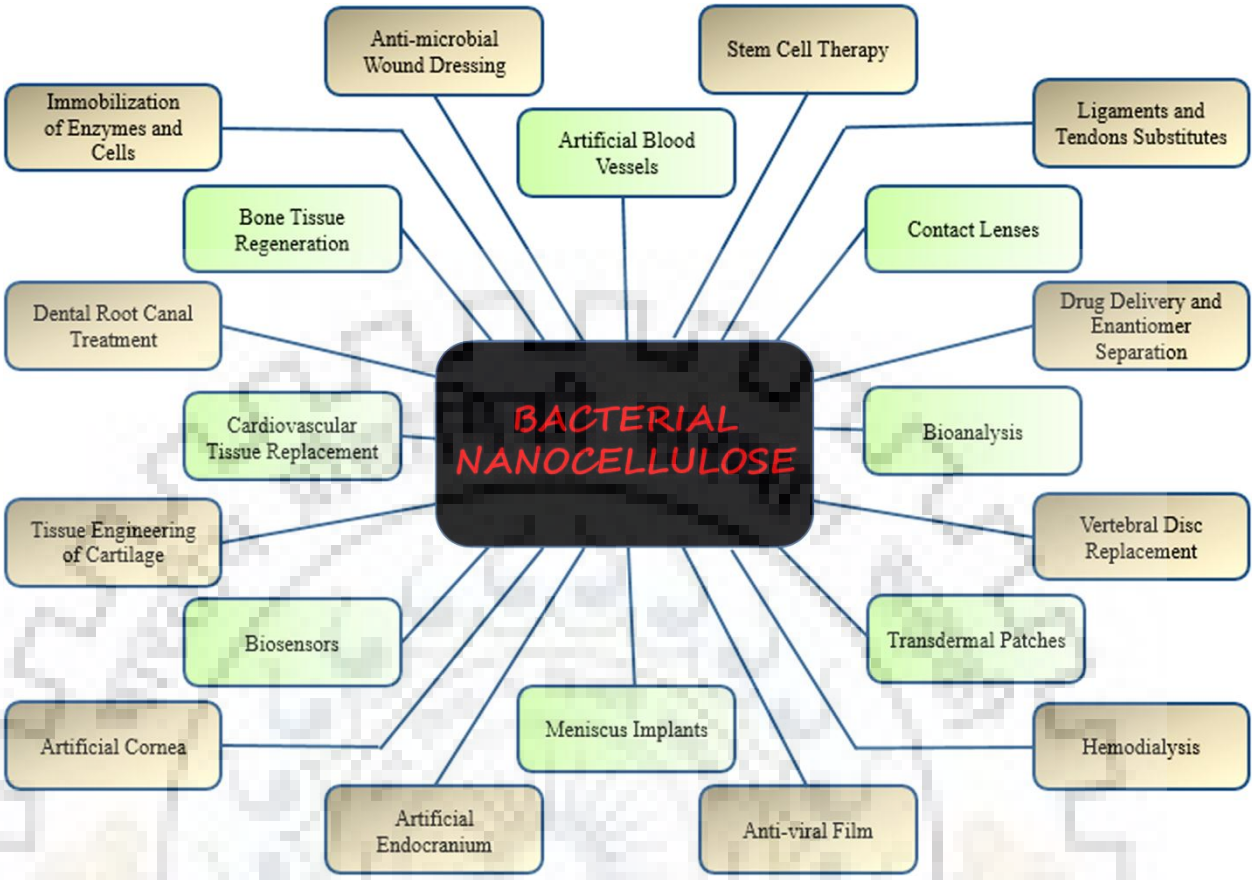

Fig. 2.5 Various biomedical and pharmaceutical applications of bacterial nanocellulose [Modified from Ullah *et al.*, 2016]

2.4.7.1 BNC in wound dressing

One of the first applications of bacterial nanocellulose in biomedical area was the wound dressing. Fontana *et al*. (1990) were the pioneers in unfolding the use of BNC to substitute the burned skin. Since then, there have been an increasing number of reports in the literature relevant to adoption of bacterial nanocellulose for wound dressing [Barud *et al*., 2016]. BNC dressings are recommended as a temporary covering for the treatment of wounds including pressure sores, skin tears, venous stasis, ischemic and diabetic wounds, second-degree burns, donor sites of skin graft, traumatic abrasions and lacerations and biopsy sites. BNC fits in all the standards and requirements of contemporary dressings including biocompatibility, mouldability, porosity, transparency, great adherence and protection from secondary infections, lack of sticking to the regenerated tissue, abilities for adsorption of exudates and water holding capacity, pain mitigation by heat adsorption (important in burns healing), which makes it a promising material for the purpose of modern wound dressing [Czaja *et al*., 2006; Kowalska-Ludwicka *et al*., 2013].

Some BNC based wound dressings are in fact available commercially such as BioFill®, Bioprocess®, XCell®, and Gengiflex® [Huang *et al*., 2014; Rajwade *et al*., 2015]. With regard to the ideal wound dressing, the biomembrane BioFill® was one of the leading commercial product that satisfy the fundamental prerequisites, including: cost-effectiveness, great adherence to the wound, permeability to water vapor, elasticity, transparency, durability, establishes a physical barrier for bacteria, hemostatic, effortless handling and it can be practiced with least possible exchanges. Moreover, the potency of BioFill® in accelerating the healing process and pain relief has been justified in more than 300 cases [Barud *et al*., 2016].

2.4.7.2 BNC in drug delivery

Among the numerous factors that have to be considered in designing an ideal drug delivery system, selection of an appropriate biomaterial is one of the critical parameter. BNC is one such biopolymer that has achieved the benchmark to be selected as an ideal drug delivery material. In past few years, a number of drug-delivery systems based on BNC have been proposed and exemplified by various researchers.

In a study by Huang *et al*., (2013), BNC membranes were used as the carrier for berberine sulphate and berberine hydrochloride to produce a controlled drug release system. Release studies and transdermal experiments carried out *in vitro*, demonstrated that the drug release time got extended significantly in the formulations using BNC as a carrier in contrast to the existing commercial carriers that were compared in the study. In an another study, incorporation of bacterial cellulose into bone cement had increased antibiotic release over 14 days as well as maintained its compression strength and fracture toughness even when loaded with 5 g of antibiotic [Mori *et al.* 2011]. Using a molecularly imprinted polymer (MIP) layer synthesis based on the controlled pore functionalization of BNC membranes, a composite membrane was developed for transdermal delivery of S-propranolol and demonstrated the controlled and stereo selective release of S-propranolol from a mixture of racemic propanol into the skin [Bodhibukkana *et al.* 2006]. Furthermore, Trovatti *et al.* (2012) had investigated the possibility of adopting BNC membranes as systems for topical or transdermal drug delivery of lidocaine hydrochloride & ibuprofen and found a uniform distribution of both drugs in the BNC membranes. The permeation rate of hydrophilic lidocaine hydrochloride in BNC membranes was lower than that obtained with the conventional formulations and indicates the benefit in the use of the system which requires long-term release of the drug. Bacterial cellulose is also employed in the synthesis of hydrogels for

drug-delivery systems. Amin *et al.* (2012) has reported that BC/AA (Bacterial Cellulose/ Acrylic Acid) hydrogel is a promising candidate for controlled drug-delivery systems. The results of swelling and *in vitro* drug-release studies of BC/AA hydrogel revealed the thermo- and pH-responsive drug release.

2.4.7.3 BNC in tissue engineering

In tissue engineering, a 3-D cell-culture system (scaffold) is needed to provide the geometrical foundation and support to the cells for attachment and proliferation. Scaffolds are the systems that closely mimic the complex and hierarchical structures of native tissue (intended to be designed) to provide the microenvironment that cells need to proliferate, migrate and differentiate.

Several synthetic and natural polymers such as polystyrene, poly-l-lactic acid (PLLA), polyglycolic acid (PGA), poly-dl-lactic-co-glycolic acid (PLGA), collagen, fibrinogen, chitosan, starch, hyaluronic acid among others, have been investigated as scaffolds to support the growth and proliferation of cells [Brien, 2011]. A few reports are also available on bacterial nanocellulose in this regard and as an intuitionistic introduction, the prospects for the various tissue engineering applications of BNC-based materials are shown in Fig. 2.6 and discussed in the subsequent sections.

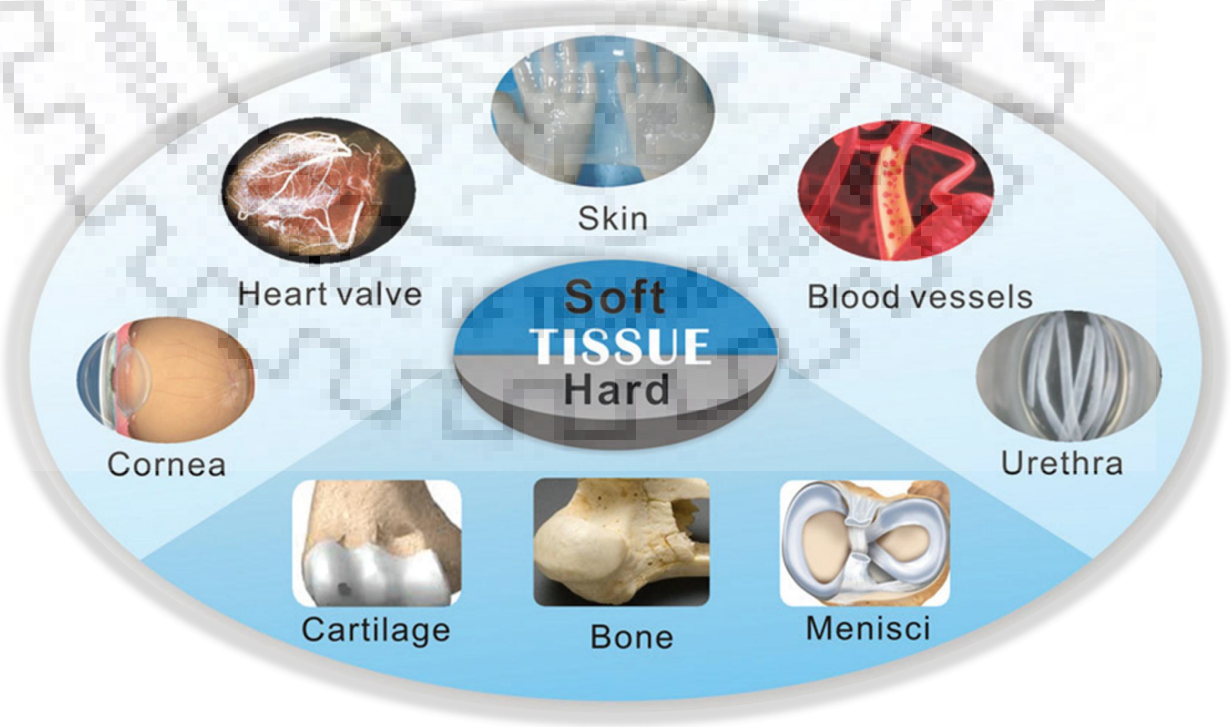

Fig. 2.6 Prospects for the various tissue engineering applications of bacterial nanocellulose [Fu *et al*., 2013]

2.4.7.3.1 BNC as artificial skin

Due to the exclusive nanofibrous network structure, mechanical features and high water content, BNC could potentially be utilized not just as a wound healing membrane but also as a semi-permanent artificial skin and can bring about epithelial recovery even in the severest epithelial damage. For patients with severe skin damage for instance, burn victims, Stevens-Johnson syndrome, etc., a cell-seeded BNC skin substitute could be an upgraded alternative to the autografting [Petersen and Gatenholm, 2011; Huang *et al*., 2014]. In order to upgrade the biodegradability and biocompatibility of BNC, Lin *et al*. (2011) formulated a macroporous BNC hydrogel *via* sequential alteration with distinct ECM fibers (collagen, elastin and hyaluronan) and growth factors (B-FGF, H-EGF and KGF) that may provide the desirable characteristics for ideal skin substitutes.

2.4.7.3.2 BNC as artificial blood vessels

Since BNC displays excellent moldability as well as provides optimal support for cell attachment and proliferation, it has been employed in the development of several synthetic prosthesis over the last years [Klemm *et al*., 2001; Schumann *et al*., 2009; Picheth *et al*., 2017]. Klemm *et al*. (2001) had publicized that BNC is an admirable candidate for the replacement of atherosclerotic coronaries as artificial vessels as it is bestowed with outstanding moldability and similar mechanical properties to of small diameter blood vessels (<5 mm). A group of researchers from Jena University, Germany synthesized the prototypes of BNC tubes (BASYC® tubes) in the form of standard vessels with different length, diameter and wall thickness, using a patented matrix technique during fermentation [Klemm *et al*., 2001, Schumann *et al*., 2009; Wippermann *et al*., 2009]. In a follow-up *in vivo* study with rats, pigs, and sheep, the BNC tubes were successfully used to substitute carotid arteries and exhibited long-term stability while maintaining the bypass unobstructed for prolonged period of time [Schumann *et al*., 2009; Wippermann *et al*., 2009]. Apart from this, the tubes exhibited superb surgical handling and could be sanitized by standard sterilization procedures.

Recently, Leitao *et al*. (2016) surgically implanted BNC grafts to the hind limb femoral artery of domestic limb. All BNC grafts exhibited good integration into the surrounding tissue without any significant signs of inflammation and fibrosis. Histological examination revealed a distinct three-layered structure having cellular adhesion and infiltration on both the adventitial and

luminal sides of the graft, and a larger BC central region without cell adhesion. Moreover, after one month of grafting, CD31 positive cells were observed on the luminal surface and were believed to be endothelial or progenitor endothelial cells, which drifted from the grafted femoral artery. Furthermore, a one month patency was attained with neo-vascularization and endothelialisation, however, after two months, the graft occluded due to thrombus formation.

2.4.7.3.3 BNC as urinary conduits

Neobladder reconstruction is unequivocally necessary for urinary diversion following cystectomy for muscle-invasive bladder cancer. The most common surgical techniques for the creation of urinary diversion are continent and conduit diversion. Continent urinary diversion involves the surgical creation of a pouch inside the body with a segment of small or large intestine which allows the patient to empty the reservoir *via* catheter. In conduit diversion a section of intestine, usually ileum is used to create a conduit that collects urine and allows it to drain through a stoma in the abdominal wall. The urine is then collected in a bag outside the body [Bodin *et al*., 2010]. However, both the continent and conduit diversion can cause several potential complications such as, urinary tract infections, bowel obstruction, skin breakdown around the stoma, hyperchloremic metabolic acidosis with hypokalemia, impaired renal function, stone formation, stenosis of the stoma, or damage to the upper urinary tract resulting from urine reflux. In this regard, tissue engineering may provide an alternative way for constructing a functional urinary conduit to store urine for patients with bladder cancer who necessitate total cystectomy.

Bodin *et al.* (2010) fabricated microporous BNC scaffolds seeded with human urine-derived stem cells (USCs) to form a tissue engineered conduit to use in urinary diversion and the results showed that scaffolds allowed 3-D growth of USCs, leading to the formation of a multilayered urothelium and cell-matrix infiltration. In an another study by Huang *et al.* (2015b), 3-D porous BNC scaffolds were prepared by gelatin sponge interfering in the BNC fermentation process and seeded with lingual keratinocytes for urethral reconstruction. The *in vivo* studies in rabbit model demonstrated that the cell seeded scaffolds enhanced urethral tissue regeneration without persuading any inflammatory reactions; and after 3 months of operation, macroscopic checkups and retrograde urethrograms of urethras revealed that all urethras had sustained wide calibers.

2.4.7.3.4 BNC as artificial cornea

This is another interesting applicability of BNC in the construction of artificial cornea. A Brazilian research group had developed and patented a special mechanism to conform BNC into correct angles and shape to produce contact lenses for cornea regeneration [Messaddeq *et al*., 2008]. In this process, wet BNC membranes were cut in a round shape and then compressed with the stick that had a semi-spherical end onto the base, under a constant temperature of 150 °C, to obtain a shape similar to a contact lens. In an extension to this work, Cavicchioli *et al*. (2015) had impregnated ciprofloxacin (CPX) with and without 2-hydroxypropyl-γ-cyclodextrin (γCD) into BNC membranes which were shaped like a contact lens by using abovementioned method in order to improve their therapeutic potential, and found that except for BC-CPX, the examined materials were promising to use as a contact lens for corneal regeneration and protection against bacteria. In an another study by Hui *et al*. (2009), using human corneal stromal cells had demonstrated that BNC scaffold supported the ingrowths of corneal stromal cells, signifying its potential for tissue engineering of cornea.

2.4.7.3.5 BNC as cartilage/meniscus implants

Due to the low regeneration potential of the cartilage tissue, the repairing of cartilage defects configures a challenge and a clinical need. Moreover, the materials for engineering artificial cartilage are required not to be only tough and resistant but also a proof of biodegradation. As BNC exhibits outstanding mechanical characteristics and low biodegradability, chondrocytes were seeded on BNC membranes and the results showed good proliferation as well as collagen type II production, signifying its suitability as a bio-mimicking scaffold for cartilage replacement [Svensson *et al*., 2005]. Further, Bodin *et al*. (2007) compared the mechanical properties of a BNC gel with traditional collagen meniscal implant material and real pig meniscus; and found that the Young's modulus of BNC gel was comparable to that of pig meniscus, and five times higher than that of traditional collagen meniscal implant. The results of promising cell proliferation, migration and controlled meniscus shape signposted that BNC can be an attractive material as meniscus implant.

Moreover, Liuzhenlin *et al*. (2011) had patented a preparation of BNC-based artificial endocranium (AE) because of its mechanical properties, foldability, non-cytotoxicity and low price. In this preparation, the wet BNC membrane was crushed and added with sodium alginate, carboxymethylcellulose and polyvinyl alcohol to get a liquid with moldability. The mixture was

then poured into a mold followed by freeze-drying to get the AE. The strength at break point, breaking elongation and hook strength values of the resulting AE were closer to that of a rabbit endocranium as well as the AE was not amenable to easy tear and off-clip during the stitching *via* sutures.

2.4.7.3.6 BNC in bone tissue engineering

Natural and synthetic implantable materials, such as polymers, metals and ceramics provide several benefits over allografts and autografts for the treatment of bone deficits. However, the use of natural materials as tissue engineering scaffolds is encouraged due to their excellent biocompatibility, biodegradability and comparatively lower cost. Numerous in depth studies have been performed for biomaterials as a substitute to allografts and autografts in treating the bone defects and nonunions [Amini *et al*., 2012; Motamedian *et al*., 2015].

With regard to BNC as a scaffold for bone tissue engineering, Grande *et al.* (2009) prepared BNC-HA (bacterial nanocellulose-hydroxyapatite) composites and got admirable results in terms of bone regeneration. Further, Saska *et al*. (2011) prepared BNC-HA nanocomposites and evaluated their biological properties and performance with respect to bone regeneration in defects of rat tibiae. The results showed that BNC-HA membranes were effective for bone regeneration and accelerated new bone formation. Lee *et al*. (2013) performed *in vivo* studies by implanting silk fibroin-BNC membranes to successfully promote the complete healing of segmental defects of zygomatic arch of rats. Further, Pigossi *et al.* (2015) analyzed the potential of BNC-HA composites associated with osteogenic growth peptide (OGP) for bone regeneration in critical-size calvarial defects in mice. The implanted specimens were analyzed at different time points by descriptive histology, gene expression of bone biomarkers and micro-computed tomography (μCT); and showed a high percentage of bone formation after 60 and 90 days. Recently, Huang *et al*. (2017) had fabricated porous BNC scaffold, and modified it by combining with gelatin *via* different crosslinking techniques and coating hydroxyapatite. *In vivo* studies in nude mice and rabbit showed new bone formation after 12 weeks of implantation at the edge of the implant which got penetrated into the center of the scaffolds, depicting the potential of scaffolds as orthopedic implant for bone deficiencies.

CHAPTER 3

Isolation of cellulose producing bacterial strains and reprogramming of culture parameters for enhanced cellulose production

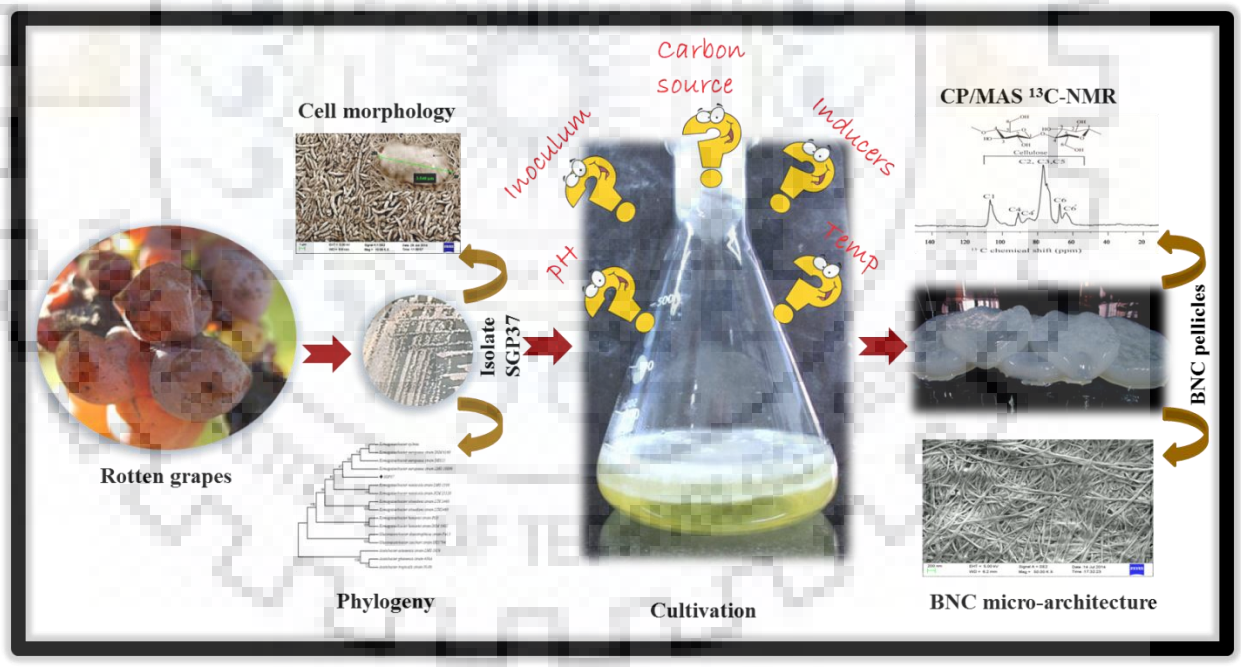

Isolation of cellulose producing bacterial strains and reprogramming of culture parameters for enhanced cellulose production

3.1 INTRODUCTION

Bacterial nanocellulose (BNC), a blooming polymer of today's era has primed a great deal of attention worldwide due to its unique properties. It is identical in chemical composition to plant cellulose, however, its physico-structural features such as ultra-fine nanofibrous network [Cacicedo *et al*., 2016], mechanical strength [Cacicedo *et al*., 2016; Jozala *et al*., 2016], ability to be molded in any shape [Zang *et al*., 2015], and extra purity (i.e. devoid of pectin, lignin, hemicellulose and other metabolic products) [Sheykhnazari *et al*., 2011; Jozala *et al*., 2016]; bestow BNC with plenteous advantages over plant cellulose and make it a potential precursor for breakthrough technologies in several vital arenas leading to cutting edge products like optoelectronic materials, acoustic membranes, ultrafiltration membranes, supercapacitors, fuel cell, polymer matrices reinforcement, cosmetics, wound dressing materials, surgical implants, tissue engineering scaffolds, drug delivery systems and other biomedical devices [Dubey *et al*., 2015; Cacicedo *et al*., 2016; Jozala *et al*., 2016; Wang *et al*., 2016]. Despite its multidimensional applicability, the widespread usage of this promising polymer hinge on the practical considerations such as the scale-up capability and production costs [Kiziltas *et al*., 2015], as if comparing with other popular commercial organic products, BNC is still expensive, therefore, its use is limited [Sheykhnazari *et al*., 2011; Mohammadkazemi *et al*., 2015]. The low conversion yield of BNC, in terms of high input of raw materials, is a major economic constraint to the commercialization of BNC at a "low" cost. In addition, there are very few microorganisms proficient in producing BNC up to an extent where its industrial use is possible. Bacteria belonging to the genera *Agrobacterium*, *Aerobacter*, *Acetobacter* (now reclassified as *Komagataeibacter*), *Achromobacter*, *Azotobacter*, *Pseudomonas*, *Rhizobium*, *Sarcina* are reported to synthesize nanocellulose [Dubey *et al*., 2015; Jozala *et al*., 2016]. However, only a few bacteria of the genus *Komagataeibacter* (preferably *Komagataeibacter xylinus*: the most referenced and used strain worldwide) were found to produce significant amount of BNC [Cacicedo *et al*., 2016; Jozala *et al*., 2016]. Since, BNC synthesis has been strictly linked to the bacterial cell metabolism; the strain type and the culture conditions have a crucial influence on BNC production, in particular regarding factors such as carbon and nitrogen sources, metabolic stimulants, temperature and pH [Castro *et al*., 2012].

In this context, the present work is undertaken with a view to search for a potential cellulose producing strain and to optimize the metabolic status of the strain towards enhanced cellulose synthesis by ameliorating the physiological dynamics to achieve a high conversion yield of BNC. This may thus enable wider applicability of this value product and open up new avenues to deliver multifarious products to the market at competitive price. Hence, this chapter depicts:

- Isolation and screening of BNC producing strains
- Molecular identification of potent BNC producing strain
- Optimization of metabolic status of the selected strain towards enhanced cellulose synthesis by ameliorating culture parameters
- Kinetic evaluation of BNC production
- Physiochemical characterization of produced BNC

3.2 MATERIALS AND METHODS

3.2.1 Chemicals and reagents

Glucose, galactose, maltose, sucrose, tartaric acid, oxalic acid, disodium hydrogen phosphate, sodium hydroxide, crystalline phenol, sodium potassium tartrate, bacteriological agar, yeast extract and bacteriological peptone were purchased from Himedia Laboratories, India. Dinitrosalicylic acid, gallic acid, xylose, fructose, sodium sulfite and sodium pyruvate were procured from SRL, India. Citric acid and acetic acid were purchased from Loba Chemie and Rankem, respectively. All the chemicals used were of analytical grade or of the highest purity available.

3.2.2 Culture media

Hestrin-Schramm (HS) medium contains (g L^{-1}): glucose, 20; yeast extract, 5; peptone, 5; disodium hydrogen phosphate, 2.7; citric acid, 1.15; pH 6.0 [Hestrin and Schramm, 1954]. 1.5 % agar was added to make HS-agar medium. The pH of the culture medium was adjusted with1 N acetic acid.

3.2.3 Isolation and screening of BNC producing bacterial strains

Samples of various rotten fruits, vegetables and vinegar were collected from local market and other places around Roorkee, India. Those samples with the odor of acetic acid were chosen for the isolation of BNC producing strains. Normal saline extracts of the selected samples were prepared and spread on HS-agar plates at 10^{-4}–10^{-5} dilution. The plates were incubated at 30 °C for 72-96 h; each distinct colony that appeared was isolated and inoculated discretely in HS broth (pH 6.0). The cultures were then incubated at 30 °C under static conditions for 1–2 weeks and observed for pellicle formation at the air-liquid interface. The strains found positive for the pellicle formation, were stored in 50 % glycerol at −80 °C.

3.2.4 Molecular identification of the potent BNC producer

The strain with thick pellicle was picked for molecular identification using 16S rRNA gene sequence analysis. Total genomic DNA was extracted using Insta Gene™ Matrix genomic DNA extraction kit (Bio-Rad, USA) and amplification of 16S rRNA gene was carried out using 27F and

1492R universal primers (Table 3.1) in PTC-225 peltier thermal cycler (MJ Research, USA) with 1 cycle of 94 °C for 3 min followed by 35 cycles of denaturation (at 94 °C for 45 sec), annealing (at 55 °C for 60 sec) and extension (at 72 °C for 60 sec), and a final extension of 72 °C for 10 min. The amplified product was purified using Montage PCR clean up kit (Millipore) and sequenced using BigDye® Terminator Cycle Sequencing kit (Applied BioSystems, USA) using 518F and 800R primers (Table 3.1) and resolved on Applied Biosystems 3730XL automated DNA sequencing system (Applied BioSystems, USA).

The sequence obtained was searched for the similarity in Genbank against 16S rRNA database via BLAST algorithm (http://www.ncbi.nlm.nih.gov/BLAST). The data generated was further processed by multi aligning the sequences using Clustal W and a phylogenetic tree was constructed using the Neighbor-Joining method by MEGA6 [Tamura *et al*., 2013].

Table 3.1 Primers used for 16S rDNA amplification and sequencing

Primers	Sequence (5′ to 3′)
27F	AGAGTTTGATCMTGGCTCAG
1492R	TACGGYTACCTTGTTACGACTT
518F	CCAGCAGCCGCGGTAATACG
800R	TACCAGGGTATCTAATCC

3.2.5 Morphological analysis of the selected BNC producer

The morphological analysis of the selected bacterial strain was carried out by field-emission scanning electron microscope (Carl Zeiss, Ultra plus, Germany), operating at an accelerated voltage of 5 kV. Samples were prepared by spreading a loopful of culture broth on a glass coverslip followed by air drying, which were then subjected for gold coating in a Denton gold sputter unit for 60 s before being mounted in the FE-SEM and the electron micrographs were captured at desired magnifications.

3.2.6 Validation of BNC via FTIR and solid state CP/MAS ^{13}C-NMR

The produced pellicle from the selected strain was purified as mentioned in Section 3.2.7 and validated for the presence of cellulose by FTIR and CP/MAS ^{13}C-NMR.

3.2.6.1 Fourier transform infrared spectroscopy (FTIR)

The purified and dried BNC pellicle was pelleted in KBr and FTIR spectrum was recorded using Thermo Nicolet NEXUS 670 FTIR spectrophotometer in the spectral range of 4000–400 cm^{-1} at the resolution of 4 cm^{-1}.

3.2.6.2 Solid-state cross-polarization/magic angle spinning ^{13}C-nuclear magnetic resonance spectroscopy (CP/MAS ^{13}C-NMR)

Solid-state CP/MAS ^{13}C-NMR spectral acquisition was carried out using Avance III 600 MHz Bruker-BioSpin NMR spectrometer, operating at 150.15 MHz. The experiment was performed at ambient temperature using Bruker 3.2 mm DVT probe. The dried BNC pellicle was ground and packed into a 3.2 mm zircon rotor, which was spun at 10 kHz. The CP contact time and the recycle delay were 1 ms and 3 s, respectively and the spectrum was acquired by accumulating 20 k scans per sample.

3.2.7 Cultivation, harvest and purification of BNC

A suspension culture for pre-inoculum was prepared by transferring a single bacterial colony into 20 mL of HS broth (pH-6), with incubation of 72 h at 30 °C under static conditions. After incubation, 20% v/v of this cell suspension was introduced into 50 mL of HS medium (pH-6) and incubated at 30 °C for 48 h under static conditions. This statically grown culture was then shaken vigorously to release the bacterial cells from BNC pellicle, and 10% v/v of the resulting cell suspension was inoculated into 250 mL Erlenmeyer flasks containing 50 mL of HS medium (pH 6.0) and incubated statically at 30 °C for 16 days. The experiment was carried out in triplicates and a set of flasks was withdrawn at each alternate day to record the (i) BNC production and (ii) residual sugar concentration in the culture medium. These conditions were designated as reference conditions of BNC production to compare it later with optimized conditions.

After incubation, pellicles formed at air-liquid interface were removed, washed thoroughly under running tap water to remove residual medium and other contaminants, and then boiled in 0.5 N NaOH for 1 h to lyse and eliminate bacterial cells, followed by boiling in distilled water (DW) for 30 min. The pellicles were further washed repeatedly with distilled water until its neutralization and whitening, dried at 60 °C to constant weight, and used for further analysis.

3.2.7.1 Valuation of residual sugar

At the end of cultivation, residual sugar in the culture media was quantified using dinitrosalicylic acid (DNS) method [Miller, 1959].

3.2.7.1.1 Preparation of reagents

3.2.7.1.1.1 DNSA reagent

1 g of dinitrosalicylic acid, 200 mg of crystalline phenol and 50 mg of sodium sulfite were dissolved simultaneously in 100 mL of NaOH (1 %) solution by stirring. The solution was kept in dark bottle and stored at 4 °C.

3.2.7.1.1.2 Rochelle salt (40 %)

40 g of sodium potassium tartrate was dissolved in 100 mL of distilled water and the solution was stored at room temperature.

3.2.7.1.2 Sugar assay

1.5 mL of culture media (diluted 100 times) was added with 1.5 mL of DNSA reagent and heated for 15 min in a boiling water bath to develop a red-brown color. After the development of the color, 0.5 mL of Rochelle salt solution (40 %) was added in this reaction mixture to stabilize the color and the tubes were allowed to cool down at RT. The absorbance was recorded at 575 nm using CARY 100 Bio UV–Vis spectrophotometer (Agilent technologies, USA) and the concentration of residual sugar was calculated using the standard curve generated by serial dilutions of glucose (for reference conditions) and fructose (for optimized conditions).

3.2.8 Reprogramming of culture parameters for enhanced BNC production

To boost up the metabolic status of the strain towards enhanced BNC synthesis, various physiological and nutritional parameters were optimized by changing one variable at a time from the reference run [Hyun *et al*., 2014]. The parameters explored were carbon sources (glucose, galactose, maltose, fructose, sucrose and xylose), modulators/additives (sodium pyruvate, ethanol,

n-propanol, isoamyl alcohol, gallic acid, tartaric acid and oxalic acid), inoculum density (1-10 %), culture medium pH (2-8) and cultivation temperature (20-40 °C).

3.2.9 Kinetic studies

After purification and drying, BNC was quantified gravimetrically and determined as g L^{-1} (dry weight (g) of BNC/ volume (L) of culture media). The residual sugar concentration of the culture medium determined using DNS method, was calculated as g (sugar) L^{-1} of culture media and BNC production rate (1), sugar consumption rate (2) and sugar to BNC conversion yield (3) were calculated as follows:

$$\text{BNC production rate (g L}^{-1}\text{ d}^{-1}) = \frac{Yield\ of\ BNC\left(\frac{g}{L}\right)\ at\ time\ t_n\ -\ Yield\ of\ BNC\left(\frac{g}{L}\right)\ at\ time\ t_0}{time\ t_n\ (d)} \quad (1)$$

$$\text{Sugar consumption rate (g L}^{-1}\text{ d}^{-1}) = \frac{Sugar\left(\frac{g}{L}\right)\ at\ time\ t_0\ -\ Sugar\left(\frac{g}{L}\right)\ at\ time\ t_n}{time\ t_n\ (d)} \quad (2)$$

$$\text{Sugar to BNC conversion yield (g/g)} = \frac{BNC\ (g)\ at\ t_{end}}{Sugar\ (g) at\ t_0\ -\ Sugar\ (g)\ at\ t_{end}} \quad (3)$$

where, t_0 is the starting time of cultivation (*i.e* Day 0), t_{end} represents the time at the end of the cultivation (*i.e* Day 16) and t_n signifies the harvesting time at particular day (*i.e* Day 2, 4, 6… 16).

3.2.10 Physicochemical characterization

BNC produced under reference and derived conditions were characterized in terms of its physicochemical properties by FE-SEM, XRD and TGA.

3.2.10.1 Field emission scanning electron microscopy (FE-SEM)

The micro-architecture of BNC pellicles were observed by FE-SEM (Carl Zeiss, Ultra plus, Germany), operating at an accelerated voltage of 5 kV. The dried pellicles were gold coated

for 90 s at the coating current of 31 mA in a Denton gold sputter unit (Biotech SC005, Switzerland) before being mounted in the FE-SEM and the micrographs were acquired at 50 k X.

3.2.10.2 X-ray diffraction (XRD)

XRD pattern of the BNC produced under reference and derived conditions was recorded with Bruker AXS D8 Advance powder X-ray diffractometer using Ni-filtered Cu-Kα radiation (λ = 1.54 Å) from 10-40° 2θ range at 2° min^{-1} scan rate. The crystallinity index of BNC was calculated using Segal method [Segal *et al*., 1959], as depicted in equation (4):

$$\text{Crystallinity Index (CrI)} = \frac{I_{200} - I_{AM}}{I_{200}} \qquad (4)$$

where, I_{200} corresponds to the maximum intensity of the lattice diffraction (200 peak) and I_{AM} is the minimum intensity between (110) and (200) peaks.

Further, allomorphic category of the produced BNC (I_α or I_β form) was also determined on the basis of Z discriminant function, developed by Wada *et al*. (2001), as given follows:

$$Z = 1693 \times d1 - 902 \times d2 - 549 \qquad (5)$$

where, d1 is the d-spacing of $(1\bar{1}0)$ peak and d2 is the d-spacing of (110) peak. $Z < 0$ indicates that cellulose is rich in I_β form while $Z > 0$ suggests that I_α is the predominant form.

3.2.10.3 Thermogravimetric analysis (TGA)

Thermogravimetric and derivative thermogravimetric (TG-DTG) analysis of the dried BNC pellicles were carried out on Thermogravimetric/Differential Thermal Analyzer (EXSTAR TG/DTA 6300, Hitachi, Tokyo, Japan) over a temperature range of 25–600 °C, at the scan rate of 10 °C min^{-1} (mass 10.5 mg) under a nitrogen atmosphere with N_2 flow rate of 200 mL min^{-1}.

3.3 RESULTS AND DISCUSSION

3.3.1 Isolation and screening of BNC producing bacterial strains

A total of 46 bacterial strains were isolated from different natural sources based on their colony size, shape and morphology (Table 3.2; Fig. 3.1). Amongst these, 4 bacterial isolates were found positive for the pellicle formation at the air-liquid interface of the culture medium when inoculated in HS medium and incubated statically for 1 week at 30 °C. All of these strains were isolated from black rotten grapes (*Vitis vinifera*) and no pellicle formation was observed in the isolates obtained from other sources. Out of these 4 strains, isolate SGP37 was competent to produce notable amounts of BNC (Table 3.3), hence selected as the most potent BNC producer for further studies.

Table 3.2 Isolation and screening of BNC producing bacterial strains from various natural sources

S. No.	Source	Total strains	No. of positive strains
1.	Rotten apple	12	None
2.	Rotten grapes	10	04
3.	Rotten orange	06	None
4.	Decomposed papaya	06	None
5.	Rotten tomato	04	None
6.	Decomposed jackfruit	04	None
7.	Decomposed guava	02	None
8.	Decomposed onion	02	None
9.	Crude vinegar	00	None

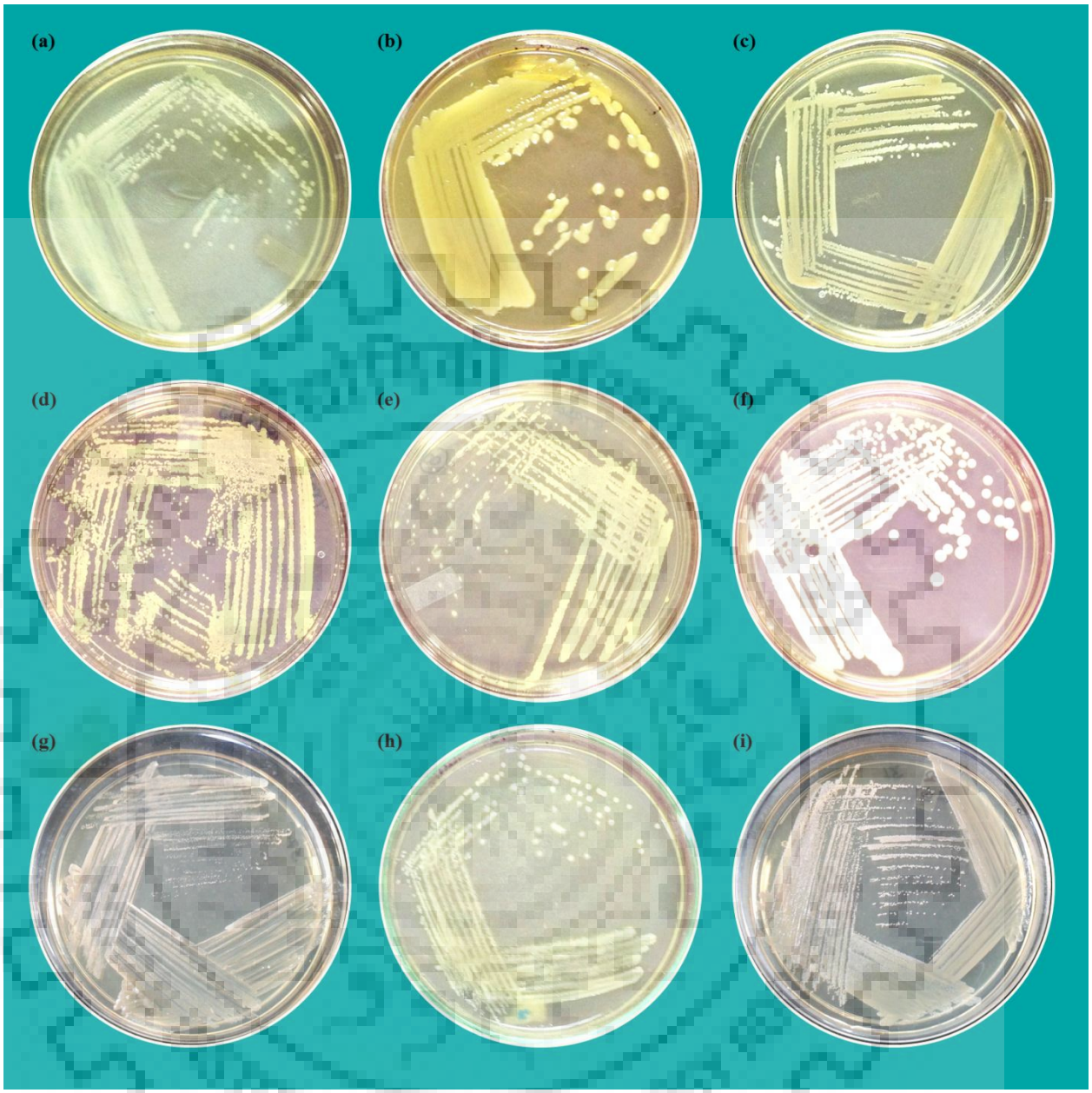

Fig. 3.1 Pure cultures of some of the isolated bacterial strains (a) SAP3 (b) SJK39 (c) SAP9 (d) SGP31 (e) SGP32 (f) SOR15 (g) SGP33 (h) STM24 (i) SGP37 (SAP: isolate from apple; SJK: isolate from jackfruit; SGP: isolate from grapes; SOR: isolate from orange; STM: isolate from tomato)

Table 3.3 Quantitative screening of BNC producing bacterial strains[a]

S. No.	Bacterial isolate	BNC yield (g L^{-1})
1.	SGP31	1.8
2.	SGP32	4.02
3.	SGP33	5.02
4.	SGP37	5.61

[a]Production of BNC in HS medium after 16 days of incubation at 30 °C

3.3.2 Molecular identification and taxonomic hierarchy of selected BNC producer

Amplification and sequencing of 16S rRNA gene of the isolate SGP37 bring in a gene sequence of ~ 1493 bp which was scrutinized for similarity search by BLAST-n against 16S rRNA database (bacteria and archaea) and indicated the isolate to be a strain of *Komagataeibacter europaeus* (formerly *Gluconacetobacter europaeus*). The sequence for the same has been deposited in the GenBank under the accession number KJ101597 and shown in the Dataset 1 as following:

Dataset 1: Nucleotide sequence of 16S rDNA of the bacterial isolate *Komagataeibacter europaeus* SGP37

```
>KJ101597.1 Komagataeibacter europaeus strain SGP37 16S ribosomal RNA gene,
partial sequence
GAAAAAGTTCCTTCGTTAGAGTTTTCGTTCTGGCTCAGAGCGAACGCTGGCGGCATGCTTAACACATGCAAGTCGCA
CGAACCTTTCGGGGTTAGTGGCGGACGGGTGAGTAACGCGTAGGGATCTGTCCATGGGTGGGGGATAACTTTGGGAA
ACTGAAGCTAATACCGCATGACACCTGAGGGTCAAAGGCGCAAGTCGCCTGTGGAGGAACCTGCGTTCGATTAGCTA
GTTGGTGGGGTAAAGGCCTACCAAGGCGATGATCGATAGCTGGTCTGAGAGGATGATCAGCCACACTGGGACTGAGA
CACGGCCCAGACTCCTACGGGAGGCAGCAGTGGGGAATATTGGACAATGGGCGCAAGCCTGATCCAGCAATGCCGCG
TGTGTGAAGAAGGTTTTCGGATTGTAAAGCACTTTCAGCGGGGACGATGATGACGGTACCCGCAGAAGAAGCCCCGG
CTAACTTCGTGCCAGCAGCCGCGGTAATACGAAGGGGGCAAGCGTTGCTCGGAATGACTGGGCGTAAAGGGCGCGTA
GGCGGTTGACACAGTCAGATGTGAAATTCCTGGGCTTAACCTAGGGGGCTGCCTTTGATACGTGGCGACTAGAGTGT
GAGAGAGGGTTGTGGAATTCCCAGTGTAGAGGTGAAATTCGTAGATATTGGGAAGAACACCGGTGGCGAAGGCGGCA
ACCTGGCTCATGACTGACGCTGAGGCGCGAAAGCGTGGGGAGCAAACAGGATTAGATACCCTGGTAGTCCACGCTGT
AAACGATGTGTGCTGGATGTTGGGTGACTTTGTCATTCAGTGTCGTAGTTAACGCGATAAGCACACCGCCTGGGGAG
TACGGCCGCAAGGTTGAAACTCAAAGGAATTGACGGGGGCCCGCACAAGCGGTGGAGCATGTGGTTTAATTCGAAGC
AACGCGCAGAACCTTACCAGGGCTTGACATGCGGAGGCCGTGTCCAGAGATGGGCATTTCTCGCAAGAGACCTCCAG
CACAGGTGCTGCATGGCTGTCGTCAGCTCGTGTCGTGAGATGTTGGGTTAAGTCCCGCAACGAGCGCAACCCTCGCC
TTTAGTTGCCAGCACGTCTGGGTGGGCACTCTAAAGGAACTGCCGGTGACAAGCCGGAGGAAGGTGGGGATGACGTC
AAGTCCTCATGGCCCTTATGTCCTGGGCTACACACGTGCTACAATGGCGGTGACAGTGGGAAGCCAGGTAGCGATAC
CGAGCCGATCTCAAAAAGCCGTCTCAGTTCGGATTGCACTCTGCAACTCGAGTGCATGAAGGTGGAATCGCTAGTAA
TCGCGGATCAGCATGCCGCGGTGGAATACCGGTTCCCGGGCCTTGTACACACCCGCCCGTCACACCATGGGGAGTTG
GTTTGACCTTAAGCCGGTGAGCGAACCGCAAGGACGCAGCCGACCACGGTCGGGTCAGCGACTGGGGTGAATCTAAG
AGGGGAACCACCCATAAAAGGGGGGCTTGG
```

Further, to analyze the evolutionary relationships of the isolate SGP37, a phylogenetic tree was constructed using some top hits obtained in contrary to 16S rRNA gene sequence of strain SGP37 after executing BLAST-n against 16S rRNA database, and found that the strain SGP37 had the closest relationship with *Komagataeibacter europaeus* strain LMG 18890 (Fig. 3.2) with 16S rRNA gene sequence homology of 99%.

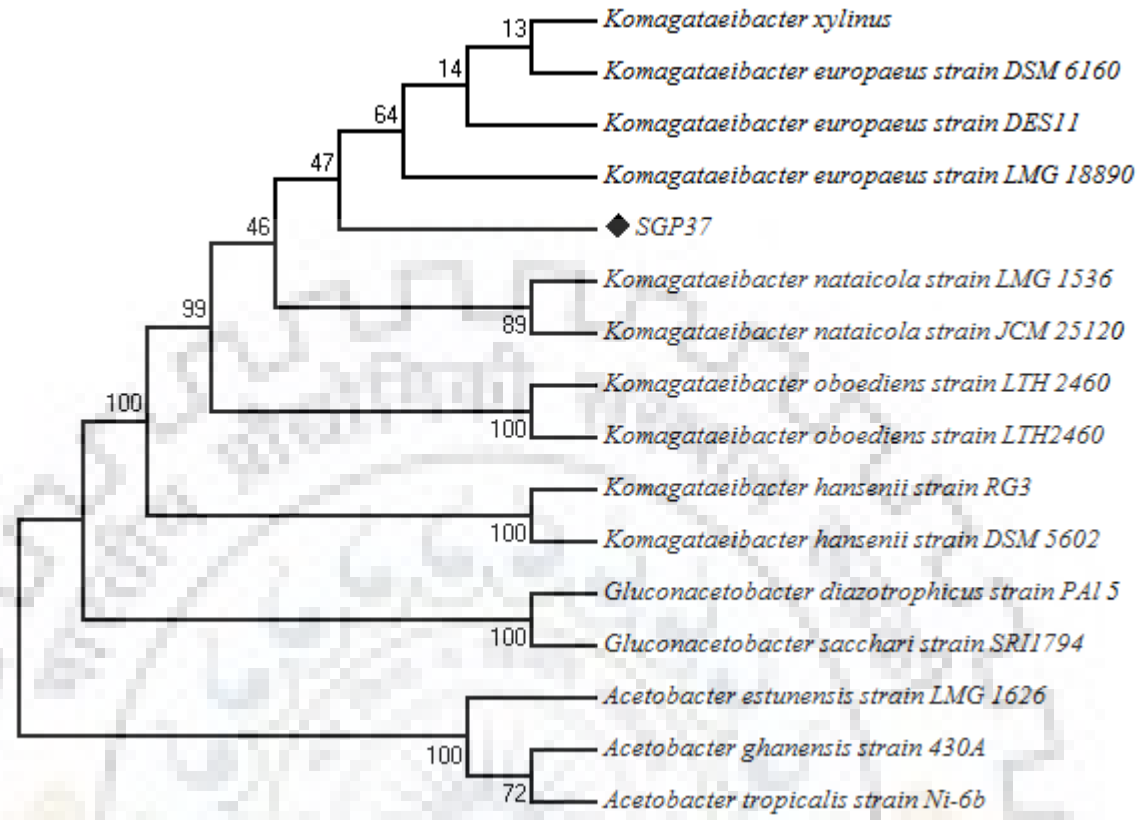

Fig. 3.2 Phylogenetic tree of the bacterial isolate SGP37 inferred by the Neighbor-Joining method using 16S rDNA sequence of the isolate and their close relatives retrieved from GenBank. The numerical values indicate the bootstrap percentiles from 1000 replicates.

3.3.3 Morphological characteristics of *Komagataeibacter europaeus* SGP37

The morphological features of *Komagataeibacter europaeus* SGP37 are shown in Fig. 3.3. The colonies were creamy white, round with upraised center and irregular edges, and sheltered with a translucent BNC layer (Fig. 3.3a). Field-emission scanning electron microscopy had demonstrated that the cells of *K. europaeus* SGP37 were rod-shaped, straight or slightly ellipsed, single or in pairs, with the size about 0.63–0.89×1.8–3.6 μm (Fig. 3.3b).

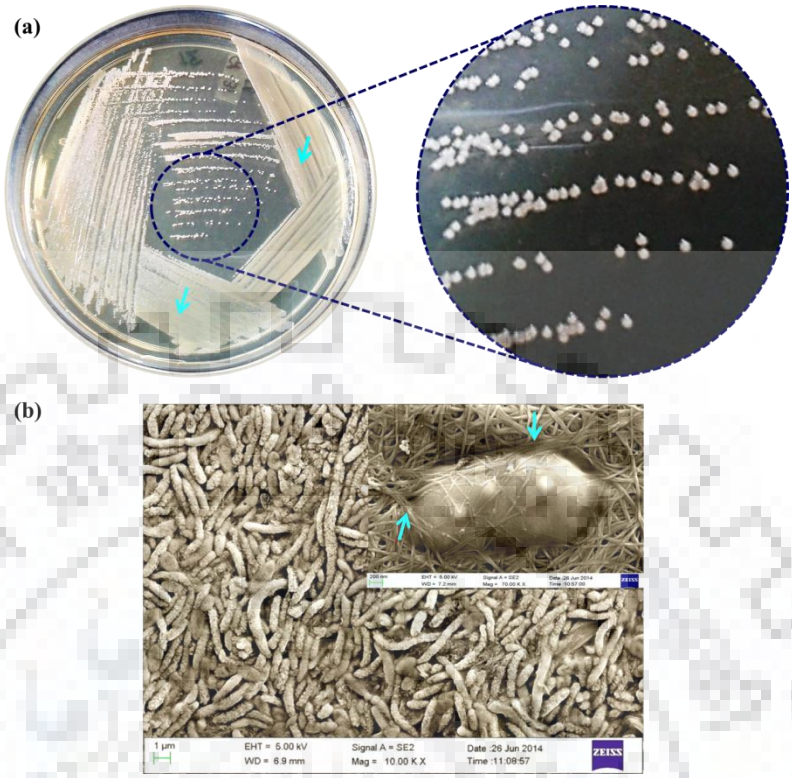

Fig. 3.3 (a) Colonial morphology of *K. europaeus* SGP37 grown on HS-agar; arrows indicating the sheath of cellulose produced by bacterial cells (b) Morphological aspects of the strain *K. europaeus* SGP37 under scanning electron microscope; inset shows a single bacterial cell (70 k X) and arrows indicate the cellulose nanofibers protruding from the bacterium.

3.3.4 Validation of pellicle produced by *K. europaeus* SGP37 for the presence of cellulose

3.3.4.1 FTIR

Prevenient analysis of the pellicle by means of FTIR had shown a broad and dominating signal shouldering around 3400-3500 cm^{-1}, depicting the stretching of -OH groups [Oh *et al*., 2005]. The peak at 2907.83 cm^{-1} represents C-H stretching [Oh *et al*., 2005], 1640.98 cm^{-1} shows O-H bending of adsorbed water [Lojewska *et al*., 2005; Yassine et al., 2016], 1421.42 cm^{-1} signalizes C-H_2 symmetric bending [Colom and Carrillo, 2002], 1375.26 cm^{-1} denotes C-H bending [Colom and Carrillo, 2002; Oh *et al*., 2005] and 1321.34 cm^{-1} indicates C-H_2 wagging [Colom and Carrillo, 2002; Oh *et al*., 2005]. The other peaks appeared at 1165.33 cm^{-1}, 1112.35 cm^{-1}, 1061.73 cm^{-1} and 897.47 cm^{-1} signifies C-O-C asymmetric bridge stretching, C-C ring stretching of cellulose, C-O-C pyranose ring skeletal vibration and C-O-C symmetric stretching in plane, respectively [Colom and Carrillo, 2002; Oh *et al*., 2005; Movasaghi *et al*., 2008; Shao *et al*., 2015]. The peaks thus obtained (Fig. 3.4) indicated the pellicle to be a pure form of cellulose;

however the results were further validated by solid state CP/MAS ^{13}C-NMR for absolute confirmation.

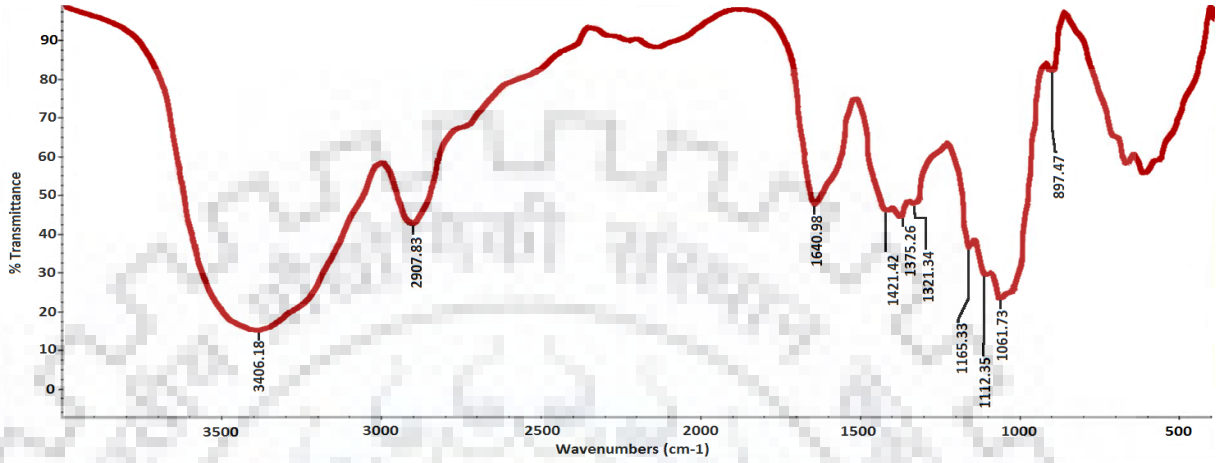

Fig. 3.4 FTIR spectrum of the pellicle produced by *K. europaeus* SGP37 in HS medium at 30 °C under static cultivation

3.3.4.2 Solid state CP/MAS ^{13}C-NMR

Solid state CP/MAS ^{13}C-NMR was used to further corroborate the result obtained with FTIR and specified the similar resonance profile as reported previously by different researchers, comprising of six characteristic peaks corresponding to six carbon atoms of glucopyranose repeating units of cellulose [Atalla and Vanderhart, 1984; Park *et al*., 2010]. As shown in Fig. 3.5, the resonance peaks with chemical shifts at 105.84, 89.63/84.01 and 65.88/62.34 ppm are assigned to the C1, C4/C4' and C6/C6' carbons respectively, and the cluster of resonance peaks observed in the region of 76-72 ppm is attributed to C2, C3, and C5 carbon atoms of hexose-ring. Further, the regions of the spectrum corresponding to C4 and C6 include a constellation of sharper resonance and a broader upfield wing *i.e.* C4/C4' and C6/C6'. The downfield peaks, C4 and C6, are unambiguously assigned to the crystalline phase while the upfield broader peaks C4' and C6' are associated with the less ordered domains of BNC [Park et al., 2010]. The result obtained, thus confirms that the pellicle produced by *K. europaeus* SGP37 is a pure form of cellulose.

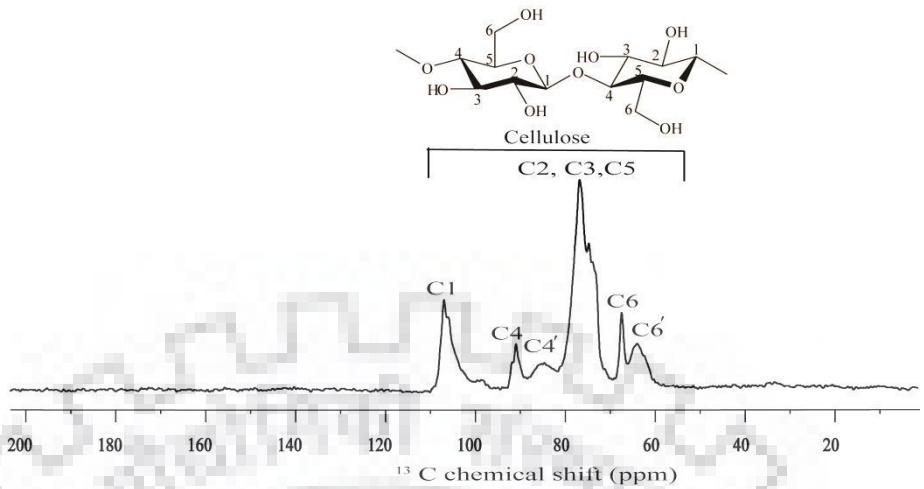

Fig. 3.5 Solid-state CP/MAS ^{13}C-NMR spectrum of the pellicle produced by *K. europaeus* SGP37 in HS medium at 30 °C under static cultivation

3.3.5 BNC production

When inoculated in HS medium containing glucose as a carbon source (pH-6) and incubated at 30°C under static conditions, the strain *K. europaeus* SGP37 led into the formation of a translucent layer at the surface of the culture medium after 24 h which continued to grow during the time and attained 3.58 ± 0.79 g L^{-1} BNC after 8 days of cultivation (Fig. 3.9 a). This yield was much higher (~2.9-3.8 fold) than obtained with *Gluconacetobacter xylinus* at similar physiological parameters [Huang *et al*., 2015c; Kuo *et al*., 2016].

3.3.5.1 Reprogramming of physiological conditions to direct metabolic flux towards enhanced BNC synthesis

The metabolic status of the strain needs to be optimized to direct as much flux as possible towards cellulose synthesis, which can be ameliorated by diverting flux from branch pathways or slackening the secretion of byproducts [Lee and Kim, 2015]. Therefore, suitable physiological parameters were defined to direct the flux towards enhanced BNC production by *K. europaeus* SGP37 as depicted in Fig. 3.6.

3.3.5.1.1 Carbon source

Carbon is the most vital component of the culture medium, as it acts as an energy source for the growth of the microorganism as well as in the production of primary and secondary metabolites. The rate at which the carbon source is metabolized can often influence the formation

of biomass and/or the production of primary or secondary metabolites. Thus, optimization of carbon source is an essential step for metabolite production prior starting with any semi-pilot/pilot production plans [Singh *et al*., 2017].

Delving into Fig. 3.6a propounded that highest BNC production (6.49 ± 0.49 g L^{-1}) was achieved in the medium containing fructose which was quite higher than produced in the reference HS medium containing glucose (5.61 ± 0.11 g L^{-1}), after 16 days of cultivation under static conditions. Sucrose was found to yield 4.01 ± 0.92 g L^{-1} of BNC while incompetent BNC production (1.4-1.9 g L^{-1}) was observed in the maltose, galactose and xylose medium. The low production of BNC in reference medium can be related to the synthesis of gluconic acid as shown in Fig. 3.7, which lowers the availability of glucose pool on the way to cellulose synthesis while fructose forms UDP-glucose (precursor molecule of cellulose synthesis) without channeling into gluconic acid [Ross *et al*., 1991]. Comparatively, low production obtained in the sucrose medium, may be because it has to be hydrolyzed to glucose and fructose in the periplasm due to impermeability of sucrose via cell membrane [Velasco-Bedran and Lopez-Isunza, 2007]. BNC production with maltose, galactose and xylose medium was always very weak, about 0.1 g L^{-1} after 8 days of incubation, as reported by Castro *et al*. (2012), and the formation of BNC from these carbon sources is possibly due to the other components of HS medium. Hence, fructose was found to be the suitable carbon source for BNC production by *K. europaeus* SGP37.

3.3.5.1.2 Inducers/modulators

Further, as shown in Fig. 3.6b, a significant rise in BNC production was observed in presence of ethanol (1.36 fold) and sodium pyruvate (1.2 fold) with the yield of 7.66 ± 0.20 and 6.76 ± 0.26 g L^{-1} respectively, while the production got downturned by 1.8 and 6.38 fold in the media subsuming n-propanol and isoamyl alcohol congruently. Further, very low amount of BNC was produced with gallic acid (0.86 ± 0.12 g L^{-1}) and tartaric acid (0.58 ± 0.27 g L^{-1}) while no production was seen when oxalic acid was added into the medium (Fig. 3.6b). The phenomenon behind enhanced production of BNC in presence of ethanol can be explicated by the context of ethanol serving as an additional energy source, directing glucose to be used only for cellulose synthesis [Velasco-Bedran and Lopez-Isunza, 2007; Li *et al*., 2012]. Additionally, the increased level of ATP generated by ethanol supplementation inhibits glucose-6-phosphate dehydrogenase, and raises glucose-6-phosphate flux towards BNC biosynthesis [Li *et al*., 2012] (Fig. 3.7). Further, pyruvate provides the flux for TCA cycle as shown in Fig. 3.7, and curtails glucose for energy

production, thus obliquely boosts BNC synthesis [Li *et al*., 2012]. Further, unlike ethanol, BNC production got diminished in presence of n-propanol and isoamyl alcohol. The underlying mechanism for this may take account of variation in the carbon chain length, as exposure to higher alcohols adversely affects the plasma membrane fluidity as well as causes protein denaturation, leading to meager fermentation [Eckert and Trinh, 2016].

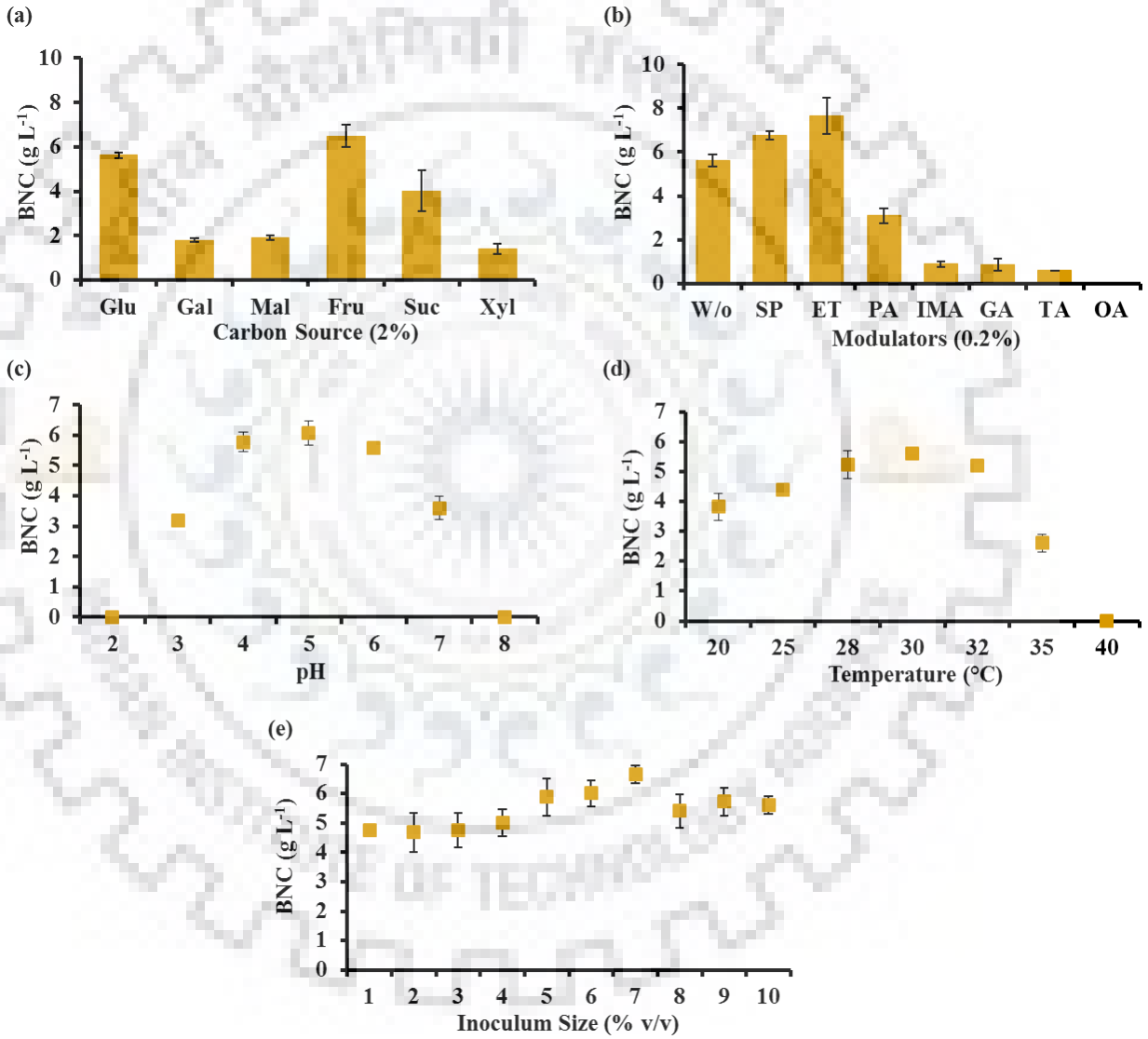

Fig. 3.6 Derivation of preeminent physiological parameters for enhanced BNC production by *K. europaeus* SGP37 using one variable at a time approach: BNC production as a function of (a) carbon sources (Glu; glucose, Gal; galactose, Mal; maltose, Fru; fructose, Suc; sucrose, Xyl; xylose), (b) modulators (W/o; without modulator, SP; sodium pyruvate, ET; ethanol, PA; n-propanol, IMA; isoamyl alcohol, GA; gallic acid, TA; tartaric acid, OA; oxalic acid), (c) pH, (d) temperature and (e) inoculum density. (All the experiments were carried out in triplicates and data are represented as Mean ± SD)

3.3.5.1.3 Culture medium pH

It has been reported that the optimal pH for BNC production varies in consonance with bacterial strain but usually been imputed within a neutral to slightly acidic pH spectrum [Castro *et al*., 2012]. A set of experiments were performed to ascertain if similar conditions favor BNC production in the current system. As shown in Fig. 3.6c, no production was marked at the lower end of examined pH range, however, the production process got consecutively upturned with further increase in the pH and maximum production (6.07 ± 0.40 g L^{-1}) was acquired at pH 5. Further increasing the pH led into the diminution in BNC yield (3.59 ± 0.38 g L^{-1} at pH 7) and a sharp fall in the production was observed after pH 7.

3.3.5.1.4 Cultivation temperature

Fig. 3.6d shows the amount of BNC produced as a function of temperature and maximum BNC production was monitored at 30 °C. The strain was also able to produce significant amount of BNC at the lower end of temperature, however, a substantial recession in the production (2.16 fold) was espied at 35 °C and further increasing the temperature to 40 °C led into the complete arrest of BNC production.

3.3.5.1.5 Inoculum density

Furthermore, the direction of initial carbon flux is also inclined by bacterial count (inoculum density) as more flux would be consumed towards energy production if cell density is too high. If the size of inoculum is too small, incommensurable bacterial count would then lead to a reduced amount of BNC synthesis. Consequently, influence of different inoculum sizes of the strain SGP37 ranging from 1% to 10% (v/v) was examined for BNC production. As the inoculum level was dwindled from 10% (control) to 7%, BNC production was found to increase from 5.61 ± 0.11 to 6.64 ± 0.31 g L^{-1} (Fig. 3.6e). A gradual decline in the production level was observed as the inoculum density was further reduced and 4.76 ± 0.05 g L^{-1} of BNC was produced at 1% inoculum size.

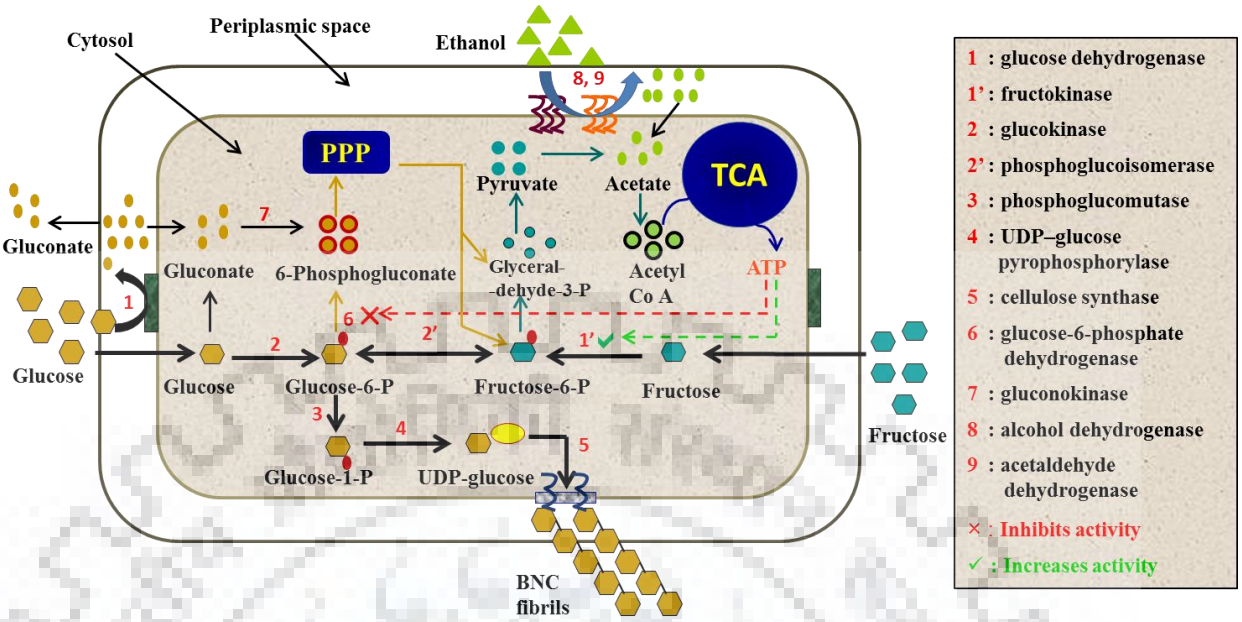

Fig. 3.7 Schematic of metabolic network for BNC synthesis (PPP: Pentose phosphate pathway; TCA: Tricarboxylic acid cycle) [Dubey *et al*., 2017].

As a result, the preeminent parameters derived above by one factor at a time were as follows: pH, 5.0; temperature, 30 °C; inoculum density, 7% (v/v) with medium composition fructose, 2% (w/v); peptone, 0.5% (w/v); yeast extract, 0.5% (w/v), citric acid, 0.115% (w/v); Na_2HPO_4, 0.27% (w/v); ethanol, 0.2% (v/v). Fig. 3.8 shows the BNC pellicles obtained after static cultivation of the strain *K. europaeus* SGP37 for 8 days under reference and derived physiological parameters. As can be appraised, the BNC pellicle produced in developed conditions was much thicker and weighed about 6.71 ± 1.15 g L^{-1} (dry weight) which was almost two fold of that obtained under reference conditions (3.58 ± 0.79 g L^{-1}).

Fig. 3.8 BNC pellicles produced by *K. europaeus* SGP37 after 8 days of static cultivation under (a) reference and (b) derived conditions. (Reference conditions: HS medium containing glucose as a carbon source with no inducer; pH, 6.0; inoculum density, 10% (v/v) and cultivation temperature, 30 °C; Derived conditions: HS medium containing fructose as a carbon source and 0.2% ethanol as an inducer; pH, 5.0; inoculum density, 7% (v/v) and cultivation temperature, 30 °C)

3.3.5.2 BNC production kinetics

Production kinetics is a most important parameter for any cell factory and/or product to be of value for industrialization. Hence, BNC production kinetics of the strain *K. europaeus* SGP37 was studied under both; reference and derived conditions and depicted in Fig. 3.9.

When the strain was grown in HS medium under standard physiological parameters, the reducing sugar was rapidly consumed from 20 g L^{-1} to 8.98 ± 0.71 g L^{-1} after 4 days of cultivation; and to 6.24 ± 0.35 g L^{-1} after 6 days, but subsequent sugar consumptions were not significant. However, BNC production continued to upsurge during this period and 5.61 ± 0.11 g L^{-1} of BNC was recorded at the expense of 15.45 ± 0.68 g L^{-1} sugar after 16 days of cultivation (Fig. 3.9a). In contrast, as delineated in Fig. 3.9b, the sugar consumption was much slower under developed conditions that about 14.93 ± 1.67 g of sugar still can be detected after 4 days of cultivation and lead into the production of 9.98 ± 0.24 g L^{-1} BNC at the expense of 12.08 ± 1.94 g L^{-1} sugar after 16 days of fermentation. The faster sugar consumption in the reference medium during early stage of the fermentation can be linked to the synthesis of gluconic acid by the membrane-bound enzyme, glucose dehydrogenase (as depicted in Fig. 3.7) while having fructose as a carbon source in the derived medium limits this conversion.

Based on the data obtained from Fig. 3.9a and b, the average sugar consumption and BNC production rates during the period were calculated. As shown in Fig. 3.9c, at day 2 of the cultivation under reference conditions, sugar consumption and BNC production rates were 1.66 ±

0.25 g L^{-1} d^{-1} and 0.95 ± 0.31 g L^{-1} d^{-1} respectively, while at day 4, a sharp rise was observed in the sugar consumption rate (2.75 ± 0.18 g L^{-1} d^{-1}) with the BNC production rate of 0.76 ± 0.21 g L^{-1} d^{-1}. However, under developed conditions, sugar consumption rate (1.93 ± 0.25 g L^{-1} d^{-1}) was slightly higher than the BNC production rate (1.55 ± 0.23 g L^{-1} d^{-1}) at day 2, and unlike reference conditions, sugar consumption (1.26 ± 0.21 g L^{-1} d^{-1}) and BNC production (1.16 ± 0.09 g L^{-1} d^{-1}) rates were almost comparable at day 4 (Fig. 3.9d). This may be due to the presence of ethanol in the developed medium which might have provided the sufficient flux for energy production and directed the fructose to be used for BNC synthesis. Despite of this, the sugar consumption rates were always much higher than the BNC production rates in the reference conditions while a little difference was observed in the consumption and production rates under developed conditions during the period.

So, if calculating the sugar to BNC conversion yield, about 0.82 g BNC/ g sugar was achieved under developed conditions, which was approximately 2.27 fold higher than the yield obtained in the reference conditions (0.36 g BNC/ g sugar) after 16 days of cultivation. A comparison of the BNC yield on consumed sugar with some previous studies [Carreira *et al*., 2011; Wu and Liu, 2012; Zhang *et al*., 2014b; Tsouko *et al*., 2015; Kuo *et al*., 2016;], acquiesced that the strain *K. europaeus* SGP37 has quite strong ability to synthesize cellulose and may offer a promising platform to reduce the production cost of BNC by a great difference.

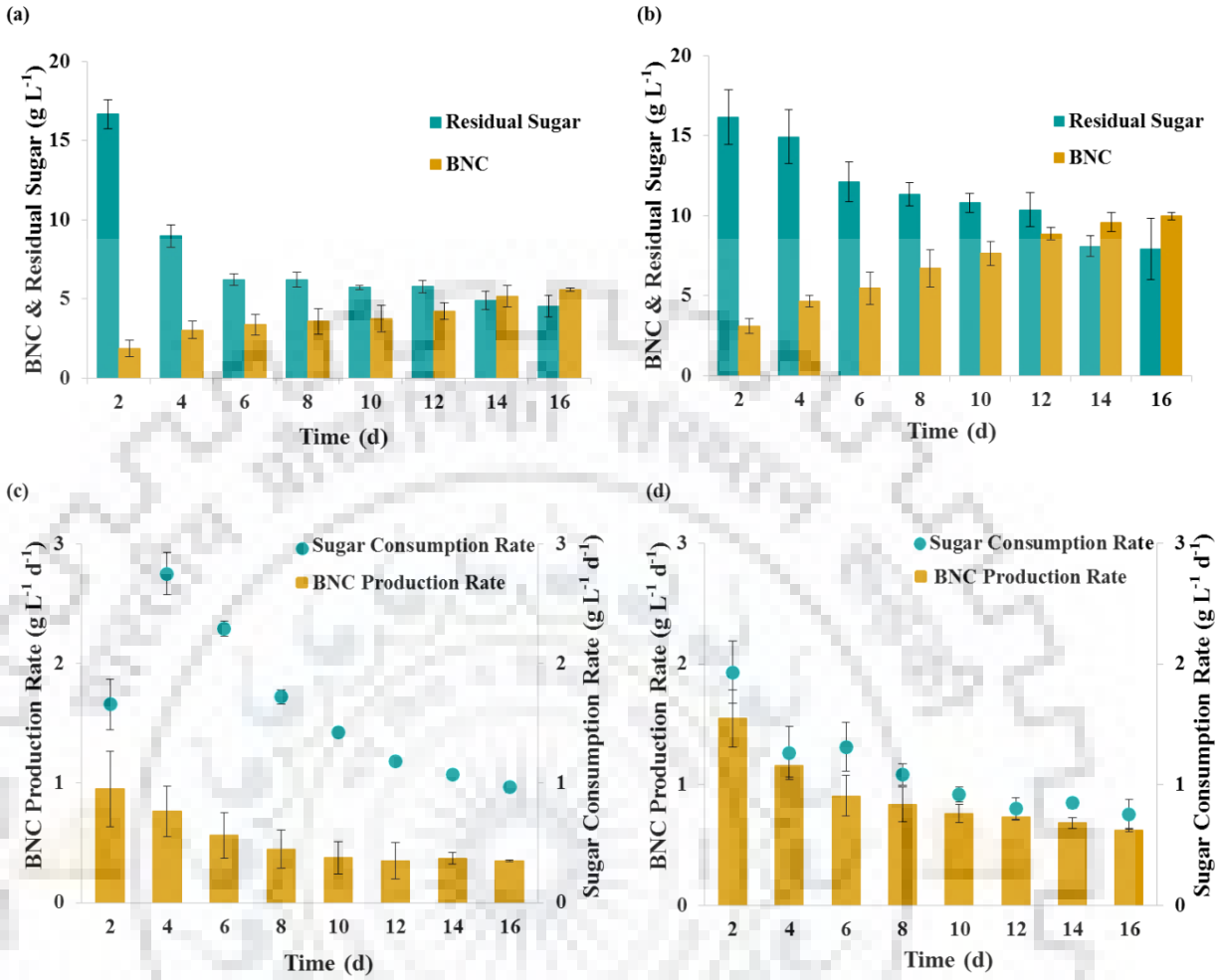

Fig. 3.9 BNC production kinetics: Fig. (a, b) shows the time course of BNC production along with sugar consumption over 16 days under (a) reference and (b) derived conditions; Fig. (c, d) shows the rates of BNC production and sugar consumption over the cultivation period under (c) reference and (d) derived conditions. (Data are the mean of three independent replicates and represented as Mean ± SD)

3.3.6 Physicochemical characterization

After purification and drying, BNC produced under reference and derived conditions were subjected for its evaluation in terms of morphology, crystallinity profile and thermal longanimity by FE-SEM, XRD and TGA, respectively.

3.3.6.1 FE-SEM

During cellulose synthesis, nascent chains of cellulose aggregate to form subfibrils which are then crystallized into microfibrils, these into bundles, and the latter into ribbons, which then accumulated together and form a gelatinous membrane at the surface of the culture medium

[Shezad *et al*., 2010]. The mechanical properties of the BNC sheets are highly dependent on the thickness and arrangement of these fibrils [Ul-Islam *et al*., 2012 and 2013].

Fig. 3.10 illustrates the field emission scanning electron micrographs of the BNC sheets produced under reference and derived conditions. Both samples had shown a densely packed reticulated structure with highly extended and randomly oriented nanoscaled fibers. The gross morphological structure seemed to be similar for both of the specimens. However, the detailed examination of the micrographs revealed profound morphological differences among BNC produced under different conditions in terms of nanofibrils morphology and arrangement. The fibrils of BNC produced under derived conditions were highly extended and almost uniform in size (diameter). In contrast, the fibrils of BNC sheets produced under reference conditions were slightly twisted, varied in size and arranged more randomly (Fig. 3.10 a; enlarged view). These micro morphological changes in the BNC sheets affect the physical properties of BNC including crystallinity, thermal stability, tensile strength etc.; and are attributed to the different cultivation conditions used for its production as the effects of culture conditions (including carbon source, cultivation temperature, culture medium pH, amount of inoculum) and the BNC purification and drying method on the fibrils morphology and arrangement have previously been reported by various groups [Horii *et al*., 1997; Shezad *et al*., 2010; Tang *et al*., 2010; Ul-Islam *et al*., 2013].

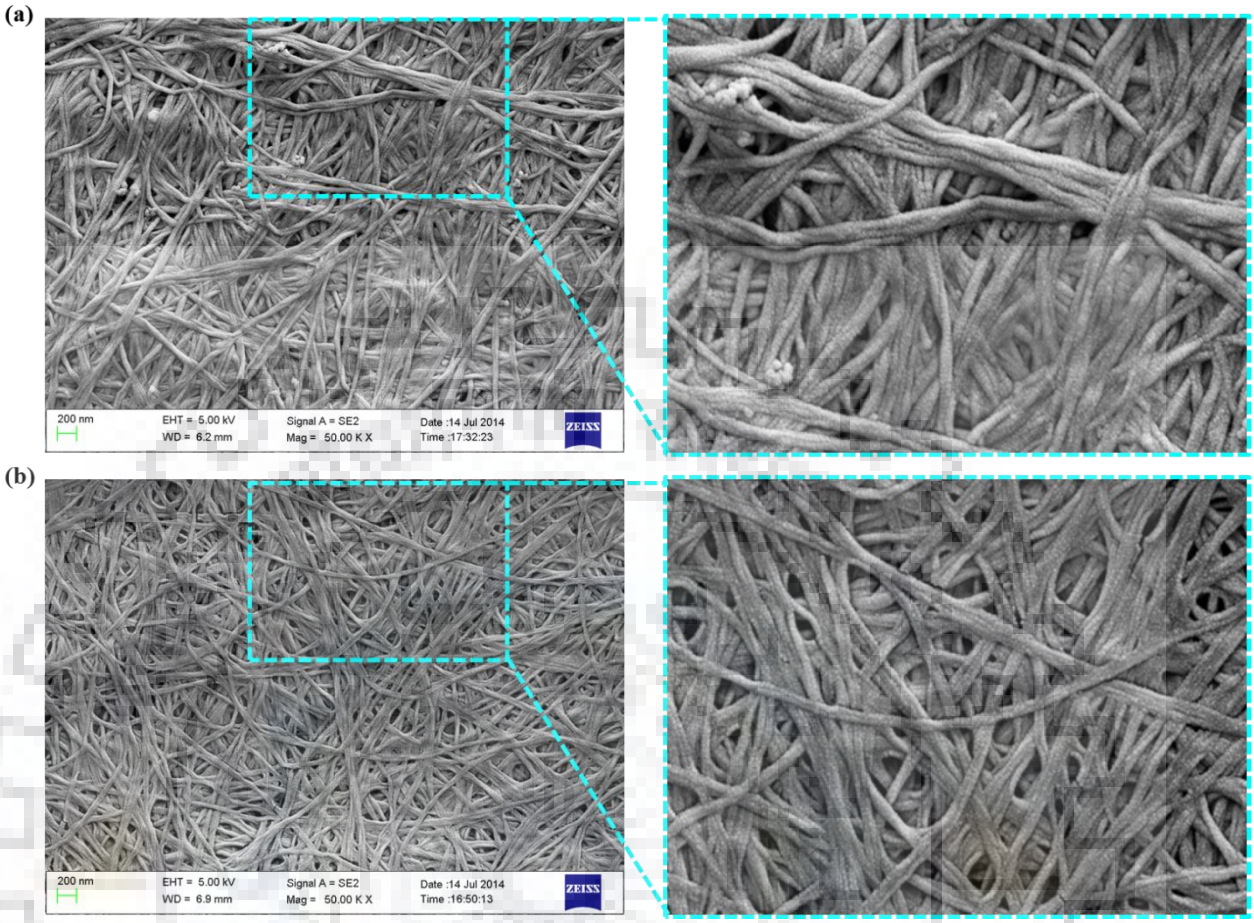

Fig. 3.10 Field-emission scanning electron micrographs illustrating the morphology and arrangement of BNC fibers produced by *K. europaeus* SGP37 under (a) reference and (b) derived conditions

3.3.6.2 XRD

The morphological changes in the ribbons of BNC are related to the changes in the crystallinity of cellulose [Sun *et al*., 2007; Shezad *et al*., 2010]; hence X-ray diffraction profile of BNC sheets produced under reference and derived conditions was recorded and depicted in Fig. 3.11.

Both the samples had shown three characteristic peaks at 2θ ~ 14.5, 16.5 and 22.5° (Fig. 3.11), corresponding to $(1\bar{1}0)$, (110) and (200) crystallographic planes of the cellulose lattice respectively, which epitomize a typical crystalline form of cellulose I [Ul-Islam *et al*., 2013; Huang *et al*., 2015]. Further, d-spacings connoting to these equatorial peaks are enumerated in Table 3.4 and the value of Z discriminant function indicated that BNC produced by *K. europaeus* SGP37 under both conditions predominantly belongs to the Iα form (triclinic lattice structure) of

cellulose [Wada et al., 2001]; however the crystallinity index of the BNC produced under derived conditions was greater than the BNC produced under reference conditions (Table 3.4).

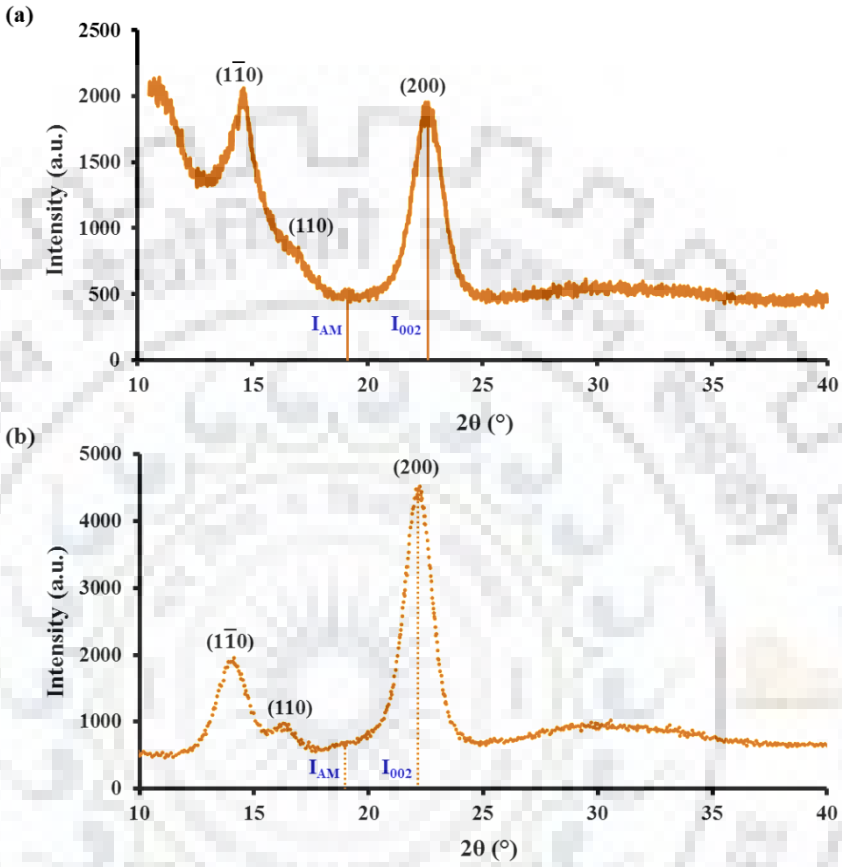

Fig. 3.11 X-ray diffraction profile of BNC sheets produced by *K. europaeus* SGP37 under (a) reference and (b) derived conditions

Table 3.4 d-Spacings, Z discriminant function, allomorphic category and crystallinity index of BNC produced by *K. europaeus* SGP37

Cultivation conditions	d-Spacing (nm)			Z-value	Dominant allomorph	CrI (%)
	d1 (1$\bar{1}$0)	d2 (110)	d3 (200)			
Reference	0.607	0.528	0.394	2.39	Iα	77.4
Optimized	0.630	0.540	0.400	30.51	Iα	87.7

3.3.6.3 TGA

The thermal stability of bacterial nanocellulose produced under reference and derived conditions was assessed by TGA-DTG analysis and results are represented as % weight loss as a function of temperature (Fig. 3.12). As evident from weight loss lineament, a marginal diminution in the weight (~1-4%) was observed in both of the samples during initial thermal treatment (60-100 °C) which attributes to the loss of adsorbed water [El-Saied *et al*., 2008; Vazquez *et al*., 2013]. Further thermal degradation exhibited two phases of weight loss in both the samples, (1) from~300 °C to~ 360 °C; a very expeditious fall in the weight (65-70%), owing to dehydration, depolymerization and decomposition of BNC which is followed by the formation of a charred residue, (2) from~450 °C to~505 °C, corresponds to the oxidation of char trailed by the formation of carbonaceous residue [El-Saied *et al*., 2008; Mohammadkazemi *et al*., 2015; Tyagi *et al*., 2016].

In terms of difference in the thermal stability of both the samples, the degradation of BNC produced under reference conditions started at ~270 °C and 39.62 % mass was remained at 350 °C, while the BNC produced under derived conditions was stable up to ~295 °C and 43.69 % residual mass was present at 350 °C which could be ascribed to its higher crystallinity index (Table 3.4) as the thermal degradation behavior is known to be influenced by the crystallinity and orientation of the fibers [Vazquez *et al*., 2013; Mohite and Patil, 2014b; Mohammadkazemi *et al*., 2015].

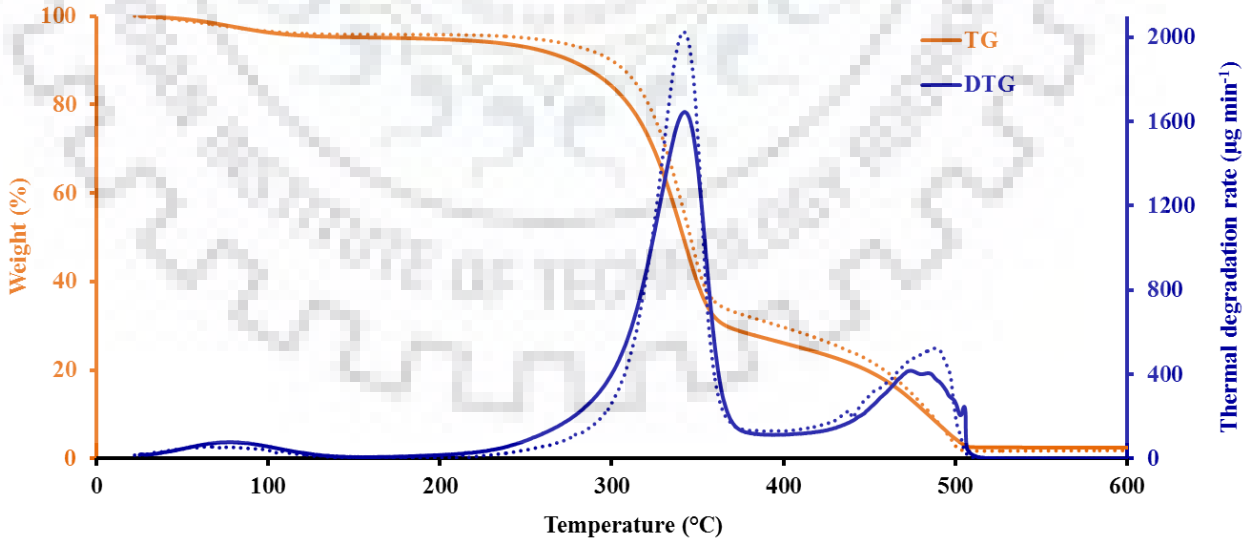

Fig. 3.12 TG-DTG curve of BNC produced by *K. europaeus* SGP37 under reference (solid lines) and derived conditions (dotted lines)

3.4 CONCLUSIONS

A novel, high yielding, cellulose producing bacterium "*Komagataeibacter europaeus* SGP37" was isolated from rotten grapes. The stagnant cultivation of *K. europaeus* SGP37 in HS medium resulted into the production of 5.61 g L^{-1} cellulose after 2 weeks of fermentation with conversion yield of 0.36 g cellulose/g sugar, at initial production rate of 0.95 g L^{-1} d^{-1}. Amelioration of physiological dynamics of the strain by devising preeminent culture conditions, enhanced the production rate of cellulose by ~1.65 fold (1.55 g L^{-1} d^{-1}) and attained 9.98 g L^{-1} cellulose with initial sugar consumption of 11.04 g L^{-1}, resulting into a very high conversion yield (0.90 g cellulose/g sugar) ever reported.

The strain with such robust competency to produce cellulose is immensely demanded by relevant cellulose diligences and we anticipate that this will pave the way to expedite and open up new avenues to deliver leading edge products at the lowest cost possible.

CHAPTER 4

Development of inexpensive production media and designing the production process for low-cost & scaled-up production of bacterial nanocellulose

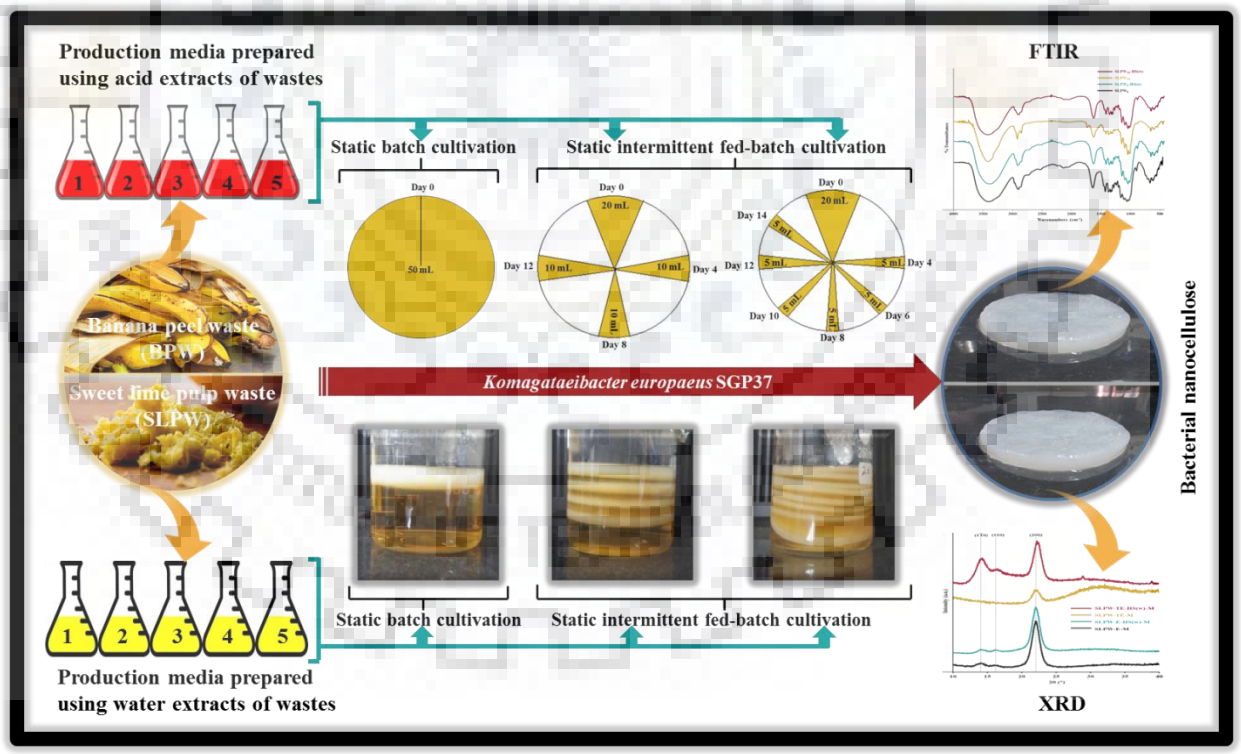

CHAPTER 4

Development of inexpensive production media and designing the production process for low-cost & scaled-up production of bacterial nanocellulose

4.1 INTRODUCTION

Bacterial nanocellulose (BNC), a polymer formed by linear coupling of glucopyranose units using microbial processes, has primed a great deal of attentiveness worldwide due to its unique physico-structural properties and multidimensional applicability viz. in the area of biomedicine, food, paper, textile, cosmetics, and materials industry [Shi *et al*., 2014; Mohite and Patil, 2014a; Dubey *et al*., 2015; Cacicedo *et al*., 2016; Jozala *et al*., 2016; Picheth *et al*., 2017]. Despite the enormous potential, its widespread usage hinge on the practical valuations such as scale-up capability and production expenditures as if comparing with other popular commercial organic merchandises, BNC is still expensive, therefore, its usage is limited [Kiziltas *et al*., 2015; Mohammadkazemi *et al*., 2015]. Consequently, the reduction of production costs and scaling up the production process are technological prerequisites for BNC to be adopted at wider scale [Cacicedo *et al*., 2016]. One of the ways to make the production process economically feasible is to search for low- or no-cost, abundant and easily available carbon sources (as during BNC production, the culture medium itself represents approximately 30 % of the total cost, Jozala *et al*., 2016) and to design a simple, less labor intensive cultivation strategy for higher productivity of BNC.

Citrus are the largest fruit crops grown across the globe (with total annual production of ~ 120 million tons) where India ranks fifth in the world with ~ 7.5 million tons of total citrus production annually [FAO, 2016]. Out of this, 25-30 % of the citrus is used by the citrus processing industries which generate a huge amount of waste every year worldwide as 50-60 % of the citrus mass remains unconsumed after processing as pulp, peels and seeds [Fan *et al*., 2016]. Further, banana is the second largest produced fruit after citrus and is cultured over 130 countries, leaded by India which produces more than 25 % of the world's total banana [Rattanavichai and Cheng, 2014; Waghmare and Arya, 2016; FAO, 2017]. Peel of banana represents 30-40% of the total fruit weight [Khawas *et al*., 2016] and is discarded as a huge waste from banana processing industries. Since, citrus pulp waste is a rich source of sugars (glucose, fructose, sucrose, trehalose etc.), fibers (pectin, xylan, glucosan etc.), organic acids (primarily citric and malic acid), vitamins (primarily ascorbic acid), minerals (primarily calcium and potassium), amino acids, oils and lipids [Fan *et al*., 2016; Sharma *et al*., 2017]; and banana peel is a rich source of starch, crude

protein, crude fat, dietary fibers, vitamins, minerals and other trace elements [Rattanavichai and Cheng, 2014] which can constitute ideal media for the growth of bacteria and could be low- or no-cost substrates for BNC production, resulting in an economic and eco-friendly approach for BNC production as the waste arising from one industry would form the raw material for the other and up-converted into a value-added product.

Further, commonly static cultivation has been used for BNC production by forming pellicles at the surface of the culture medium [Krystynowicz *et al*., 2002; Hsieh *et al*., 2016] and once the pellicle reaches to a certain thickness, the growth of bacterial cells as well as BNC production slows down as the pellicle limits the access of oxygen to the lower part (liquid zone) of the pellicle and nutrients to the upper part (aerobic zone) of the pellicle, results into a low productivity of BNC. While the nutrients and oxygen availability to bacterial cells in agitated culture are sufficient as the growth is not restricted to the air-liquid interface and better productivity of BNC may be anticipated, but the shear pressure exerted on some bacterial strains induces formation of cellulose nonproducing mutants (Cel^{-}), leading to diminished cellulose production [Krystynowicz *et al*., 2002].

In this context, the present work is aimed towards (i) developing inexpensive culture media for BNC production using sweet lime pulp waste (SLPW) and banana peel waste (BPW) as low- or no-cost substrates to make the production process cost effective, followed by (ii) designing a simple production process strategy to scale-up the production process for higher productivity of BNC, using the bacterial isolate *Komagataeibacter europaeus* SGP37 as a BNC producer. Henceforth, this chapter embodies:

- ☞ Production of BNC in various SLPW and BPW media under static batch cultivation
- ☞ Production of BNC in various SLPW and BPW media under static intermittent fed-batch cultivation
- ☞ Evaluating the effect of SLPW and BPW on physicochemical properties of produced BNC

4.2 MATERIALS AND METHODS

4.2.1 Materials

Sweet lime pulp waste (SLPW) and banana peel waste (BPW) were collected from local fruit markets, Roorkee, India. The chemicals and reagents used were procured from standard suppliers and were of highest purity available.

4.2.2 Preparation of extracts from SLPW and BPW

For preparing sweet lime pulp waste-extract ($SLPW_E$), 250 g of pulp was ground to a fine paste in 500 mL of distilled water and hydrolyzed at 90 °C for 1 h. The hydrolysate was then centrifuged at 10000 rpm for 10 min and supernatant was collected as stock solution. In an another vessel, 250 g of SLPW ground to a fine paste and added with 500 mL of 1 N H_2SO_4, was hydrolyzed at 90 °C for 1 h and centrifuged at 10000 rpm for 10 min. The collected supernatant was labelled as sweet lime pulp waste-acid treated extract ($SLPW_{TE}$).

The same procedure was followed to prepare banana peel waste-extract (BPW_E) and banana peel waste-acid treated extract (BPW_{TE}).

Further, total sugar and reducing sugar in the resulting extracts were determined by the phenol-sulfuric acid method [Masuko *et al.*, 2005] and dinitrosalicylic acid (DNS) method [Miller, 1959], respectively.

4.2.3 Valuation of sugar content in SLPW and BPW extracts

4.2.3.1 Total sugar content

Total sugar concentration of the SLPW and BPW extracts was determined using phenol-sulfuric acid microplate method [Masuko *et al*., 2005]. In brief, 50 µL of the extract (diluted 20 times) was added with 150 µL of concentrated H_2SO_4 in a 96-well microplate with rapid mixing which was then followed by addition of 30 µL of phenol (5%; in water). The plate was then incubated at 90 °C for 5 min in a water bath; and after cooling down, the absorbance was recorded at 490 nm using Synergy HTX multimode reader (BioTek Instruments Inc. USA) and the

concentration of sugar was calculated using the standard curve generated by serial dilutions of glucose.

4.2.3.2 Total reducing sugar content

Reducing sugar concentration of the SLPW and BPW extracts was quantified using dinitrosalicylic acid (DNS) method [Miller, 1959], as described in Chapter 3, Section 3.2.7.1.

4.2.4 Microorganism and culture media

Komagataeibacter europaeus SGP37 isolated from rotten grapes (Chapter 3; Dubey *et al*., 2017) was used for BNC production. Hestrin-Schramm (HS) medium (20 g L^{-1} glucose, 5 g L^{-1} yeast extract, 5 g L^{-1} peptone, 2.7 g L^{-1} disodium hydrogen phosphate, 1.15 g L^{-1} citric acid, pH 6; Hestrin & Schramm, 1954) was used as seed medium for preparation of pre-inocula and various formulations of SLPW and BPW extracts as listed in Table 4.1 and 4.2, respectively, were used as production media for BNC production.

Table 4.1 Production media prepared using SLPW extracts for BNC production[a]

Production Media	Media Components						pH
	Carbon Source	Yeast Extract (g L^{-1})	Peptone (g L^{-1})	Citric Acid (g L^{-1})	Na_2HPO_4 (g L^{-1})	Ethanol (%)	
$SLPW_E$	100% $SLPW_E$	-	-	-	-	-	5
$SLPW_E$-HS	100% $SLPW_E$	5	5	1.15	2.7	0.2	5
50% $SLPW_E$-HS	50% $SLPW_E$	5	5	1.15	2.7	0.2	5
25% $SLPW_E$-HS	25% $SLPW_E$	5	5	1.15	2.7	0.2	5
$SLPW_E$-HS(w)	100% $SLPW_E$ Fructose (20 g L^{-1})	5	5	1.15	2.7	0.2	5
$SLPW_{TE}$	100% $SLPW_{TE}$	-	-	-	-	-	5
$SLPW_{TE}$-HS	100% $SLPW_{TE}$	5	5	1.15	2.7	0.2	5
50% $SLPW_{TE}$-HS	50% $SLPW_{TE}$	5	5	1.15	2.7	0.2	5
25% $SLPW_{TE}$-HS	25% $SLPW_{TE}$	5	5	1.15	2.7	0.2	5
$SLPW_{TE}$-HS(w)	100% $SLPW_{TE}$ Fructose (20 g L^{-1})	5	5	1.15	2.7	0.2	5

[a]($SLPW_E$ Medium: Sweet lime pulp waste-extract ($SLPW_E$) as a sole nutrient source; $SLPW_E$-HS Medium: Sweet lime pulp waste-extract ($SLPW_E$) supplemented with components of HS medium except sugar; $SLPW_E$-HS(w) Medium: Sweet lime pulp waste-extract ($SLPW_E$) supplemented with all the components of HS medium including sugar; $SLPW_{TE}$ Medium: Sweet lime pulp waste-acid treated extract ($SLPW_{TE}$) as a sole nutrient source; $SLPW_{TE}$-HS Medium: Sweet lime pulp waste-acid treated extract ($SLPW_{TE}$) supplied with HS medium components except sugar; $SLPW_{TE}$-HS(w) Medium: Sweet lime pulp waste-acid treated extract ($SLPW_{TE}$) supplied with all the components of HS medium including sugar. Media were prepared by dissolving all the components in respective dilutions of the extracts instead of distilled water. Here, the composition of the HS medium used was same as optimized in Chapter 3 for enhanced BNC production by *K. europaeus* SGP37)

Table 4.2 Production media prepared using BPW extracts for BNC production[a]

Production Media	Media Components						pH
	Carbon Source	Yeast Extract (g L^{-1})	Peptone (g L^{-1})	Citric Acid (g L^{-1})	Na_2HPO_4 (g L^{-1})	Ethanol (%)	
BPW_E	100% BPW_E	-	-	-	-	-	5
BPW_E-HS	100% BPW_E	5	5	1.15	2.7	0.2	5
50% BPW_E-HS	50% BPW_E	5	5	1.15	2.7	0.2	5
25% BPW_E-HS	25% BPW_E	5	5	1.15	2.7	0.2	5
BPW_E-HS(w)	100% BPW_E Fructose (20 g L^{-1})	5	5	1.15	2.7	0.2	5
BPW_{TE}	100% BPW_{TE}	-	-	-	-	-	5
BPW_{TE}-HS	100% BPW_{TE}	5	5	1.15	2.7	0.2	5
50% BPW_{TE}-HS	50% BPW_{TE}	5	5	1.15	2.7	0.2	5
25% BPW_{TE}-HS	25% BPW_{TE}	5	5	1.15	2.7	0.2	5
BPW_{TE}-HS(w)	100% BPW_{TE} Fructose (20 g L^{-1})	5	5	1.15	2.7	0.2	5

[a](BPW_E Medium: Banana peel waste-extract (BPW_E) as a sole nutrient source; BPW_E-HS Medium: Banana peel waste-extract (BPW_E) supplemented with components of HS medium except sugar; BPW_E-HS(w) Medium: Banana peel waste-extract (BPW_E) supplemented with all the components of HS medium including sugar; BPW_{TE} Medium: Banana peel waste-acid treated extract (BPW_{TE}) as a sole nutrient source; BPW_{TE}-HS Medium: Banana peel waste-acid treated extract (BPW_{TE}) supplied with HS medium components except sugar; BPW_{TE}-HS(w) Medium: Banana peel waste-acid treated extract (BPW_{TE}) supplied with all the components of HS medium including sugar. Media were prepared by dissolving all the components in respective dilutions of the extracts instead of distilled water. Here the composition of the HS medium used was same as optimized in Chapter 3 for enhanced BNC production by *K. europaeus* SGP37)

4.2.5 BNC production

Pre-inoculum was prepared by transferring a single bacterial colony into 20 mL of HS broth containing glucose as a carbon source (pH 6) followed by 72 h of incubation at 30 °C under static conditions. After incubation, 20% v/v of this cell suspension was introduced into 50 mL of fresh HS medium (pH 6) and incubated at 30 °C for another 48 h under static conditions. This statically grown culture was then flustered vigorously to release the bacterial cells from BNC pellicle and the resulting cell suspension was used as seed culture and inoculated in the production media (as prepared above using SLPW and BPW extracts) at different cultivation conditions as given in Fig. 4.1; and incubated statically at 30 °C for 16 days.

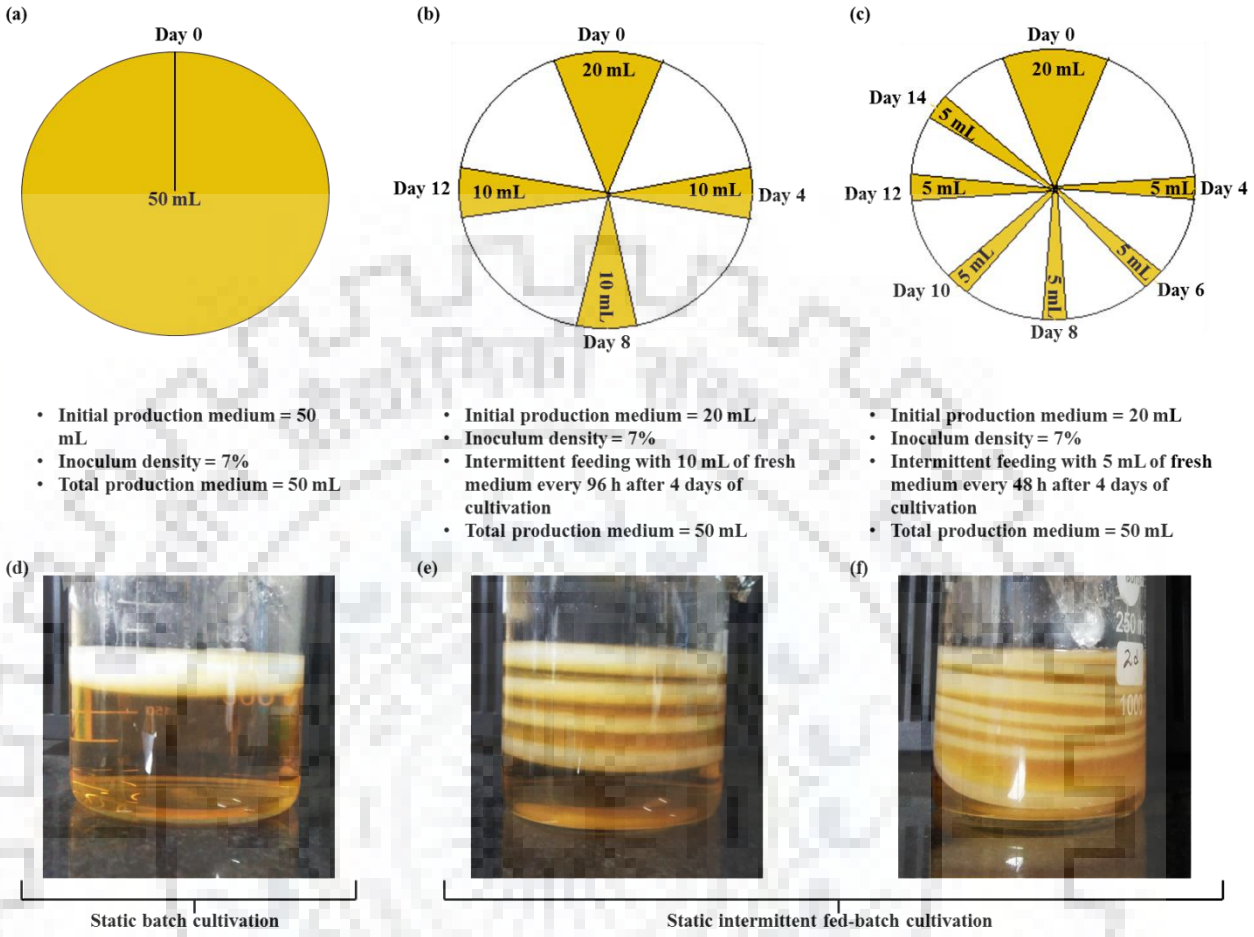

Fig. 4.1 Schematic representation of bacterial nanocellulose (BNC) production under static batch cultivation (a, d) and static intermittent fed-batch cultivation with fresh medium addition every 96 h (b, e) and 48 h (d, f); in static intermittent fed-batch cultivation the fresh medium was added at the top of the pellicles at respective time junctures to meet organism both the high oxygen plea and the nutrients at the same time, resulted into a steady BNC production and hence the higher productivity of BNC may be expected.

4.2.6 BNC purification and quantification

After the incubation period, BNC pellicles were harvested from culture vessel and purified via NaOH method as described in Chapter 3, Section 3.2.7. The pellicles were then dried at 60 °C to constant weight and quantified gravimetrically as g L^{-1} (dry weight (g) of BNC/volume (L) of culture medium).

The total residual sugar of the culture media at the end of the cultivation was determined using phenol-sulfuric acid method as described above in Section 4.2.3.1 and calculated as g (sugar) L^{-1} of culture medium.

The efficiency of BNC production in different production medium at different cultivation conditions was evaluated after 16 days of cultivation and % substrate consumption (i) & % substrate to BNC conversion yield (ii) were calculated as follows:

$$\% \text{ substrate consumption} = \frac{TS_i - TS_f}{TS_i} \times 100 \qquad \text{(i)}$$

$$\% \text{ substrate to BNC conversion yield} = \frac{BNC\left(\frac{g}{L}\right) at\ t_{end}}{TS_i - TS_f} \times 100 \qquad \text{(ii)}$$

where, TS_i and TS_f are the initial and final concentrations of total sugar (g L^{-1}) and t_{end} represents the time at the end of the cultivation (*i.e* Day 16).

4.2.7 Physicochemical characterization

The BNC membranes produced using SLPW and BPW extracts were characterized in terms of chemical structure, morphology, crystallinity profile and thermal longanimity by FTIR, FE-SEM, XRD and TGA, respectively, in order to assess the effect of SLPW and BPW on physicochemical properties of BNC.

4.2.7.1 Fourier transform infrared spectroscopy (FTIR)

FTIR analysis of the purified and dried BNC samples was performed using Thermo Nicolet NEXUS 670 FTIR spectrophotometer in the spectral region of 4000–450 cm^{-1} at 4 cm^{-1} resolution.

4.2.7.2 Field emission scanning electron microscopy (FE-SEM)

BNC pellicles produced in different SLPW and BPW media were observed by FE-SEM (FEI Quanta 200 FEG) at an accelerated voltage of 15 kV. Briefly, the dried pellicles were gold coated for 90 s in a Denton gold sputter unit before being mounted in the FE-SEM and the micrograph was acquired at 10 k X.

4.2.7.3 X-ray diffraction (XRD)

X-ray diffraction pattern of the dried BNC pellicles was acquired with Bruker AXS D8 Advance powder X-ray diffractometer using Ni-filtered Cu-Kα radiation (λ = 1.54 Å). The data were collected in 10-40° 2θ range at 2° min^{-1} scan rate and the crystallinity index was calculated according to the method defined by Segal *et al*. (1959), as described in Chapter 3, Section 3.2.10.2, equation (iii); and the allomorphic type of the produced BNC (I_α or I_β form) was determined on the basis of Z discriminant function, developed by Wada *et al*. (2001), as illustrated in Chapter 3, Section 3.2.10.2, equation (iv).

4.2.7.4 Thermogravimetric analysis (TGA)

TGA analysis of the BNC was done using Thermogravimetric/Differential Thermal Analyzer (EXSTAR TG/DTA 6300, Hitachi, Tokyo, Japan) over a temperature range of 25-600 °C at 10 °C min^{-1} scan rate (sample mass ~10.5 mg). All the measurements were performed under a nitrogen atmosphere with N_2 flow rate of 200 mL min^{-1}.

4.3 RESULTS AND DISCUSSION

4.3.1 Sugar content in SLPW and BPW extracts

4.3.1.1 SLPW

Table 4.3 illustrates the concentration of total sugar and reducing sugar in $SLPW_E$ (sweet lime pulp waste-extract) and $SLPW_{TE}$ (sweet lime pulp waste-acid treated extract). The concentration of total sugar was comparable in both of the extracts (~60 g L^{-1}) while $SLPW_{TE}$ was found to have higher amount of reducing sugar (33.44 ± 2.21 g L^{-1}) than $SLPW_E$ (15.72 ± 0.76 g L^{-1}). This may be due to the enhanced hydrolysis of polysaccharides present in SLPW by the coupled acid and heat treatment.

4.3.1.2 BPW

In comparison to SLPW extracts, quite low sugar content was found in BPW extracts with 16.78 ± 1.63 g L^{-1} and 15.56 ± 1.85 g L^{-1} of total sugar in BPW_E and BPW_{TE}, respectively, as manifested in Table 4.3. Further, in contrast to the SLPW extracts, negligible amount of reducing sugar was observed in BPW extracts as depicted in Table 4.3; this may be because the cell wall of banana is very complex to breakdown into simpler constituents.

Table 4.3 Contents of reducing sugar and total sugar in SLPW and BPW extracts[a]*

	Sweet lime pulp waste (SLPW)		Banana peel waste (BPW)	
	$SLPW_E$	**$SLPW_{TE}$**	**BPW_E**	**BPW_{TE}**
Reducing sugar (g L^{-1})	15.72 ± 0.76	33.44 ± 2.21	0.34 ± 0.16	0.62 ± 0.17
Total sugar (g L^{-1})	60.04 ± 5.05	62.54 ± 4.04	16.78 ± 1.63	15.56 ± 1.85

[a]($SLPW_E$: sweet lime pulp waste-extract; $SLPW_{TE}$: sweet lime pulp waste-acid treated extract; BPW_E: banana peel waste-extract; BPW_{TE}: banana peel waste-acid treated extract)

*Data are the mean of three independent replicates and represented as Mean ± SD.

4.3.2 BNC production using SLPW extracts

4.3.2.1 Static batch cultivation

4.3.2.1.1 $SLPW_E$ and $SLPW_{TE}$ as a sole nutrient source

The water and acid extracts of SLPW viz. $SLPW_E$ and $SLPW_{TE}$, were unswervingly used as the production media without addition of any other extra nutrients for BNC production by *K. europaeus* SGP37 under static batch cultivation for 16 days. After cultivation, a dry BNC film of 6.30 ± 1.56 g L^{-1} was obtained from $SLPW_E$ medium and 4.20 ± 1.21 g L^{-1} was acquired with $SLPW_{TE}$ medium (Table 4.4) which was quite lower with that harvested from modified HS medium (9.98 ± 0.24 g L^{-1}) under similar physiological parameters (Chapter 3, Fig. 3.9b). However, the BNC production values obtained from SLPW extracts are already promising as these are considerably higher than those reported previously for other agro-industrial residues without any supplementation; for instance, 2.8 g L^{-1} of BNC after 13 days from pineapple peel juice [Castro *et al*., 2011]; 0.85 g L^{-1} after 4 days from dry olive mill residue [Gomes *et al*., 2013] and 0.10 g L^{-1} of BNC after 28 days from hot water extracted wood sugars [Kiziltas *et al*., 2015].

Further, at the end of the cultivation, 27.30 ± 2.36 g L^{-1} and 30.48 ± 5.99 g L^{-1} of sugar was still present in $SLPW_E$ and $SLPW_{TE}$ medium, respectively (Table 4.4) which suggest that sugar was not the limiting factor for lower BNC production in SLPW extracts. Hence, it was speculated that scarcity of other nutrients in the culture medium may have hindered the growth of microorganism and consequently the lower BNC production despite of sufficient sugar availability in the culture medium.

4.3.2.1.2 $SLPW_E$ and $SLPW_{TE}$ supplemented with the components of HS medium

Aiming to improve the BNC production by overcoming the foretold nutrients deficit of the SLPW extracts, some complementary nutrient sources, namely yeast extract (0.5% w/v), peptone (0.5% w/v), citric acid (0.115% w/v), Na_2HPO_4 (0.27% w/v) and ethanol (0.2% v/v) were added to the $SLPW_E$ and $SLPW_{TE}$. This addition was made on the basis of composition of the HS medium optimized in Chapter 3. A substantial increase (~ 2.5 fold) in BNC production was observed for both $SLPW_E$-HS (14.3 ± 0.75 g L^{-1}) and $SLPW_{TE}$-HS (11.4 ± 1.90 g L^{-1}) when compared with the results obtained without supplementation (Table 4.4). However, at the end of

the cultivation, approximately 37% sugar (22.27 ± 2.75 g L^{-1}) was still present in the $SLPW_E$-HS medium (Table 4.4) which may be due to (i) either the strain was not able to utilize all the sugars present in the $SLPW_E$-HS (as the concentration of reducing sugar in $SLPW_E$ was only 15.72 ± 0.76 g L^{-1}; Table 4.3) or/and (ii) the thickness of BNC pellicle produced, had limited the access of oxygen to the culture media and consequently the growth of the microorganism, resulting into lower levels of sugar consumption.

Further, despite the higher reducing sugar concentration in $SLPW_{TE}$-HS (33.44 ± 2.21 g L^{-1}; Table 4.3), the lower BNC production can be related to the presence of some possible inhibitory compounds in $SLPW_{TE}$ such as furfurals released during acid hydrolysis and also the phenolic compounds, which might have impeded the metabolism of *K. europaeus* SGP37 and thus the BNC production [Gomes *et al*., 2013; Zhang *et al*., 2014a, 2014b]. Moreover, a significant rise (4-5 fold) in BNC production was observed when the extracts were supplemented with HS medium components including the sugar source (fructose, 2% w/v); the BNC yields were 26.2 ± 1.50 g L^{-1} in $SLPW_E$-HS(w) and 22.4 ± 0.78 g L^{-1} in $SLPW_{TE}$-HS(w) (Table 4.4), however 28.48 % and 55.7 % sugar was still unutilized in $SLPW_E$-HS(w) and $SLPW_{TE}$-HS(w), respectively following 16 days of cultivation.

Table 4.4 BNC production in varying SLPW media under static batch cultivation of *Komagataeibacter europaeus* SGP37 for 16 days at 30 °C[a]*

Production medium	Total Sugar (g L^{-1})	Yield of BNC (g L^{-1})	Residual Sugar (g L^{-1})	Substrate consumption (%)	Substrate to BNC conversion (%)
Sweet lime pulp waste-extract ($SLPW_E$)					
$SLPW_E$	60.04 ± 5.05	6.30 ± 1.56	27.30 ± 2.36	54.53	19.24
$SLPW_E$-HS	60.04 ± 5.05	14.3 ± 0.75	22.27 ± 2.75	62.90	37.86
50% $SLPW_E$-HS	30.02 ± 2.52	8.40 ± 1.60	7.73 ± 0.45	74.25	37.68
25% $SLPW_E$-HS	15.01 ± 1.26	5.05 ± 1.07	3.64 ± 0.42	75.74	44.41
$SLPW_E$-HS(w)	80.04 ± 5.05	26.2 ± 1.50	22.8 ± 2.36	71.51	45.77
Sweet lime pulp waste-acid treated extract ($SLPW_{TE}$)					
$SLPW_{TE}$	62.54 ± 4.04	4.20 ± 1.21	30.48 ± 5.99	51.26	13.10
$SLPW_{TE}$-HS	62.54 ± 4.04	11.4 ± 1.90	24.72 ± 4.47	60.47	30.14
50% $SLPW_{TE}$-HS	31.27 ± 2.02	11.7 ± 2.13	6.48 ± 1.11	79.27	47.19
25% $SLPW_{TE}$-HS	15.63 ± 1.01	9.85 ± 1.85	2.95 ± 0.24	81.13	77.65
$SLPW_{TE}$-HS(w)	82.54 ± 4.04	22.4 ± 0.78	46.0 ± 8.08	44.26	61.30

[a]($SLPW_E$: Sweet lime pulp waste-extract as a sole nutrient source; $SLPW_E$-HS: Sweet lime pulp waste-extract supplemented with components of HS medium except sugar; $SLPW_E$-HS(w): Sweet lime pulp waste-extract supplemented with all the components of HS medium including sugar; $SLPW_{TE}$: Sweet lime pulp waste-acid treated extract as a sole nutrient source; $SLPW_{TE}$-HS: Sweet lime pulp waste-acid treated extract supplied with HS medium components except sugar; $SLPW_{TE}$-HS(w): Sweet lime pulp waste-acid treated extract supplied with all the components of HS medium including sugar. Refer Table 4.1 for details.)
*All the experiments were carried out in triplicates and data are represented as Mean ± SD.

Thus, it would be desired and imperative to determine the optimal concentrations of the extracts for obtaining higher conversion levels and yields. Henceforth, different dilutions of the extracts were prepared (Table 4.1), in order to optimize carbon substrate concentration, and, at the same time, to reduce the effect of possible inhibitory compounds present. All the nutrients of HS medium except sugar were added to the respective dilutions of the extracts and the results obtained are presented in Table 4.4. For the production media prepared using $SLPW_E$, BNC production get downturned following dilution and, 8.40 ± 1.60 g L^{-1} and 5.05 ± 1.07 g L^{-1} of BNC was produced in 50% $SLPW_E$-HS and 25% $SLPW_E$-HS, respectively. These low production values of BNC could be related to the lower concentration of reducing sugar in the diluted $SLPW_E$-HS.

Unlike $SLPW_E$-HS, the dilutions of $SLPW_{TE}$-HS had resulted into almost comparable yields of BNC *i.e.* $SLPW_{TE}$-HS (11.4 ± 1.90 g L^{-1}), 50% $SLPW_{TE}$-HS (11.7 ± 2.13 g L^{-1}) and 25% $SLPW_{TE}$-HS (9.85 ± 1.85 g L^{-1}). This could be due to the higher levels of reducing sugars present

in the acid-treated extract and the decreasing concentration of the possible inhibitory compounds present in these extract following dilutions.

4.3.2.2 Static intermittent fed-batch cultivation

In static batch cultivation, BNC pellicle is produced at the air-liquid interface of culture medium; and after the pellicle covers the entire surface and grows thicker, microorganisms on the surface of the pellicle find it difficult to come across to culture nutrients, and those below the pellicle find it hard to reach oxygen, resulting into lower yields of BNC despite having sufficient substrate in the culture media.

As illustrated in Fig. 4.1d, once the pellicle entirely blocked the air-liquid interface, the nutrients might be insufficient in the upper part of BNC and the oxygen might be limited within the lower part of BNC; it prohibit the microorganisms from simultaneous contact with oxygen and nutrients. To resolve this constraint, an intermittent feeding of the culture medium was practiced directly onto the existing pellicle to meet organism both the high oxygen plea and nutrients concurrently, as depicted in Fig. 4.1e, f.

The results obtained are shown in Table 4.5. Using $SLPW_E$-HS(w) medium under static batch cultivation, 26.2 ± 1.50 g L^{-1} of BNC was obtained after 16 days (Table 4.4). In contrast, a marked augmentation in the BNC yield was observed when intermittent fed-batch (IFB) cultivation was adopted and kept the other parameters constant. The BNC yield had increased to 36.6 ± 0.55 g L^{-1} and 38 ± 0.85 g L^{-1} when $SLPW_E$-HS(w) medium was fed intermittently at periodical interval of 96 h and 48 h, respectively. The similar paradigm was seen in $SLPW_{TE}$-HS(w) medium; 27.0 ± 2.20 g L^{-1} BNC in IFB-96 h and 28.9 ± 1.34 g L^{-1} BNC in IFB-48 h (Table 4.5), compared to 22.4 ± 0.78 g L^{-1} BNC in batch cultivation.

Table 4.5 BNC production in SLPW media under static intermittent fed-batch cultivation of *K. europaeus* SGP37 for 16 days at 30 °C*

Production medium	Total Sugar ($g\ L^{-1}$)	Yield of BNC ($g\ L^{-1}$)	Residual Sugar ($g\ L^{-1}$)	Substrate consumption (%)	Substrate to BNC conversion (%)
Intermittent feeding every 96 h (IFB-96h)					
$SLPW_E$-HS(w)	80.04 ± 5.05	36.6 ± 0.55	16.39 ± 2.75	79.52	57.50
$SLPW_{TE}$-HS(w)	82.54 ± 4.04	27.0 ± 2.20	43.3 ± 8.63	47.54	68.80
Intermittent feeding every 48 h (IFB-48h)					
$SLPW_E$-HS(w)	80.04 ± 5.05	38 ± 0.85	17.2 ± 2.95	78.51	60.47
$SLPW_{TE}$-HS(w)	82.54 ± 4.04	28.9 ± 1.34	45.5 ± 7.76	44.87	78.02

*All the experiments were carried out in triplicates and data are represented as Mean ± SD.

According to Hornung *et al*. (2006), in static culture, BNC production primarily depends on the growth and ability (for BNC synthesis) of the bacteria within the aerobic zone, as only that part of the total number of cells which dwell within this aerobic zone is actively able to produce cellulose. Therefore by supplementing nutrients directly in this aerobic zone (onto the existing BNC pellicle) would enable the microbes to keep producing BNC without any inadequacy of either nutrients or oxygen; and that suitably inculcates about the enhanced BNC yields as achieved during intermittent fed-batch cultivation.

Moreover, relatively higher BNC yield was observed in both $SLPW_E$-HS(w) and $SLPW_{TE}$-HS(w) when 5 ml of media was fed every 48 h than 10 ml of media every 96 h. The underlying reason for this may be that bacteria prefer to be in the aerobic zone, so it took time for them to diffuse to the new air-liquid interface and then start producing BNC if the distance between the existing pellicle and the new air-liquid interface is larger (due to the volume of the media fed). Consequently, some carbon in the form of energy may have used in this process and could be related to the lower BNC yield in contrary to higher sugar consumption in IFB-96 h. Hsieh *et al*. (2016) had also reported that the period for new pellicle formation is roughly proportional to the distance between the former pellicle and the new air-liquid interface; and thus support our findings.

4.3.2.3 BNC production efficiency

In order to better attempt the value of this residual waste and the cultivation strategy, % substrate consumption and substrate to BNC conversion yield were calculated. The results are

delineated in Table 4.4 for static batch cultivation and in Table 4.5 for static intermittent fed-batch cultivation.

As depicted in Table 4.4, the lowest substrate to BNC conversion yield (19.24 % for $SLPW_E$ and 13.10 % for $SLPW_{TE}$) was obtained when SLPW extracts were used as a sole nutrient source. However, when the extracts were satiated with the components of HS medium except sugar, the conversion had increased to 37.86 % and 30.14 % for $SLPW_E$-HS and $SLPW_{TE}$-HS, respectively. Further, dilution of $SLPW_{TE}$ (while supplemented with the components of HS medium) had made a substantial increase in the conversion yield of BNC and reached to 77.65 % in 25% $SLPW_{TE}$-HS medium under static batch cultivation, which is comparable to that obtained in modified HS medium (82%) under similar physiological parameters (Chapter 3, Section 3.3.5.2).

In consideration of static batch cultivation, maximum BNC production was achieved in $SLPW_E$-HS(w) medium (26.2 ± 1.50 g L^{-1}) and $SLPW_{TE}$-HS(w) medium (22.4 ± 0.78 g L^{-1}) bring in the conversion yield of 45.77 % and 61.30 %, respectively. Hence, the duos were chosen for intermittent feeding strategy to evaluate if any further increase in BNC production and conversion yield can be achieved. A notable increase was observed in both $SLPW_E$-HS(w) and $SLPW_{TE}$-HS(w) medium when fed intermittently and the maximum conversion yield was obtained in $SLPW_{TE}$-HS(w) medium (78.02 %) under IFB-48 h (Table 4.5) which is remarkably higher than those reported for other agro-industrial residues [Carreira *et al*., 2011; Wu and Liu, 2012; Gomes *et al*., 2013].

4.3.3 BNC production using BPW extracts

4.3.3.1 Static batch cultivation

4.3.3.1.1 BPW_E and BPW_{TE} as a sole nutrient source

When BPW extracts were used as a sole nutrient source for BNC production by *K. europaeus* SGP37, a BNC yield of 1.20 ± 0.23 g L^{-1} and 0.90 ± 0.11 g L^{-1} was obtained from BPW_E and BPW_{TE} medium, respectively (Table 4.6) which was much lower than that obtained with SLPW extracts while served unswervingly under similar physiological conditions (Table 4.4). It could be due to either the bacteria were not able to utilize the sugars present in BPW extracts for

BNC synthesis and/or the deficit of other nutrients may have hindered the metabolism of microorganism and consequently the BNC synthesis.

4.3.3.1.2 BPW_E and BPW_{TE} supplemented with the components of HS medium

Addition of some complementary nutrient sources based on the composition of HS medium (except sugar) optimized in the previous chapter to the BPW extracts had made a remarkable increase (~4-6 fold) in the BNC yield with 5.53 ± 0.68 g L^{-1} BNC in BPW_E-HS medium and 4.20 ± 0.43 g L^{-1} BNC in BPW_{TE}-HS medium (Table 4.6). Further, when the extracts were provided with all the components of HS medium including sugar source (fructose, 20 g L^{-1}), the BNC yield had reached to 14.2 ± 2.95 g L^{-1} in BPW_E-HS(w) medium and 11.8 ± 0.17 g L^{-1} in BPW_{TE}-HS(w) medium. Moreover, as can be comprehended from Table 4.6, in both cases either the BPW extracts were supplemented with all the components of HS medium (*i.e.* BPW_E-HS(w) and BPW_{TE}-HS(w) medium) or omitted with the sugar source (*i.e.* BPW_E-HS and BPW_{TE}-HS medium), BNC yield was always higher in the media prepared using water extract of BPW (*i.e.* BPW_E) which is quite similar with that happened with SLPW extracts (Table 4.4).

A gradual reduction of BNC yield was observed when the BPW extracts were diluted to 50% and 25% except for the 50% BPW_{TE}-HS medium. The reduction in the BNC yield following dilution is obviously due to the lowered concentration of sugar in the diluted extracts.

Table 4.6 BNC production in varying BPW media under static batch cultivation of *Komagataeibacter europaeus* SGP37 for 16 days at 30 °C[a]*

Production medium	Total Sugar (g L^{-1})	Yield of BNC (g L^{-1})	Residual Sugar (g L^{-1})	Substrate consumption (%)	Substrate to BNC conversion (%)
Banana peel waste-extract (BPW_E)					
BPW_E	16.78 ± 1.63	1.20 ± 0.23	7.17 ± 0.53	57.27	12.48
BPW_E-HS	16.78 ± 1.63	5.53 ± 0.68	3.86 ± 0.29	76.99	42.80
50% BPW_E-HS	8.39 ± 0.82	4.40 ± 0.36	1.89 ± 0.23	77.47	67.69
25% BPW_E-HS	4.19 ± 0.41	3.21 ± 0.45	1.02 ± 0.17	75.68	101.10
BPW_E-HS(w)	36.78 ± 1.63	14.2 ± 2.95	15.49 ± 3.12	57.88	66.69
Banana peel waste-acid treated extract (BPW_{TE})					
BPW_{TE}	15.56 ± 1.85	0.90 ± 0.11	6.20 ± 0.51	60.15	9.61
BPW_{TE}-HS	15.56 ± 1.85	4.20 ± 0.43	5.01 ± 0.41	67.80	39.81
50% BPW_{TE}-HS	7.78 ± 0.92	4.60 ± 0.32	2.25 ± 0.37	71.07	83.18
25% BPW_{TE}-HS	3.89 ± 0.46	3.03 ± 0.41	1.17 ± 0.24	69.92	111.39
BPW_{TE}-HS(w)	35.56 ± 1.85	11.8 ± 0.17	21.65 ± 1.28	39.11	84.83

[a](BPW_E: Banana peel waste-extract as a sole nutrient source; BPW_E-HS: Banana peel waste-extract supplemented with components of HS medium except sugar; BPW_E-HS(w): Banana peel waste-extract supplemented with all the components of HS medium including sugar; BPW_{TE}: Banana peel waste-acid treated extract as a sole nutrient source; BPW_{TE}-HS: Banana peel waste-acid treated extract supplied with HS medium components except sugar; BPW_{TE}-HS(w): Banana peel waste-acid treated extract supplied with all the components of HS medium including sugar. Refer Table 4.2 for details.)

*All the experiments were carried out in triplicates and data are represented as Mean ± SD.

4.3.3.2 Static intermittent fed-batch cultivation

In consideration of static batch cultivation of *K. europaeus* SGP37 in BPW media, maximum BNC production was achieved in BPW_E-HS(w) medium (14.2 ± 2.95 g L^{-1}) and BPW_{TE}-HS(w) medium (11.8 ± 0.17 g L^{-1}) with total sugar consumption of 57.8 % and 39.11 %, respectively. Since notable amount of sugar was still present at the end of the cultivation hence the duos were selected for the static intermittent fed-batch cultivation for any further augmentation in the BNC yield which may have been confined in the batch cultivation due to the pellicle thickness as explained in Section 4.3.2.2. The results obtained are shown in Table 4.7 and as can be seen, a remarkable increase in the BNC yield was observed for both BPW_E-HS(w) and BPW_{TE}-HS(w) medium, with 22.83 ± 3.80 g L^{-1} and 24.30 ± 2.17 g L^{-1} of BNC in IFB-96h and IFB-48h, respectively for BPW_E-HS(w) medium; and 20.50 ± 3.53 g L^{-1} and 21.26 ± 2.76 g L^{-1} of BNC in IFB-96h and IFB-48h, respectively for BPW_{TE}-HS(w) medium.

Table 4.7 BNC production in BPW media under static intermittent fed-batch cultivation of *K. europaeus* SGP37 for 16 days at 30 °C*

Production medium	Total Sugar ($g\ L^{-1}$)	Yield of BNC ($g\ L^{-1}$)	Residual Sugar ($g\ L^{-1}$)	Substrate consumption (%)	Substrate to BNC conversion (%)
Intermittent feeding every 96 h (IFB-96h)					
BPW_E-HS(w)	36.78 ± 1.63	22.83 ± 3.80	12.24 ± 1.42	66.72	93.03
BPW_{TE}-HS(w)	35.56 ± 1.85	20.50 ± 3.53	13.06 ± 1.82	63.27	91.11
Intermittent feeding every 48 h (IFB-48h)					
BPW_E-HS(w)	36.78 ± 1.63	24.30 ± 2.17	12.50 ± 2.15	66.01	100.08
BPW_{TE}-HS(w)	35.56 ± 1.85	21.26 ± 2.76	13.47 ± 2.33	62.12	96.24

*All the experiments were carried out in triplicates and data are represented as Mean ± SD.

4.3.3.3 BNC production efficiency

Based on the BNC yield and the total sugar left at the end of the cultivation, % sugar consumption and % sugar to BNC conversion yield were calculated and the results are delineated in Table 4.6 for static batch cultivation and in Table 4.7 for static intermittent fed-batch cultivation.

As shown in Table 4.6, like SLPW extracts, the lowest sugar to BNC conversion yield (12.48 % for BPW_E and 9.61 % for BPW_{TE}) was obtained when the extracts were directly used as the production media without any supplementation. However, when the extracts were provided with the components of HS medium (except sugar), the conversion was reached to 42.80% and 39.81% for BPW_E-HS and BPW_{TE}-HS medium, respectively. Further, as can be appraised from Table 4.6, unlike SLPW extracts, dilution of BPW extracts (while supplemented with the components of HS medium except sugar source) had made no significant change in the substrate consumption which suggest that the residual sugar present in the media at the end of the cultivation was not utilizable by the bacterium *K. europaeus* SGP37. However, the conversion yield got increased following dilution in both BPW_E-HS and BPW_{TE}-HS medium and reached to 101.10% and 111.39% in 25% BPW_E-HS and 25% BPW_{TE}-HS medium, respectively. The possible reason for this may be the concentration of potassium in these BPW media which regulates the intracellular level of c-di-GMP in a very specific manner and ultimately the cellulose synthesis [Weinhouse *et al*., 1997; Lee *et al*., 2014]. Moreover, the higher than 100% sugar to BNC conversion indicates that nutrients other than the sugars present in the media, were metabolized by *K. europaeus* SGP37 to synthesize BNC. The similar findings are reported by Wu and Liu (2013)

where a conversion yield of 120% was attained when the HS medium was supplemented with 87.5% thin stillage (TS) wastewater from rice wine distillery [Wu and Liu, 2013].

Further, in static batch cultivation, supplementation of HS medium components including sugar source (Fructose, 20 g L^{-1}) had led 66.69% sugar to BNC conversion for BPW_E-HS(w) medium and 84.83% sugar to BNC conversion for BPW_{TE}-HS(w) medium which got upturned to 100.08% and 96.24% for BPW_E-HS(w) and BPW_{TE}-HS(w) medium, respectively when intermittent feeding strategy (IFB-48h) was applied, as depicted in Table 4.7.

4.3.4 Physicochemical characterization

The BNC membranes produced using SLPW and BPW media (with/without supplementation of HS medium components) were characterized in terms of chemical structure, morphology, crystallinity profile and thermal stability by FTIR, FE-SEM, XRD and TGA, respectively, in order to assess the effect of these feedstocks on physicochemical properties of BNC.

4.3.4.1 FTIR

Fig. 4.2 and 4.3 shows the FTIR spectra of BNC produced in different SLPW and BPW media respectively, under static batch cultivation. As can be seen, the FTIR spectral profiles of all the BNC produced by different means were almost similar except minor shifting and some broadening or decreasing in the intensity of the peaks. For details, Tables 4.8 and 4.9 display the values of FTIR spectral bands of BNC produced in different SLPW and BPW media, respectively.

The shifting, broadening and/or decreasing in the intensity of the peaks in some of the BNC samples could be attributed to the rearrangements of cellulose chains in different production media otherwise the obtained spectral profiles were similar to the BNC produced using standard HS medium as stated in the previous study [Dubey *et al*., 2017; Chapter 3, Section 3.3.4.1] and demonstrate the characteristic signature of cellulose.

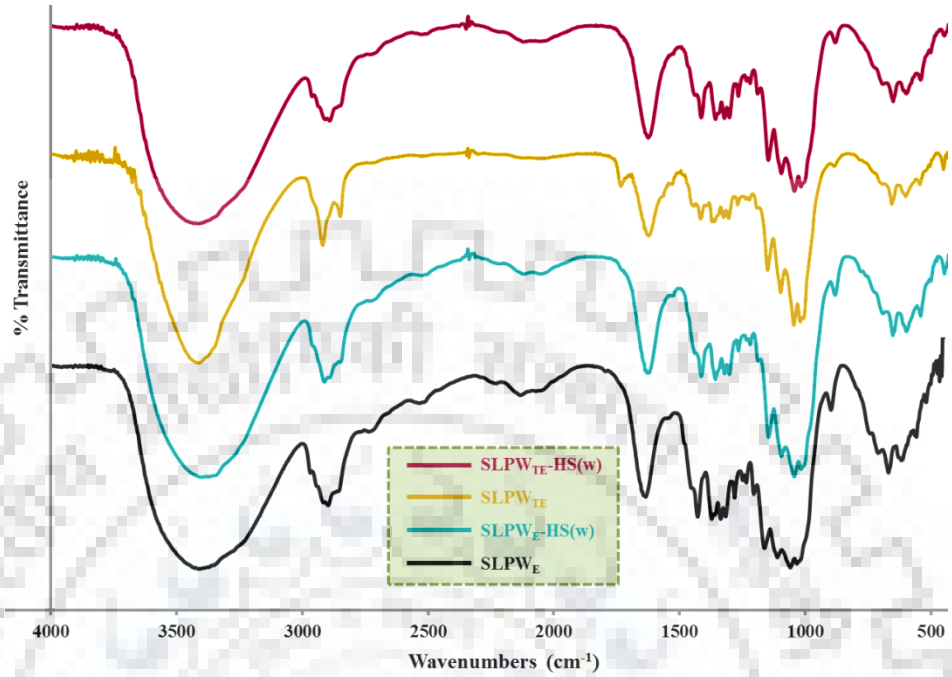

Fig. 4.2 FTIR spectral profiles of bacterial nanocellulose (BNC) produced in various SLPW media under static batch cultivation.

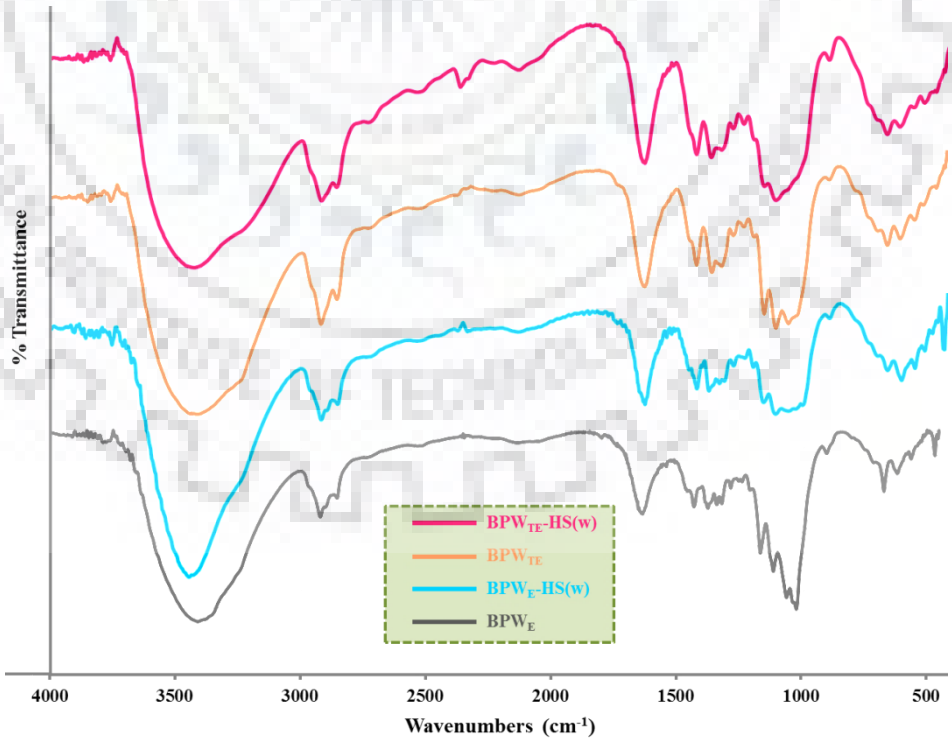

Fig. 4.3 FTIR spectral profiles of bacterial nanocellulose (BNC) produced in various BPW media under static batch cultivation.

Table 4.8 FTIR spectral bands of bacterial nanocellulose produced by *K. europaeus* SGP37 in various SLPW media under static batch cultivation[a]

Wavenumber (cm^{-1})				Assignment	References
$SLPW_E$	**$SLPW_E$-HS(w)**	**$SLPW_{TE}$**	**$SLPW_{TE}$-HS(w)**		
3410.14	3402.64	3412.94	3421.70	γO-H (H-bonded)	Oh *et al*., 2005
2897.31	2920.01	2923.69	2898.77	γC-H	Oh *et al*., 2005
1634.39	1639.32	1633.22	1638.26	δH-O-H (H_2O absorbed)	Yassine *et al*., 2016
1428.23	1428.55	1428.43	1428.75	δC-H_2 (symmetric)	Oh *et al*., 2005
1371.99	1372.37	1383.80	1372.04	δC-H	Oh *et al*., 2005
1316.73	1317.08	1317.05	1316.97	C-H_2 wagging	Oh *et al*., 2005
1281.34	1281.45	1282.02	1281.57	δC-H	Oh *et al*., 2005
1234.80	1234.98	1235.10	1235.07	δC-OH in plane at C-6	Oh *et al*., 2005
1162.71	1162.57	1162.88	1163.10	γC-O-C (asymmetric bridge stretching)	Fan *et al*., 2016
1111.19	1111.33	1111.40	1111.71	γC-C ring (polysaccharides, cellulose)	Movasaghi *et al*., 2008
1060.02	1060.18	1059.55	1060.04	C-O-C (pyranose ring skeletal vibration)	Shao *et al*., 2015
898.25	898.89	898.52	898.40	γC-O-C (in plane, symmetric stretching)	Oh *et al*., 2005

[a]Key to symbols: γ: stretching, δ: bending

Table 4.9 FTIR spectral bands of bacterial nanocellulose produced by *K. europaeus* SGP37 in various BPW media under static batch cultivation[a]

Wavenumber (cm^{-1})				Assignment	References
BPW_E	**BPW_E-HS(w)**	**BPW_{TE}**	**BPW_{TE}-HS(w)**		
3409.10	3446.68	3416.51	3415.36	γO-H (H-bonded)	Oh *et al*., 2005
2919.52	2920.71	2921.22	2919.16	γC-H	Oh *et al*., 2005
1633.13	1633.41	1633.78	1633.31	δH-O-H (H_2O absorbed)	Yassine *et al*., 2016
1428.02	1427.16	1427.98	1427.79	δC-H_2 (symmetric)	Oh *et al*., 2005
1372.41	1379.10	1367.51	1369.36	δC-H	Oh *et al*., 2005
1317.01	1319.86	1324.28	1326.80	C-H_2 wagging	Oh *et al*., 2005
1281.33	1279.87	1280.13	1283.07	δC-H	Oh *et al*., 2005
1236.45	1236.88	1241.86	1244.81	δC-OH in plane at C-6	Oh *et al*., 2005
1162.82	1165.84	1159.41	1159.02	γC-O-C (asymmetric bridge stretching)	Fan *et al*., 2016
1111.34	1114.36	1113.15	1112.55	γC-C ring (polysaccharides, cellulose)	Movasaghi *et al*., 2008
1058.90	1063.83	1062.96	1060.67	C-O-C (pyranose ring skeletal vibration)	Shao *et al*., 2015
897.92	899.02	897.47	896.75	γC-O-C (in plane, symmetric stretching)	Oh *et al*., 2005

4.3.4.2 FE-SEM

Further, the micro-structural differences between the BNC pellicles produced in various media was reconnoitered by field emission scanning electron microscope (FE-SEM) and for each medium, the BNC fibers dispersion and interfacial adhesion is manifested in Fig. 4.4 and 4.5. All the BNC samples revealed a heterogeneous reticulated structure consisting of some newly formed loosely-knitted randomly oriented cellulose nanofibers and a closely packed extensively intertwined network of highly extended nanofibers, with no significant difference in the fiber size and fiber distribution among the samples except for the BNC membrane produced in BPW_{TE} medium where the cellulose fibers were quite aggregated and more disorganized.

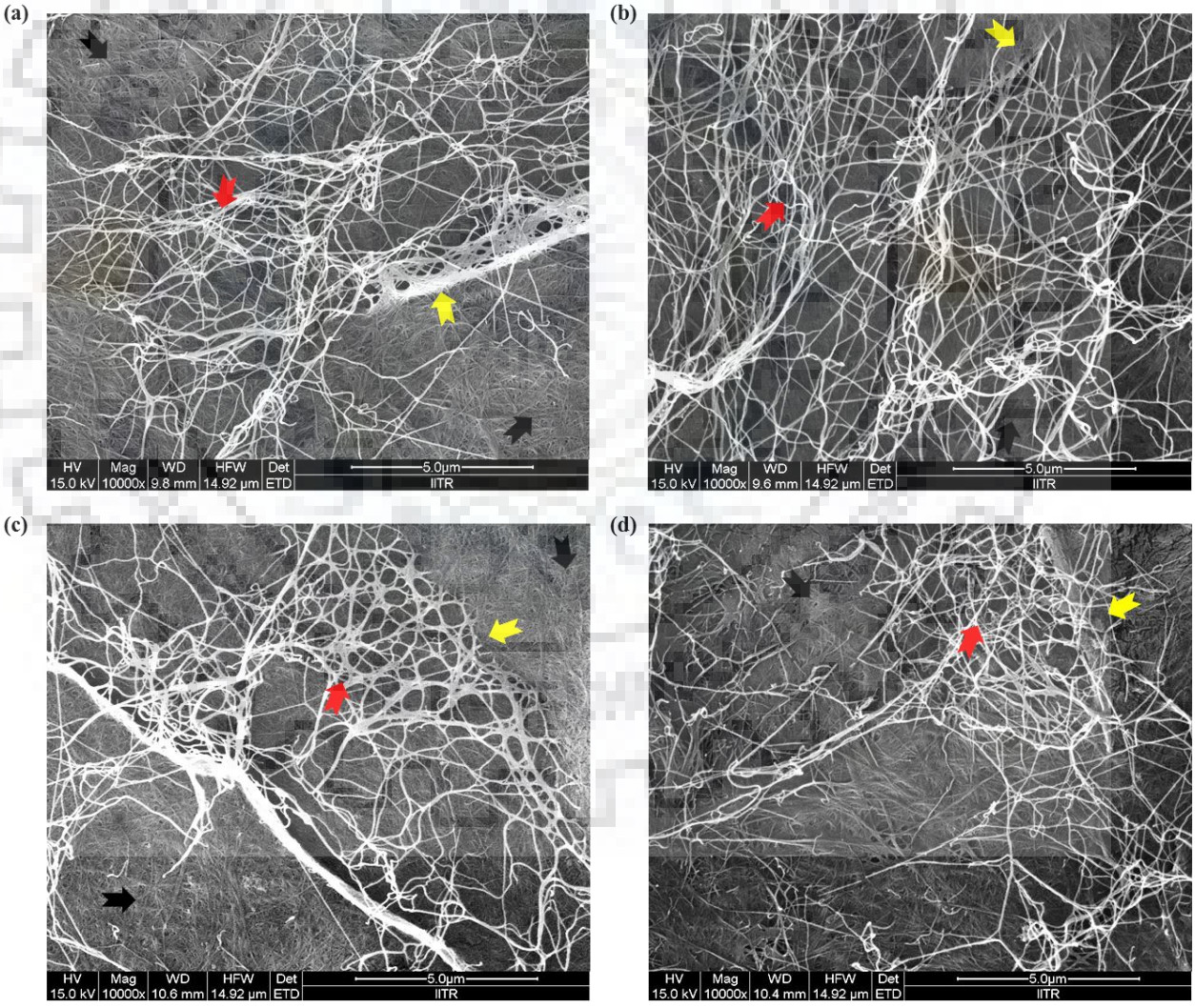

Fig. 4.4 Field emission scanning electron micrographs illustrating the micro-architecture of bacterial nanocellulose (BNC) produced in (a) $SLPW_E$, (b) $SLPW_{TE}$, (c) $SLPW_E$-HS(w) and (d) $SLPW_{TE}$-HS(w) under static batch cultivation (black arrow indicating densely packed cellulose nanofibers; red arrow representing loosely-knitted cellulose nanofibers and yellow arrow specifying the interfacial adhesion).

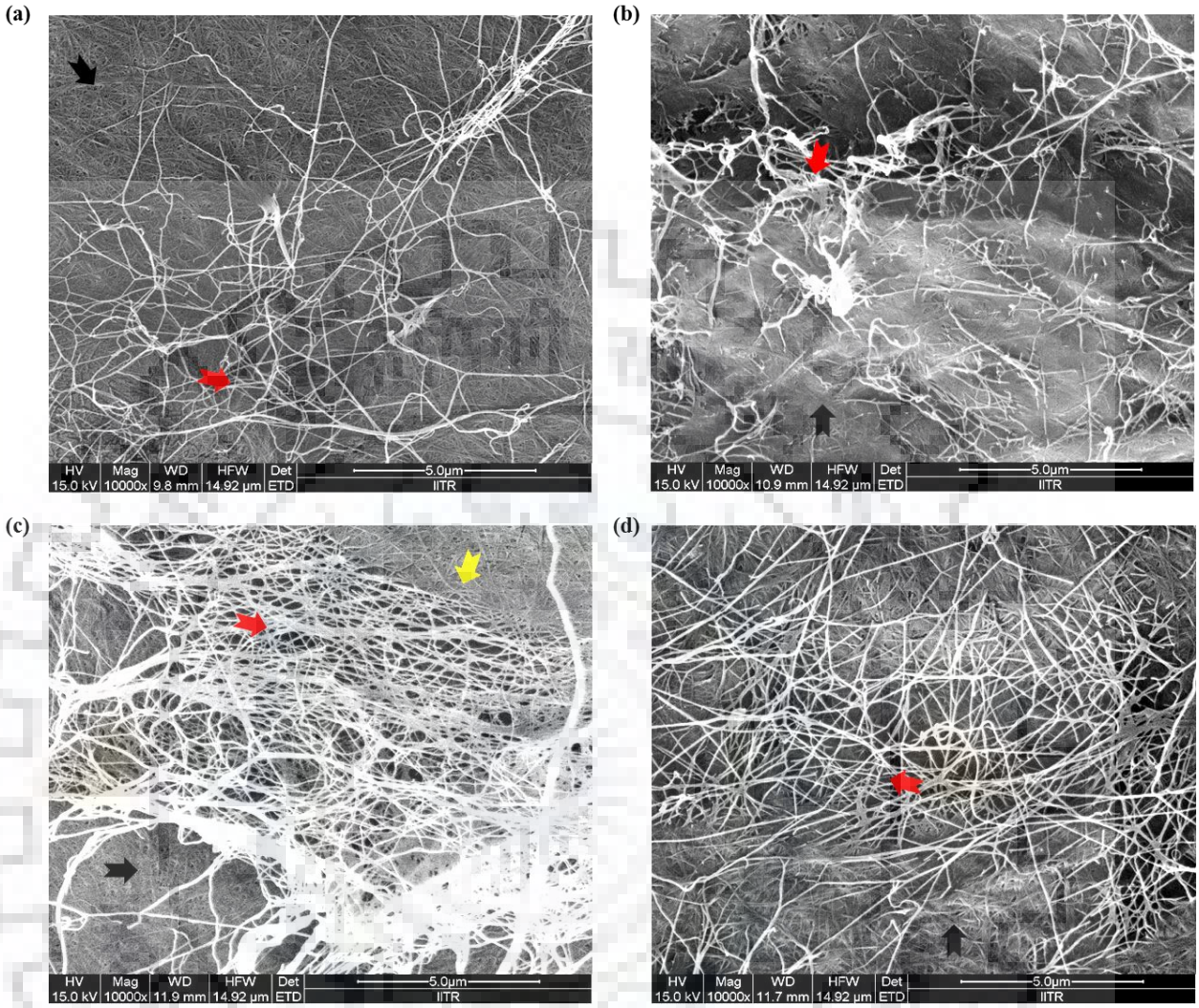

Fig. 4.5 Field emission scanning electron micrographs illustrating the micro-architecture of bacterial nanocellulose (BNC) produced in (a) BPW_E, (b) BPW_{TE}, (c) BPW_E-HS(w) and (d) BPW_{TE}-HS(w) under static batch cultivation (black arrow indicating densely packed cellulose nanofibers; red arrow representing loosely-knitted cellulose nanofibers and yellow arrow specifying the interfacial adhesion).

4.3.4.3 XRD

Fig. 4.6 and 4.7 shows the X-ray diffraction patterns of bacterial nanocellulose produced in different SLPW and BPW media, respectively. All the BNC samples (except the one produced in $SLPW_{TE}$) had exhibited three characteristic peaks at 2θ ~ 14.5, 16.5 and 22.5°, corresponding to $(1\bar{1}0)$, (110) and (200) crystallographic planes of the cellulose lattice respectively, which demonstrate a typical crystalline form of cellulose I [Tyagi & Suresh, 2016]. No reflections, instead, were found in correspondence of 2θ = 12.1 and 20.8, which are characteristic of cellulose II [Gea *et al.*, 2011]. Further, cellulose I is typically composed of two allomorphs *i.e.* Iα and Iβ

forms, the ratio of which is dependent on the microbial species, nutrient source and cultivation conditions [Castro *et al*., 2011; Tyagi & Suresh, 2016; Reiniati *et al*., 2017a]. According to Wada *et al*. (2001), these two allomorphs can be classified on the basis of characteristic set of d-spacings, as mentioned in Chapter 3, Section 3.2.10.2, Equation (iv). Table 4.10 and 4.11 enumerates the d-spacings connoting to the above-mentioned equatorial peaks and shows the dominancy of Iα allomorph in all the samples except the BNC obtained from $SLPW_{TE}$ whose spectrum was similar to that obtained by Gu and Catchmark, (2012) when the culture medium was provided with the xyloglucan, and indicates the dominancy of Iβ allomorph.

Further, Cr.I (%) of the BNC samples produced in water extracted SLPW medium (either used as a sole nutrient source *i.e.* $SLPW_E$ or supplemented with the components of HS medium *i.e.* $SLPW_E$-HS(w)) was little higher than that obtained with the optimized HS medium (87.7 %) under similar physiological parameters (Chapter 3, Table 3.4) while a decrease in the Cr.I (%) was observed in the BNC harvested from acid extracted SLPW media (viz. $SLPW_{TE}$ and $SLPW_{TE}$-HS(w)), as depicted in Table 4.10.

With regard to BNC produced in BPW media, highest crystallinity index was observed in BPW_E-HS(w) which was almost similar to that obtained in the optimized HS medium while the crystallinity index of the BNC samples produced from acid extracted BPW medium was greater than the BNC obtained from acid extracted SLPW media (Table 4.11).

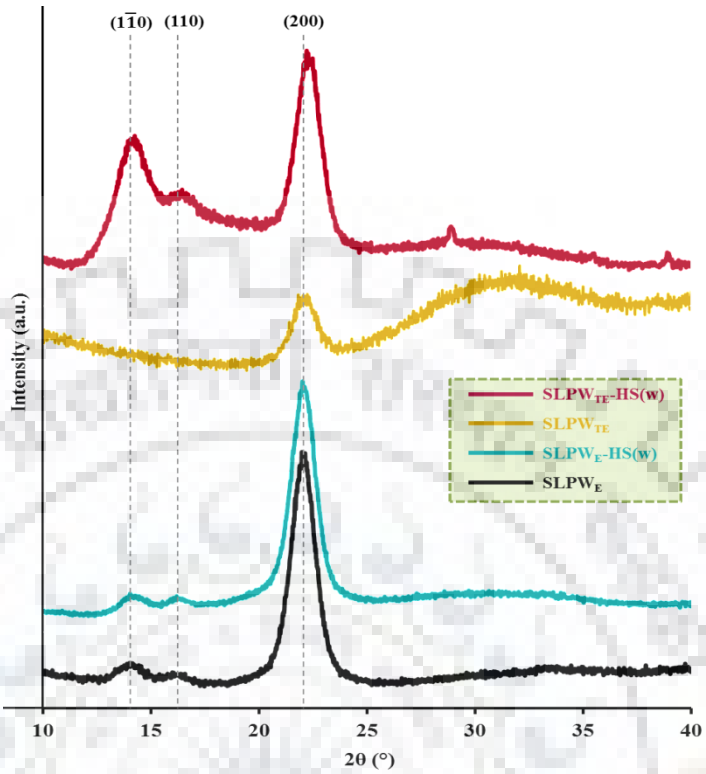

Fig. 4.6 X-ray diffraction patterns of bacterial nanocellulose produced by *K. europaeus* SGP37 in various SLPW media under static batch cultivation.

Table 4.10 d-Spacings, allomorphic category and crystallinity index of BNC produced by *K. europaeus* SGP37 in various SLPW media under static batch cultivation

Production medium	d-Spacing (nm)			Dominant allomorph	CrI (%)
	d1 (1$\bar{1}$0)	d2 (110)	d3 (200)		
$SLPW_E$	0.627	0.551	0.402	Iα	89.6
$SLPW_E$-HS(w)	0.619	0.546	0.402	Iα	88.8
$SLPW_{TE}$	-	-	0.399	Iβ	67.3
$SLPW_{TE}$-HS(w)	0.625	0.541	0.399	Iα	65.7

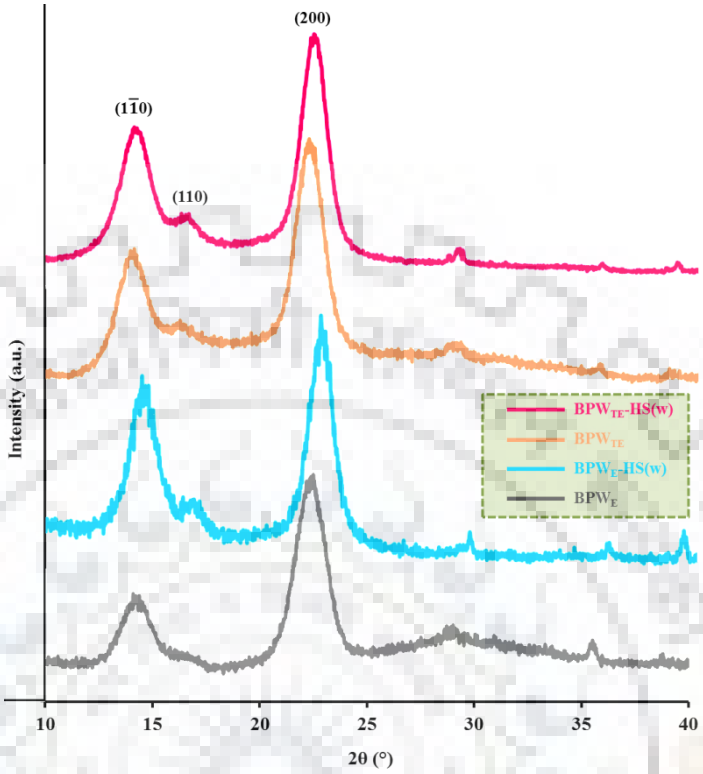

Fig. 4.7 X-ray diffraction patterns of bacterial nanocellulose produced by *K. europaeus* SGP37 in various BPW media under static batch cultivation.

Table 4.11 d-Spacings, allomorphic category and crystallinity index of BNC produced by *K. europaeus* SGP37 in various BPW media under static batch cultivation

Production medium	d-Spacing (nm)			Dominant allomorph	CrI (%)
	d1 (1$\bar{1}$0)	d2 (110)	d3 (200)		
BPW_E	0.621	0.533	0.395	Iα	85.46
BPW_E-HS(w)	0.608	0.526	0.390	Iα	87.36
BPW_{TE}	0.632	0.546	0.401	Iα	72.91
BPW_{TE}-HS(w)	0.626	0.535	0.396	Iα	82.59

4.3.4.4 TGA

TG-DTG curves of the dried BNC pellicles obtained from various SLPW and BPW media are shown in Fig. 4.8 and 4.9, respectively. The corresponding data are listed in Table 4.12 and 4.13 which summarizes the main degradation stages, maximum weight loss temperature and the respective degradation rates.

As shown in Table 4.12, BNC produced in water extracted SLPW media viz. $SLPW_E$ and $SLPW_E$-HS(w) showed the higher DTG values than the BNC harvested from acid extracted SLPW media which could be ascribed to their higher crystallinity index (Table 4.10) as the thermal degradation behavior is known to be influenced by the crystallinity and orientation of the fibers [Vazquez *et al*., 2013; Mohammadkazemi *et al*., 2015]. Similarly, the lower DTG values for the BNC obtained from $SLPW_{TE}$ and $SLPW_{TE}$-HS(w) medium could be attributed to their lower crystallinity, which is in the agreement with the results obtained by Mohammadkazemi *et al*. (2015). The similar pattern was observed for the BNC produced using BPW media as manifested in Table 4.13.

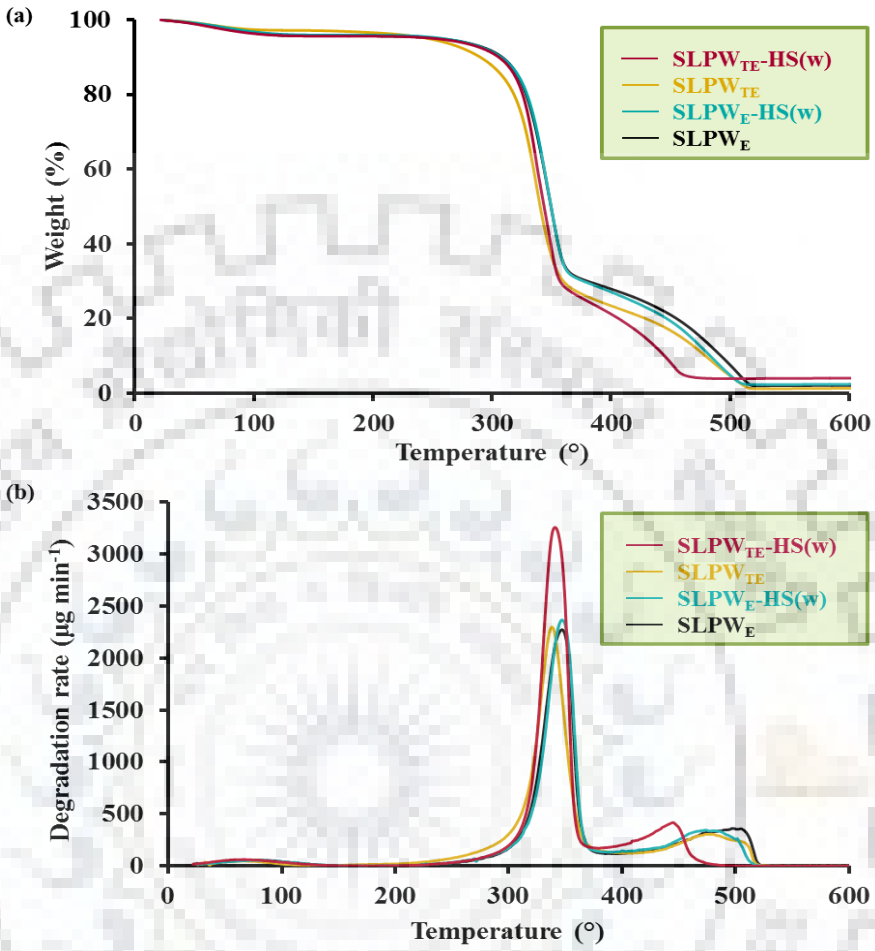

Fig. 4.8 (a) Thermogravimetric (TG) and (b) differential thermogravimetric (DTG) curves of bacterial nanocellulose produced by *K. europaeus* SGP37 in various SLPW media under static batch cultivation.

Table 4.12 Thermal degradation properties of bacterial nanocellulose produced by *K. europaeus* SGP37 in various production media prepared using sweet lime pulp waste as a feedstock

Production medium	Degradation stage	DTG peak (°)	Degradation rate (µg min^{-1}) at DTG peak
SLPW$_{E}$	1st	348	2270
	2nd	504	360
SLPW$_{E}$-HS(w)	1st	348	2360
	2nd	477	330
SLPW$_{TE}$	1st	338	2300
	2nd	481	300
SLPW$_{TE}$-HS(w)	1st	342	3250
	2nd	446	410

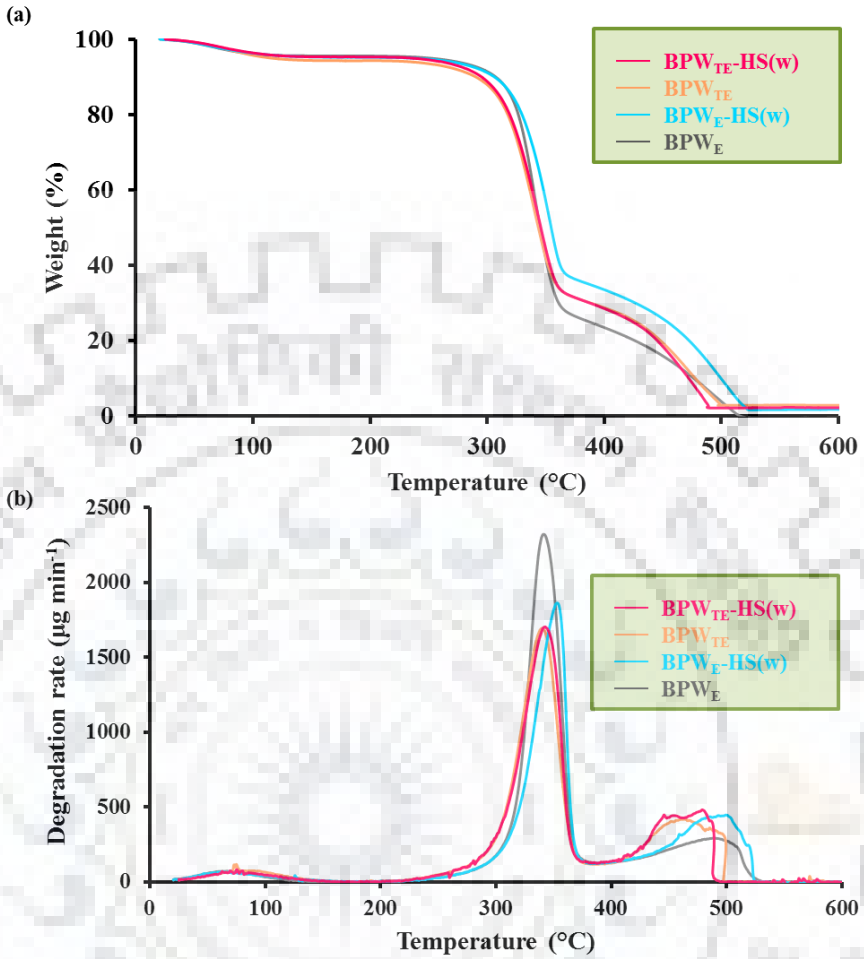

Fig. 4.9 (a) Thermogravimetric (TG) and (b) differential thermogravimetric (DTG) curves of bacterial nanocellulose produced by *K. europaeus* SGP37 in various BPW media under static batch cultivation.

Table 4.13 Thermal degradation properties of bacterial nanocellulose produced by *K. europaeus* SGP37 in various production media prepared using banana peel waste as a feedstock

Production medium	Degradation stage	DTG peak (°)	Degradation rate (µg min^{-1}) at DTG peak
BPW$_{E}$	1st	342	2320
	2nd	495	284
BPW$_{E}$-HS(w)	1st	353	1862
	2nd	492	440
BPW$_{TE}$	1st	339	1690
	2nd	459	414
BPW$_{TE}$-HS(w)	1st	343	1702
	2nd	478	476

4.4 CONCLUSIONS

The present study was aimed towards reducing the production cost of bacterial nanocellulose (BNC) by developing an inexpensive production medium followed by scaling-up the production process for higher productivity by designing a simple production process strategy to circumvent the major constraints of BNC commercialization at wider scale. Thus, sweet lime pulp waste (SLPW) and banana peel waste (BPW) were explored as a low- or no-cost feedstocks for green, sustainable and economic production of BNC using the isolate *K. europaeus* SGP37. The feedstocks were used alone and in amalgamation with other nutritional supplements under static batch and static intermittent fed-batch cultivation and demonstrated to have a great potential to serve as an alternative feedstock for BNC production. SLPW itself supported the growth of *K. europaeus* SGP37 to produce BNC with the yield of 6.30 ± 1.56 g L^{-1} after 16 days of static batch cultivation while passable results were obtained with BPW. Inclusion of other nutritional supplements and shifting of cultivation strategy from static batch to static intermittent fed-batch (IFB-48 h) had led into commendable BNC yields in both of the production media with 38 ± 0.85 g L^{-1} in $SLPW_E$-HS(w) and 24.30 ± 2.17 g L^{-1} in BPW_E-HS(w) with the substrate to BNC conversion of 60.47 % and 100.08 %, respectively. The BNC production yields reported here are, so far, the highest in a process using agro-industrial waste and *K. europaeus* bacterium; and opens up new avenues for future valorization of other biological wastes.

CHAPTER 5

Effect of various purification approaches on purity and physicochemical properties of BNC

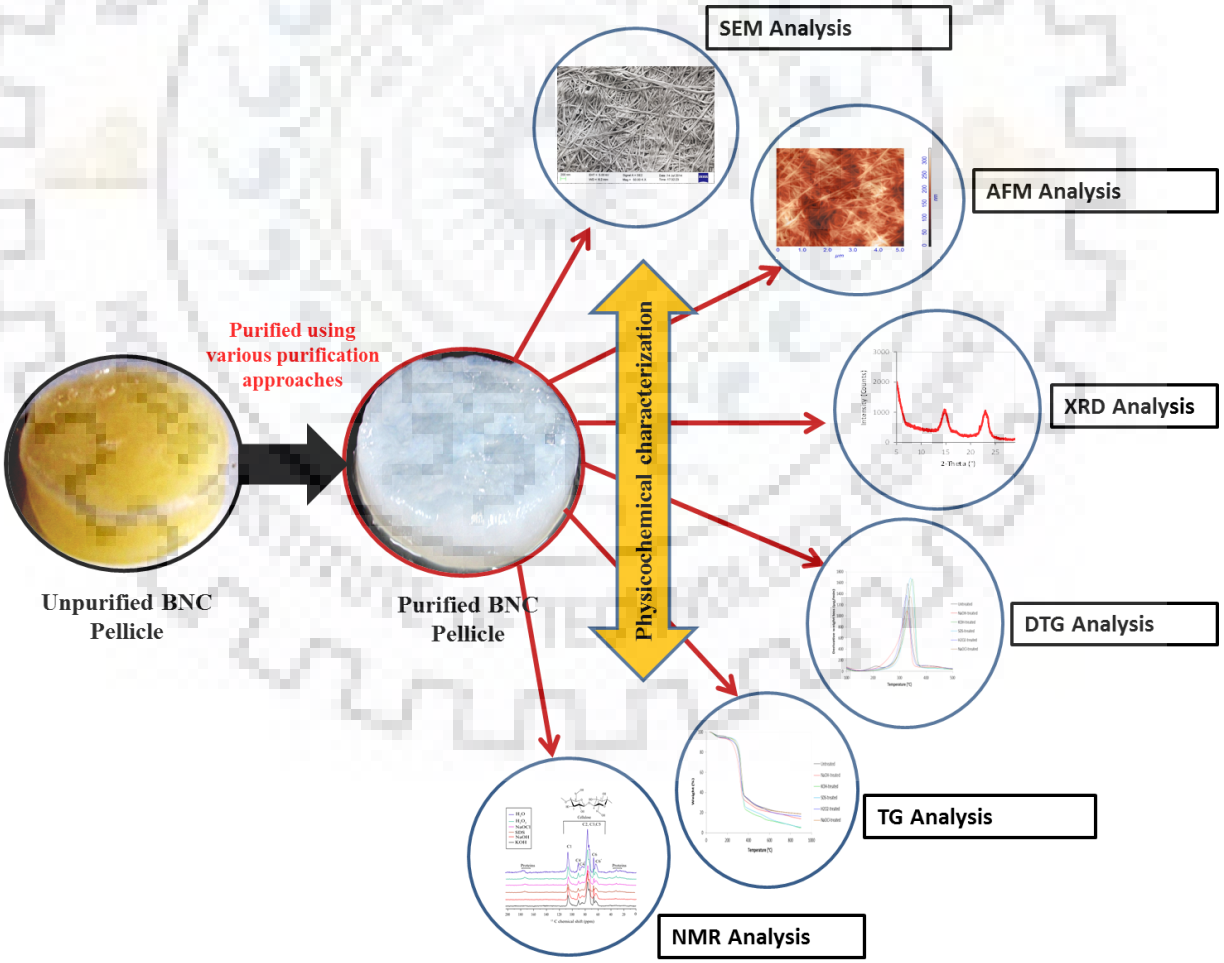

Effect of various purification approaches on purity and physicochemical properties of BNC

5.1 INTRODUCTION

Bacterial nanocellulose (BNC) synthesis befalls in a multi-step series of enzymatic reactions starting with the incorporation of monomeric glucose into β-1, 4-glucan chains that combine and forms subfibrils. About 10-100 subfibrils intertwine together to form crystalline nanofibrils (~3.5 nm in diameter) [Santos *et al*., 2015; Cacicedo *et al*., 2016]. Then, these nanofibrils are gathered in bundles, which in turn are united to form ribbons with 40–60 nm width [Cacicedo *et al*., 2016]. Ribbons interweave with ribbons from other bacterial cells, forming a two-dimensional layer. Finally, parallel layers interact with one another by hydrogen bonds and Van der Waals forces, generating a gelatinous membrane at the surface of the culture broth [Santos *et al*., 2015].

As discussed earlier also, due to this unique nanofibrillar structure, BNC acquires excellent physicochemical properties such as higher crystallinity and mechanical strength, which make it a material with multifarious applications in the fields as diverse as paper, textile, food and biomedicine [Shi *et al*., 2014; Mohite and Patil, 2014; Dubey *et al*., 2015; Cacicedo *et al*., 2016; Jozala *et al*., 2016; Picheth *et al*., 2017]; however, it's features and possible practices are mainly dependent on its structure.

A purification step has to be added to eliminate the bacteria and the culture medium components from the BNC before it is subjected to a relevant application. Several purification approaches such as NaOH, KOH and SDS were used for killing the bacteria [Sakairi *et al*., 1998; George *et al*., 2005; Moniri *et al*., 2017]; however alkaline treatment using NaOH is normally used for removal of bacterial cells from BNC pellicle [Chawla *et al*., 2009; Sulaeva *et al*., 2015]. However, Gea *et al*. (2011) had reported that this alkaline treatment is often accompanied with the undesirable alteration of the crystal structure from cellulose I to cellulose II to some extent, which in turn affects its physicochemical properties.

The concentration of NaOH used for this alteration differs, contingent on the type and the origin of cellulose being treated. Previous groups have reported that the transformation of cellulose I to cellulose II occurs at concentrations of NaOH above 6%; some reported that it is also affected by the immersion time used to treat the samples [Gea *et al*., 2011]. However, observation related to transformation of cellulose I to cellulose II due to alkalization remains unexplained and debatable.

In the course of the polymorphic transformation from cellulose I to cellulose II, a change in the cellulose chains conformation from parallel to anti-parallel ensues, which is accompanied by the breaking of several primary inter- and intra-molecular hydrogen bonds in cellulose I. This process initiates with fiber swelling due to water absorption, leading to a significant increase in the mobility of the cellulose chains. Thereafter, the alkaline solution penetrates the amorphous areas of the cellulose, before saturating the cellulose and disrupting the crystalline regions; and forms new crystalline frames after the mercerizing solution is washed off [Gea *et al*., 2011]. This transformation impacts into significantly decreased mechanical properties of the cellulose.

Hence, the present study was carried out to evaluate the impact of various treatment approaches onto the purity and physicochemical properties of BNC in order to find out precisely a process that can remove the bacteria and other culture medium components from BNC pellicle but, at the same time, preserves it physico-chemical features. Thus, the chapter includes:

- ☞ Purification of BNC pellicles using various purifying agents
- ☞ Physicochemical characterization of purified BNC pellicles in terms of its purity, morphology, crystallinity and thermal stability

5.2 MATERIALS AND METHODS

5.2.1 Materials

Sodium hydroxide, potassium hydroxide and sodium dodecyl sulfate were purchased from Himedia, India. Hydrogen peroxide and sodium hypochlorite were procured from SRL, India. All the chemicals used were of analytical grade or of the highest purity available.

5.2.2 Microorganism and culture media

Komagataeibacter europaeus SGP37 isolated from rotten grapes (Chapter 3) was used for BNC production. Hestrin-Schramm (HS) medium (20 g L^{-1} glucose, 5 g L^{-1} yeast extract, 5 g L^{-1} peptone, 2.7 g L^{-1} disodium hydrogen phosphate, 1.15 g L^{-1} citric acid, pH 6) was used as the seed and the production medium.

5.2.3 Production of BNC

A suspension culture for pre-inoculum was prepared by transferring a single bacterial colony into 20 mL of HS broth (pH-6), with incubation of 72 h at 30 °C under static conditions. After incubation, 20% v/v of this cell suspension was added into 50 mL of HS medium (pH-6) and incubated at 30 °C for 48 h under static conditions. This statically grown culture was then shaken vigorously to release the bacterial cells from BNC pellicle, and 10% v/v of the resulting cell suspension was inoculated into 250 mL Erlenmeyer flasks containing 50 mL of HS medium (pH 6.0) and incubated statically at 30 °C for 16 days.

5.2.4 Purification of BNC

After incubation, pellicles formed at air-liquid interface were removed, washed thoroughly under running tap water to remove residual medium and other contaminants, and then the pellicles were treated with 0.5 M NaOH, 0.5 M KOH, 10% SDS, 0.5 M NaOCl and 0.5 M H_2O_2 separately, at 100 °C for 1 h to lyse and eliminate bacterial cells, followed by boiling in distilled water (DW) for 30 min. These are hereafter referred to as NaOH-treated BNC, KOH- treated BNC, SDS-treated BNC, NaOCl- treated BNC and H_2O_2- treated BNC respectively. Some of the pellicles were just boiled in DW for 1 h without any purifying agent and these samples were named as

water washed or untreated BNC. All the pellicles were further washed repeatedly with distilled water until its neutralization, dried at 60 °C to constant weight, and used for further analysis.

5.2.5 Physicochemical characterization

5.2.5.1 CP/MAS ^{13}C-NMR

Solid-state CP/MAS ^{13}C-NMR spectral acquisition was carried out using Avance III 600 MHz Bruker-BioSpin NMR spectrometer, operating at 150.15 MHz. The experiment was performed at ambient temperature using Bruker 3.2 mm DVT probe. The dried BNC pellicles were ground and packed into a 3.2 mm zircon rotor, which was spun at 10 kHz. The CP contact time and the recycle delay were 1 ms and 3 s, respectively and the spectra were acquired by accumulating 20 k scans per sample.

5.2.5.2 AFM

AFM measurement of the BNC membranes was conducted on NTEGRA-MDT (Moscow, Russia) atomic force microscopy using the program NOVA in tapping mode.

5.2.5.3 FE-SEM

The micro-morphology of BNC pellicles were observed by FE-SEM (Carl Zeiss, Ultra plus, Germany). The dried pellicles were gold coated for 90 s at the coating current of 31 mA in a Denton gold sputter unit (Biotech SC005, Switzerland) before being mounted in the FE-SEM and the micrographs were acquired at 50 k X.

5.2.5.4 XRD

XRD patterns of the BNC pellicles purified using various agents were recorded with Bruker AXS D8 Advance powder X-ray diffractometer using Ni-filtered Cu-Kα radiation (λ = 1.54 Å) from 10-30° 2θ range at 2° min^{-1} scan rate. The crystallinity index of BNC was calculated using Segal method [Segal *et al*., 1959], as described in Chapter 3, Section 3.2.10.2, eq. (4).

Further, the allomorphic category of the purified BNC (I_α or I_β form) was also determined on the basis of Z discriminant function, developed by Wada *et al*. (2001), as defined in Chapter 3, Section 3.2.10.2, eq. (5).

5.2.5.5 TGA

Thermogravimetric and derivative thermogravimetric (TG-DTG) analysis of the dried BNC pellicles were carried out on Thermogravimetric/Differential Thermal Analyzer (EXSTAR TG/DTA 6300, Hitachi, Tokyo, Japan) over a temperature range of 25–600 °C, at the scan rate of 10 °C min^{-1} (mass 10.5 mg) under a nitrogen atmosphere with N_2 flow rate of 200 mL min^{-1}.

5.3 RESULTS AND DISCUSSION

5.3.1 Solid-state cross-polarization/magic angle spinning ^{13}C-nuclear magnetic resonance spectroscopy (CP/MAS ^{13}C-NMR)

Purity of the treated and untreated BNC membranes was monitored using solid-state CP/MAS ^{13}C-NMR, and the signals generated were assigned according to the literature available [Atalla and Vanderhart, 1984; Park *et al*., 2010; Yamazawa *et al*., 2013]. Only the BNC treated with NaOH and KOH had shown the pure fingerprints of cellulose as described in Chapter 3 while the other treated samples were found to be contaminated by proteins which may be due to the presence of bacterial smidgens left after purification (Fig. 5.1).

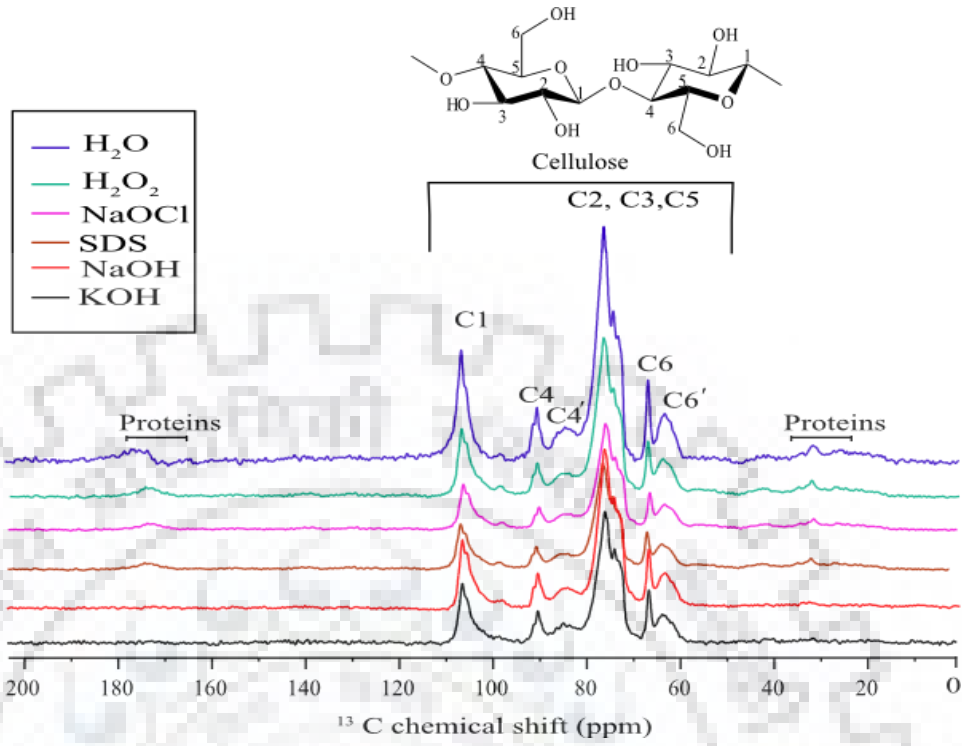

Fig. 5.1 CP/MAS ^{13}C-NMR spectra of untreated and treated bacterial nanocellulose

5.3.2 Atomic force microscopy (AFM)

AFM measurement in tapping mode was conducted on NTEGRA-MDT atomic force microscopy using the program NOVA which revealed some rod like structures (which may be bacterial cells) in the BNC samples treated with H_2O_2 and NaOCl (Fig. 5.2 e, f) while NaOH, KOH and SDS treated BNC membranes had shown a clear reticulated mat of BNC nanofibers (Fig. 5.2 b, c, d).

5.3.3 Field emission scanning electron microscopy (FE-SEM)

To validate the results obtained with AFM, the micro-architecture of BNC pellicles was reconnoitered by field-emission scanning electron microscope (FE-SEM) and revealed a densely packed, extensively interwoven network of highly extended fibers which were crossed, superimposed and randomly oriented (Fig. 5.3). The size of the ribbons was in the range of 40-60 nm. Further, rod like bacterial cells were observed in untreated, H_2O_2-treated and NaOCl-treated BNC membranes (Fig. 5.3 a, e, f) while some cloudy aggregations of bacterial cell debris were found in the SDS treated BNC membrane (Fig. 5.3 d). These can be compared with the NaOH-

treated and KOH treated BNC (Fig. 5.3 b, c) where the bacterial cells and other impurities can no longer be seen on the surface of the membranes which confirms the results of AFM. These results are in consistent with the results obtained from NMR which demonstrated the purity of NaOH-treated and KOH treated BNC.

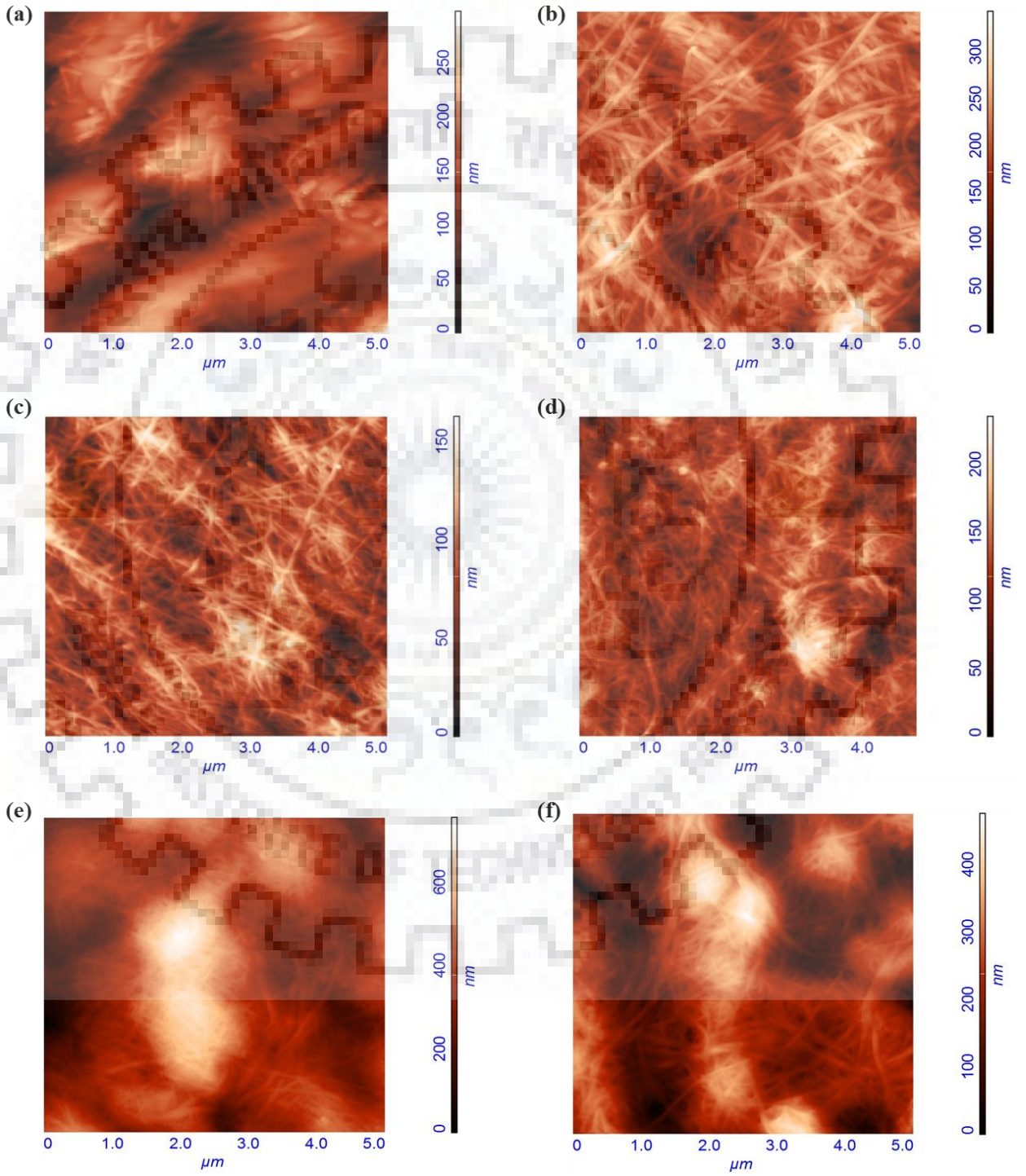

Fig. 5.2 AFM micrographs of (a) untreated, (b) NaOH-treated, (c) KOH-treated, (d) SDS-treated, (e) H_2O_2- treated, and (f) NaOCl-treated BNC membranes

Fig. 5.3 FE-SEM micrographs of (a) untreated, (b) NaOH-treated, (c) KOH-treated, (d) SDS-treated, (e) H_2O_2-treated and (f) NaOCl-treated BNC membranes

5.3.4 X-ray diffraction (XRD)

Since only NaOH, KOH and SDS treatments were found effective in purifying BNC, thus the next studies were carried out on the BNC samples treated using these agents only. Fig. 5.4 shows the XRD patterns of BNC membranes treated with the above mentioned purifying agents. Three distinct peaks were appeared at 2θ equalling to ~14.5°, 16° and 22.5° which were assigned to the reflexion planes of (1 $\bar{1}$ 0), (110) and (200), respectively. This XRD pattern showed a typical crystalline form of cellulose I, and was in agreement with the relative reports [Gea *et al*., 2011; Tyagi & Suresh, 2016]. All the samples showed Iα form of cellulose and the crystallinity index were in the order KOH>NaOH>SDS with 79.4%, 77.4% and 76.5%, respectively.

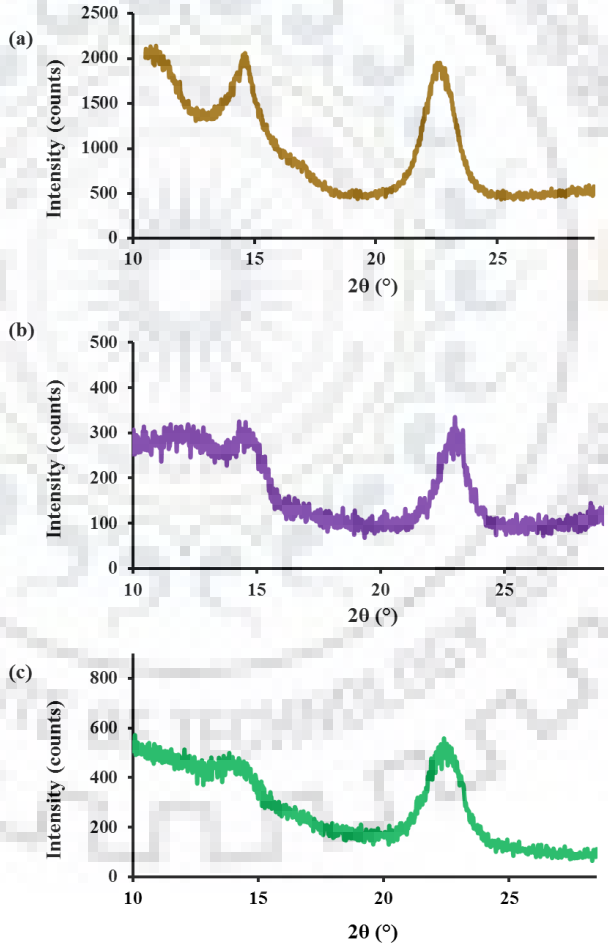

Fig. 5.4 X-ray diffractograms of (a) NaOH-treated, (b) KOH-treated, (c) SDS-treated BNC membranes

5.3.5 Thermogravimetric analysis (TGA)

The percent weight loss for NaOH-treated BNC at 300 °C was 15.92%, while for other treated membranes *viz* KOH and SDS treated; it was 15.23% and 11.12%, respectively. In case of NaOH-treated BNC, 50% weight loss was manifested at 341 °C, while it was 346 °C and 342 °C for KOH and SDS treated BNC, respectively. Moreover, the main DTG peak for NaoH-treated BNC was appeared at 343 °C while the main DTG peaks for KOH and SDS treated BNC were observed at 351 °C and 339 °C, respectively (Fig. 5.5).

Though, the results obtained from TGA and XRD analysis does not vary too much, but together these results suggests that the KOH treatment is more effective over the most commonly used NaOH treatment for the purification of BNC.

(a)

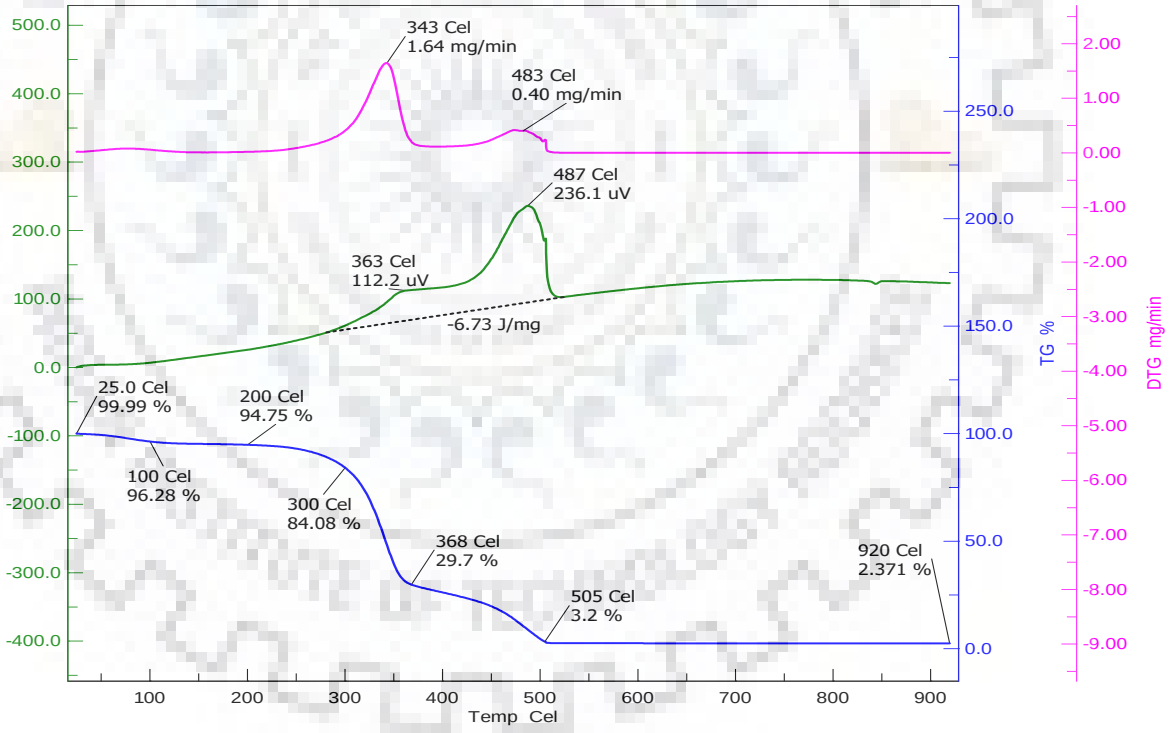

(b)

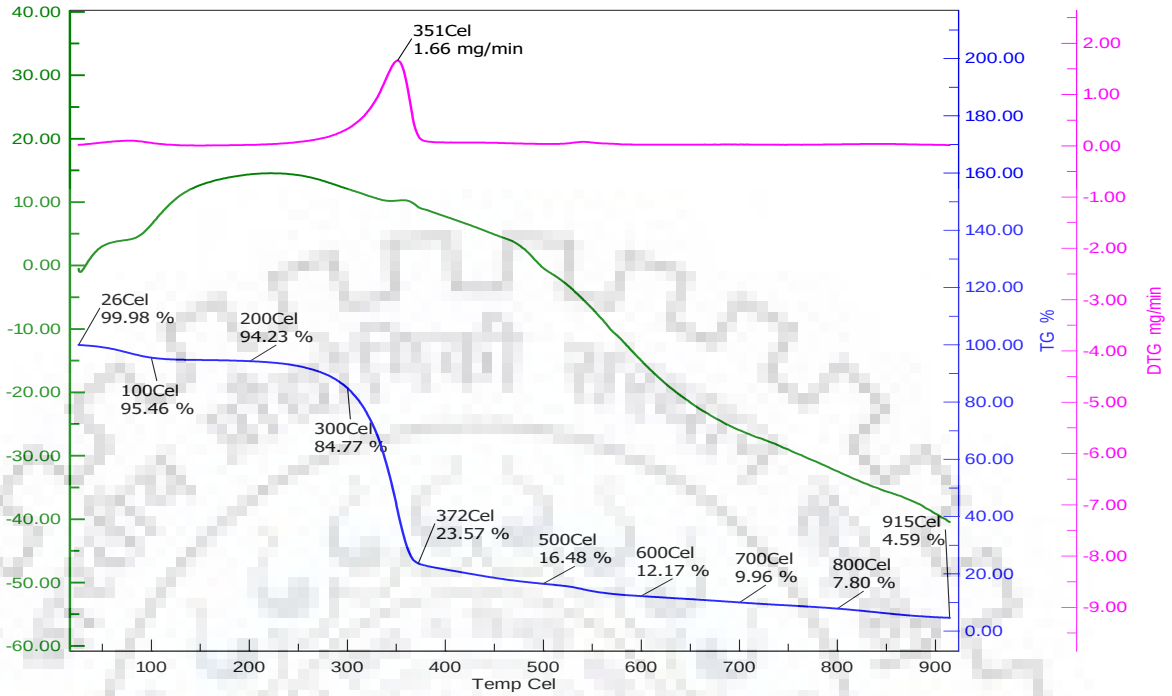

(c)

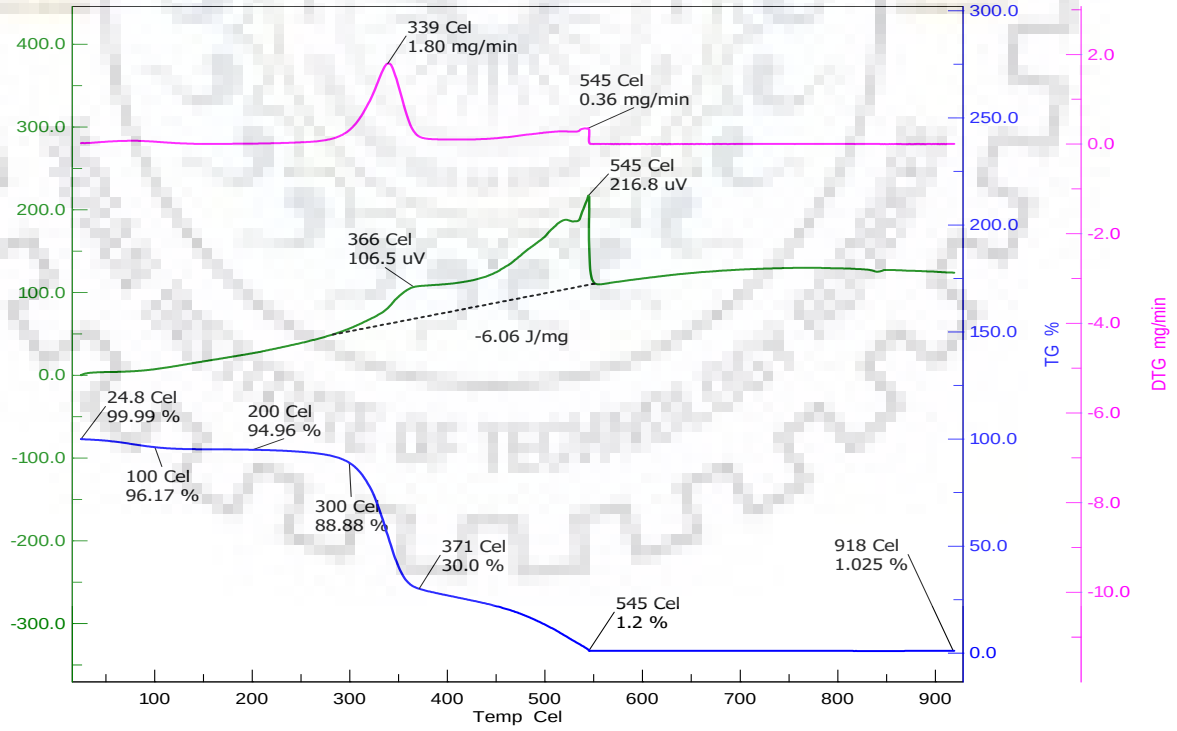

Fig. 5.5 TG-DTG curve of BNC purified using (a) NaOH, (b) KOH and (c) SDS

5.4 CONCLUSIONS

This study was carried out to evaluate the impact of various treatment approaches onto the purity and physicochemical properties of BNC in order to find out precisely a process that can remove the bacteria from BNC pellicle but, at the same time, prevents the polymorphic transformation of cellulose I to cellulose II. BNC treated with NaOH and KOH had shown the pure fingerprints of cellulose while the other treated samples were found to be contaminated by proteins which may be due to the presence of bacterial smidgens left after purification. AFM and FE-SEM analyses also revealed the presence of bacterial cells and some other cloudy aggregations in all the BNC membranes except the BNC purified using NaOH and KOH. However, the BNC membrane purified using KOH method was more crystalline and thermally stable than the membrane purified using NaOH. Together, these results suggested that the KOH treatment of the pellicle was effectively able to remove the bacterial cells and other contaminants from the BNC membrane and at the same time was able to maintain the physicochemical properties of BNC.

CHAPTER 6

Preparation of 3-D microporous-nanofibrous BNC scaffolds and evaluation of their potential for bone tissue engineering

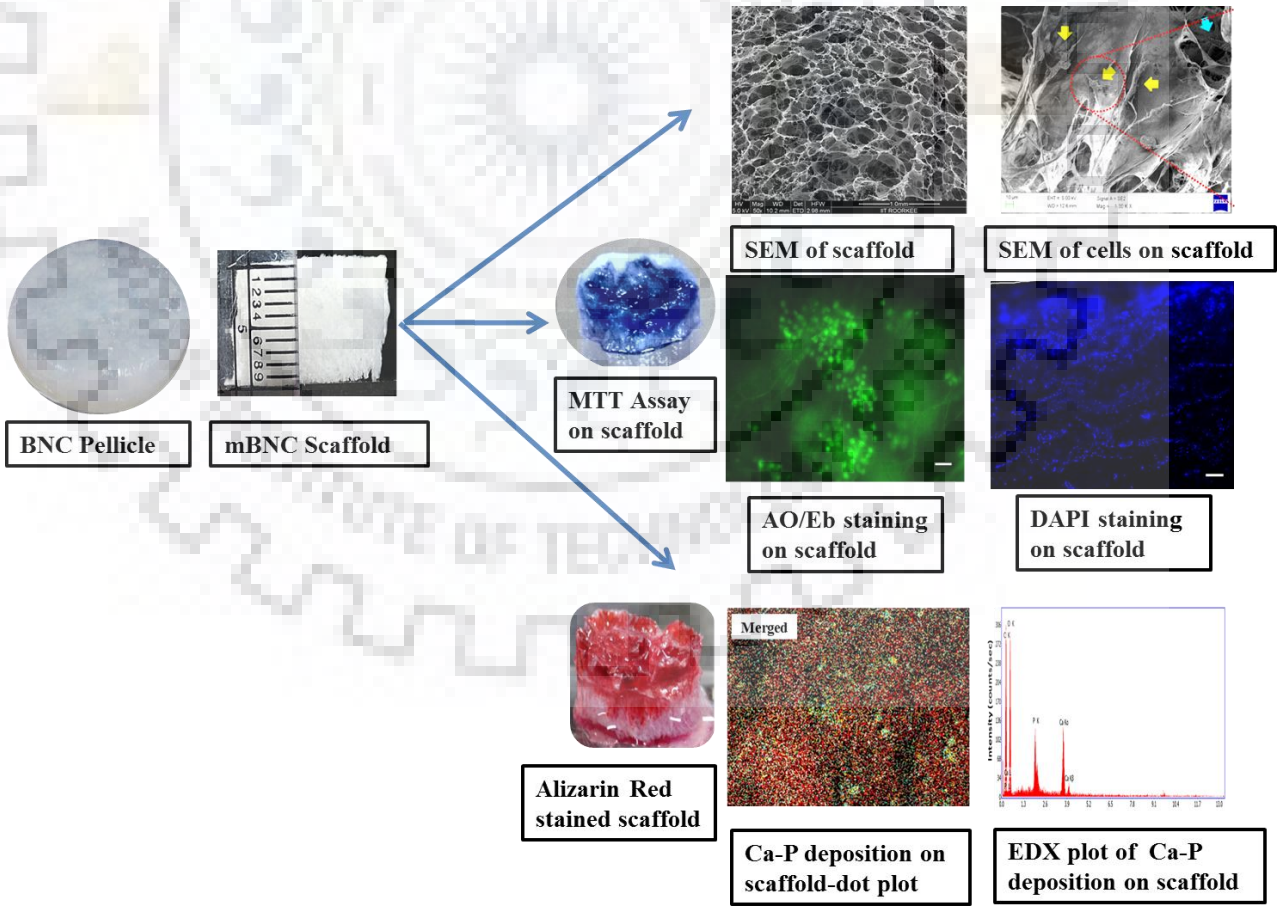

6.1 INTRODUCTION

The deformation and deterioration of bone due to the age or some pathological conditions such as trauma, congenital defects and tumor creates large tissue deficits that do not heal normally, and necessitates bone grafts to stimulate the healing process. This deteriorated bone can be supplanted by autologous, allogenous or xenografting; but the two last options risk graft rejection and pathogen transmission [Zaborowska *et al*., 2010]. Though the autologous bone graft exhibits the best clinical outcome but the limitation of donor tissue in terms of shape, size and quantity makes it incongruous for the repair of larger bone discrepancies. Besides, it involves surgery at multiple sites to harvest the donor tissue, which may compromise normal bone structure. Metals and ceramics primarily used in the hip implants [Katti, 2004], could be the another graft option but they do not provide optimal mechanical assets and exhibit poor osseointegration [Katti, 2004] and eventually fail due to infection or fatigue loading [Salgado *et al*., 2004]. Every year, approximately one million cases require bone-graft procedures which make bone the second most transplanted tissue after blood [Zaborowska *et al*., 2010]. Cumulatively, these findings accentuate the major clinical need for new bone grafting materials; and efforts have been underway for the past few years to search for the strategies and alternate materials that can be processed easily into larger, complex structures and can direct the body's own repair mechanism.

In this concern, tissue engineering offers almost illimitable possibilities by supplanting the damaged and/or diseased parts with new tissues grown *in vitro*, to meet the requirements of repair sites. One of the fundamental essentials in tissue engineering is the three-dimensional biomaterial scaffold which serves as a template to provide structural support to the cells for adhesion, infiltration, proliferation and differentiation [Hutmacher, 2000]. Bone cells *in vivo* live in the extracellular matrix (ECM) which is organized as a 3-D porous network with hierarchical structures from nanometer length scale multi-fibrils to macroscopic tissue architecture [Li *et al*., 2006] and acts as a structural and biochemical support for the cell growth. Thus, an ideal scaffold for bone tissue engineering should mimic the topographies and spatial structures of native ECM to facilitate the proliferation and differentiation of seeded cells for effective bone regeneration. Therefore, a significant attention has been paid to methods for the fabrication of porous 3-D scaffolds which resemble the microenvironment of natural ECM. To date, a number of 3-D

scaffolds have been fabricated using various natural and synthetic polymers, such as gelatin, collagen, chitosan, polyglycolic acid (PGA), poly (lactic acid) (PLA), poly [lactic-co-(glycolic acid)] (PLGA) among others, and have been used for the tissue engineering of bone [Amini *et al*., 2012; Motamedian *et al*., 2015].

Distinguished from the aforementioned polymers, bacterial cellulose owns a natural 3-D nanofibrils network (hence also termed as bacterial nanocellulose or BNC) which has a similar shape to that of the collagen nanofibrils of natural ECM [Gao *et al*., 2011]. Meanwhile, it displays unique mechanical properties with excellent biocompatibility, *in situ* moldability and high water holding capacity [Cacicedo *et al*., 2016; Jozala *et al*., 2016], all these make BNC a superb scaffolding candidate for bone tissue engineering. However, the major downside of this naturally woven scaffold is the lack of cell infiltration which constrains its practical usage as tissue engineering scaffold [Gao *et al*., 2011].This is caused by inadequate pore size ensuing from tightly packed BNC fiber layers [Bachdahl *et al*. 2006], which is hard for cells to penetrate; thus hinders tissue in-growth. It has been documented that the pore size of scaffold is a crucial parameter in the development of scaffolds for tissue engineering and the pores must be interconnected and large enough to allow cell growth and migration, nutrient flow, vascularization, new tissue formation and remodeling so as to facilitate host tissue integration upon implantation [Xiong *et al*., 2014]. In this context, creation of pores suitable for cell growth and migration would be pertinent for effective 3- dimensional tissue in-growth which would lead into efficient regeneration of bone.

Thus, the goal of this study was to prepare 3-dimensional microporous-nanofibrous scaffolds using bacterial nanocellulose and to evaluate the potential of these scaffolds for bone tissue engineering. To this end, microporous-nanofibrous BNC scaffolds (mBNC) were prepared and thoroughly characterized in terms of their morphology, chemical structure, crystallinity, thermal stability and biodegradability which were then followed by culturing C3H10T1/2 mesenchymal stem cells on these scaffolds to assess the cell attachment, proliferation, infiltration and osteoblastic differentiation for effective regeneration of bone tissue.

6.2 MATERIALS AND METHODS

6.2.1 Chemicals, cells, culture media and kits

Dulbecco's Modified Eagle's medium (DMEM), fetal bovine serum (FBS), trypsin, dexamethasone, phosphate buffer saline (PBS), cell culture-grade dimethyl sulfoxide (DMSO), lysozyme, MTT (3-(4, 5-dimethylthiazol-2-yl)-2, 5-diphenyltetrazolium bromide), acridine orange (AO), ethidium bromide (EtBr), alizarin red and bone morphogenetic protein-2 (BMP-2) were purchased from Himedia Laboratories, India. HMDS (Bis(trimethylsilyl)amine) and DAPI (4',6-diamidino-2-phenylindole) were acquired from Sigma Aldrich. The kits for LDH (lactate dehydrogenase) assay was obtained from Himedia Laboratories, India and C3H10T1/2 mesenchymal stem cells were procured from National Centre for Cell Science (NCCS), Pune, India.

6.2.2 Preparation of 3-D mBNC scaffolds

BNC pellicles were produced and purified using the methods described in Chapter 3 and 3-D microporous-nanofibrous BNC scaffolds were prepared using these pellicles by freeze drying method with minor modifications [Xiong *et al*., 2014]. Briefly, the BNC pellicles were crushed using a home-made blender at 4000 rpm for 5 min and the resulting BNC emulsion was then poured into appropriate molds and freeze-dried at -50 °C for 48 h. The resulting scaffolds were stored at room temperature (RT) and used for further studies.

6.2.3 Characterization of scaffolds

6.2.3.1 Field emission scanning electron microscopy (FE-SEM)

The microscopic morphology of mBNC scaffolds was observed by FE-SEM (FEI Quanta 200 FEG) at an accelerated voltage of 15 kV. Briefly, the scaffolds were gold coated for 90 s in a Denton gold sputter unit before being mounted in the FE-SEM and the micrographs were acquired at desired magnifications.

6.2.3.2 Fourier transform infrared spectroscopy (FTIR)

FTIR analysis of mBNC scaffolds was performed using Thermo Nicolet NEXUS 670 FTIR spectrophotometer in the spectral region of 4000–450 cm^{-1} at 4 cm^{-1} resolution to find out any changes in the chemical structure of BNC after scaffold preparation.

6.2.3.3 X-ray diffraction (XRD)

X-ray diffraction pattern of the freeze dried BNC scaffolds was acquired with Bruker AXS D8 Advance powder X-ray diffractometer using Ni-filtered Cu-Kα radiation (λ = 1.54 Å). The data were collected in 10-40° 2θ range at 2° min^{-1} scan rate and the crystallinity index was calculated according to the method defined by Segal et al. (1959), as described in Chapter 3, Section 3.2.10.2, equation (4) to find out any changes in the crystallinity level.

6.2.3.4 Thermogravimetric analysis (TGA)

TGA analysis of the scaffolds was done using Thermogravimetric/Differential Thermal Analyzer (EXSTAR TG/DTA 6300, Hitachi, Tokyo, Japan) over a temperature range of 25-600 °C at 10 °C min^{-1} scan rate (sample mass ~10.5 mg). All the measurements were performed under a nitrogen atmosphere with N_2 flow rate of 200 mL min^{-1}.

6.2.4 Degradation behavior of the scaffolds

The degradation ratio of the mBNC scaffolds was measured at different time points for 2 months in PBS (phosphate buffer saline) and PBS containing 0.2 % lysozyme. Briefly, the scaffolds were incubated in the above mentioned solutions at 37 °C for the different time points (15 days, 30 days and 60 days) and at respective time junctures, the scaffolds were removed, washed thrice with deionized water to remove salts and immersed in 100% ethanol for 2 h which was then followed by drying at room temperature till constant weight. The weight loss of the scaffolds (as a measure of degradation) was observed by weighing the dried samples.

6.2.5 Cell culture

C3H10T1/2 mesenchymal stem cells were plated in a 5 cm cell culture dish (NEST Biotechnology, USA) at a density of 50,000 cells/cm^2, using expansion/proliferation media (denoted PM) consisted of Dulbecco's Modified Eagle's Medium (DMEM), 10% fetal bovine serum (FBS), 1% penicillin (100 U/mL) and 1% streptomycin (100 mg/mL) and propagated at 37 °C in a humidified atmosphere of 5% CO_2, till 80% confluency. After confluency, the cells were trypsinized and used for the seeding on scaffolds.

6.2.6 Cell seeding on 3-D mBNC scaffolds

Before cell seeding, the scaffolds were autoclaved at 121 °C for 20 min followed by UV sterilization for 2 h. The scaffolds were then transferred to 12-well tissue culture plates (NEST Biotechnology, USA), washed three times with sterile PBS and then incubated at 37 °C for 12 h in cell culture medium (proliferation medium) before cell seeding.

After incubation, C3H10T1/2 cells (passage 10) were seeded onto the scaffolds at a cell density of 1,00,000 cells/scaffold and the plate was kept at 37 °C under humidified atmosphere with 5% CO_2 for cell attachment. After 4 h of incubation, 2 mL of proliferation media was added into each well and the plates were again placed in a humidified incubator at 37 °C and 5% CO_2 for the duration of the experiments and the culture medium was changed at each alternate day.

6.2.7 Cell attachment

Field emission scanning electron microscopy (FE-SEM) analysis of the scaffolds was performed to see the cell adhesion. After 12 h of incubation, the cell seeded scaffolds were washed twice with PBS and fixed with 4% formaldehyde for 30 min. After further washing with PBS, the scaffolds were dehydrated in a series of ethanol solutions with increasing concentrations (10% to 100% at 5 min interval) and finally dried with hexamethyldisilazane (HDMS). For FE-SEM analysis, the dried cell seeded scaffolds were sputter coated with gold for 90 sec and observed by FE-SEM (Carl Zeiss, Ultra plus, Germany), operating at an accelerated voltage of 5 kV.

6.2.8 Cell proliferation and viability

MTT assay, LDH Assay and live/dead cell assay of the cell seeded scaffolds were performed after 1, 4 and 7 days of incubation to assess the cell viability and proliferation.

6.2.8.1 MTT assay

C3H10T1/2 cells (1,00,000 cells/scaffold) were cultured on mBNC scaffolds for 1, 4 and 7 days in 12-well tissue culture plate before being subjected to MTT assay. The scaffolds that were not seeded with the cells were taken as control to ignore the non-specific adsorption of MTT onto the scaffolds.

MTT reagent at a working concentration of 0.5 mg/ml was added to the each well at the above mentioned time points and the plate was incubated in darkness for 4 h at 37 °C with 5% CO_2. After incubation, the solution in the wells was removed carefully and 500 µL of DMSO was added in each well. The plate was then placed on a shaker under darkness for 1 h to dissolve the MTT formazan crystals. Subsequently, 100 µL of the dissolved formazan solution of each well was transferred to the individual wells of 96-well plate and the absorbance was recorded at 570 nm using microplate reader (Fluostar optima, BMG labtech, Germany).

6.2.8.2 LDH assay

The cytotoxicity of the mBNC scaffolds was assessed by quantifying lactate dehydrogenase (LDH) leakage into the culture medium caused by cell membrane damage [Tazi *et al*., 2012]. The quantity of LDH released is relational to the number of damaged or lysed cells.

The cells were seeded onto the scaffolds at a density of 1,00,000 cells/scaffold and incubated for 1, 4 and 7 days. The culture medium was removed at each respective time point and the release of LDH into the medium was determined by the LDH activity assay kit according to the manufacturer's instructions (Himedia, India). Briefly, 100 µL of the culture medium was transferred to a 96-well plate and added with the 50 µL of reconstituted substrate mix (LDH reagent) provided in the kit. The plate was then incubated in the dark at room temperature for 15 min. To stop the reaction, 50 µL of stop solution (provided in the kit) was added to each well and absorbance was recorded at 570 nm using microplate reader. Treatment of cells with lysis solution

(provided in the kit) served as a 100% positive control of cell damage and the fresh culture media (PM) served as background control. The LDH release was calculated using the following formula:

Total LDH release (%) = (Experimental – Background control) / (Positive control-Background control)*100

6.2.8.3 Live/dead cell assay

To further assess the cell viability of the C3H10T1/2 cells on mBNC scaffold, the cells were grown on the scaffolds for 1, 4 and 7 days. After incubation, the cell seeded scaffolds were rinsed gently with PBS and stained with equal volumes (1 µl) of live/dead assay reagents (acridine orange (AO) and ethidium bromide (EtBr) (5 mg/mL) for 30 secs. Cells were then visualized under inverted fluorescence microscope (Evos, AMG groups, USA) and the images were captured using change-coupled device (CCD) camera equipped with the microscope.

6.2.9 Cell infiltration

At 1, 4 and 7 days of culture, the cell seeded scaffolds were removed from the tissue culture plate, washed twice with PBS and fixed in 4% formaldehyde for 30 min at room temperature. After incubation, the scaffolds were again washed with PBS and dehydrated using gradient series of ethanol (10% to 100% at 10 min interval). The scaffolds were then embedded in the wax and cut transversely into ~5 µm thin slices using microtome. The slices were then rehydrated using decreasing concentration of ethanol (100% to 10% at 10 min interval), permeabilized with 0.1% Triton-X100 for 20 min and then stained with DAPI. Cells were then visualized under inverted fluorescence microscope and the images were captured using CCD camera.

6.2.10 Osteogenic studies

For osteogenic studies, two experimental groups of scaffolds were maintained in 12-well tissue culture plates: (1) cell seeded scaffolds cultured in osteogenic induction medium (OM) consisting of DMEM supplemented with 10% FBS, 100 units/mL penicillin, and 100 µg/mL streptomycin, 10 mM β-glycerol-2-phosphate,10 nM dexamethasone, 50 µg/mL ascorbic acid and (2) a control group of cell-seeded scaffolds cultured in proliferation medium (PM) consisting of DMEM supplemented with 10% FBS, 100 units/mL penicillin, and 100 µg/mL streptomycin only .

These two groups were further divided into two subgroups as depicted in Fig. 6.1. In one subgroup, the cells were seeded as such without any pretreatment of any growth factor while in another subgroup the cells were preconditioned with osteogenic growth hormone BMP-2 (50 ng/mL) for 15 min at 37 °C in a humidified atmosphere of 5% CO_2 prior seeding. The experiment was performed for 21 days; differentiation and proliferation media were changed every second day.

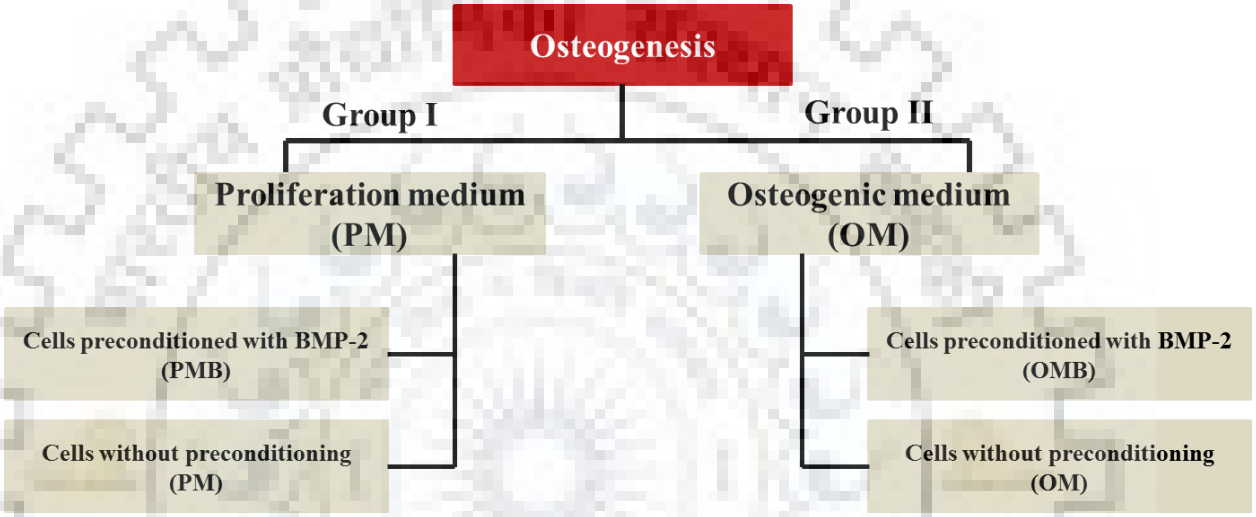

Fig. 6.1 Cell culture strategy in proliferation and osteogenic medium

6.2.10.1 Evaluation of osteogenic differentiation

6.2.10.1.1 Alizarin red S staining

The mineralization/calcification by the constructs (cell seeded scaffolds) was evaluated using alizarin red S staining of calcium deposits. The samples were collected after 7, 14 and 21 days, rinsed twice with PBS, fixed with 4% formaldehyde for 30 min, and then rinsed thrice for 5 min with deionized water. Alizarin Red S stain solution (1%) was added to each well and incubated for 20 min at room temperature. Excess dye was removed by washing with deionized water. The scaffolds were then dipped 20 times in acetone, 20 times in 50% acetone–xylene solution, followed by clearing in 100% xylene. Images were obtained using bright field inverted microscope equipped with CCD camera.

6.2.10.1.2 Visualization of calcium nodules under FE-SEM

For the visualization of calcium nodules onto the cell seeded scaffolds, field emission scanning electron microscopy (FE-SEM) was performed after 21 days. Briefly, scaffolds were washed twice with PBS and fixed with 4% formaldehyde for 30 min. After further washing with PBS, the scaffolds were dehydrated in a series of ethanol solutions with increasing concentrations (10% to 100% at 5 min interval) and finally dried with hexamethyldisilazane (HDMS). The dried cell seeded scaffolds were gold coated for 90 s in a Denton gold sputter unit before being mounted in the FE-SEM (FEI Quanta 200 FEG), which was equipped with EDX spectrometry. The micrographs were acquired at 1000 X and EDX analysis was done for the detection and distribution of calcium and phosphorus within these tissue scaffolds.

6.2.11 Statistical analysis

All quantitative data were expressed as the mean ± standard deviation. Statistical comparisons were performed using oneway ANOVA with SPSS 13.0 for Windows software (SPSS Inc., Chicago, IL, USA). P values less than 0.05 were considered statistically significant.

6.3 RESULTS AND DISCUSSION

6.3.1 Preparation and physicochemical characterization of 3-D mBNC scaffolds

6.3.1.1 Macro and micro morphology of 3-D mBNC scaffolds

Nanofibrous bacterial cellulose is easier to obtain than other nanofibrous biomaterials, since it does not require complex technology such as electrospinning, self-assembly, phase separation, etc. Beside this, it exhibits ultrahigh mechanical strength, high water holding capacity and comparatively low production cost; all these make BNC an excellent biomaterial (Svensson *et al*., 2005; Hong *et al*., 2006; Gao *et al*., 2011). However, as a scaffold for tissue engineering, a major drawback of this biomaterial is the lack of cell infiltration (Zaborowska *et al*., 2010). This is caused by inadequate pore size ensuing from the densely packed BNC fiber layers (as shown in Chapter 3). Hence, the seeded cells live only on the surface of the BNC and vascularization of the scaffold is inhibited, thereby restricting tissue in-growth. Thus, BNC must be further processed into a macro-porous material and pores must be interconnected and large enough to allow cell growth and migration, nutrient flow, vascularization and new tissue formation.

Fig. 6.2 depicts the macroscopic morphology of the prepared 3-D macroporous-nanofibrous bacterial cellulose (3-D mBNC) scaffolds. The prepared scaffolds were ~ 9 mm in thickness and ~ 18 mm in diameter. However, the size and shape of the scaffolds could be controlled by choosing the molds of specific dimension in order to meet the desired size and shape requirements of clinical therapies.

Further, the micro-morphology of the scaffolds was analyzed through FE-SEM (Fig. 6.3). As manifested, the mBNC scaffolds had a highly porous microarchitecture compared to native BNC membrane (Chapter 3, Fig. 3.10) and displayed an irregular open pore geometry with an interconnected pore morphology characterized by macro-pores, micro-pores and nano-pores. Thus, the prepared scaffolds may facilitate the diffusion of cells, nutrients and wastes resulting into 3-dimensional cellular ingrowth.

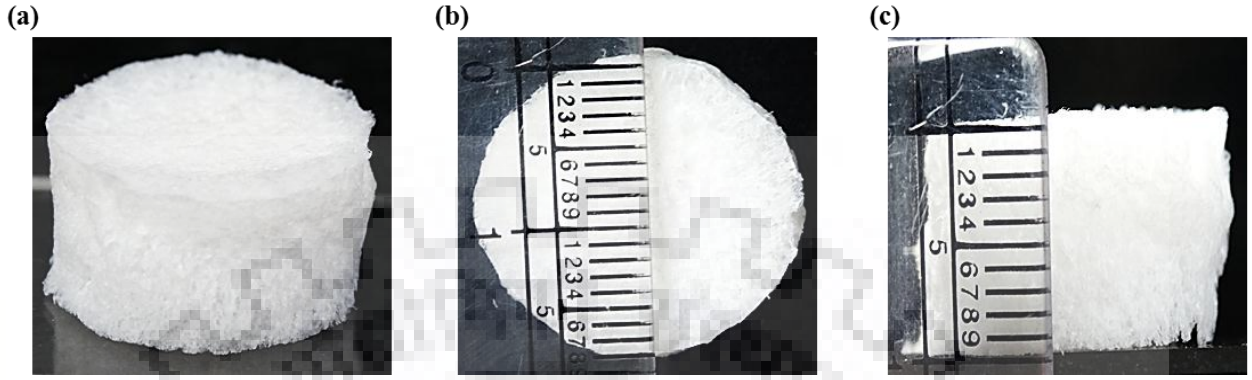

Fig. 6.2 Macroscopic aspects of mBNC scaffold in terms of its three dimensionality and size: (a) 3-D view, (b) top view with scale and (c) side view with scale

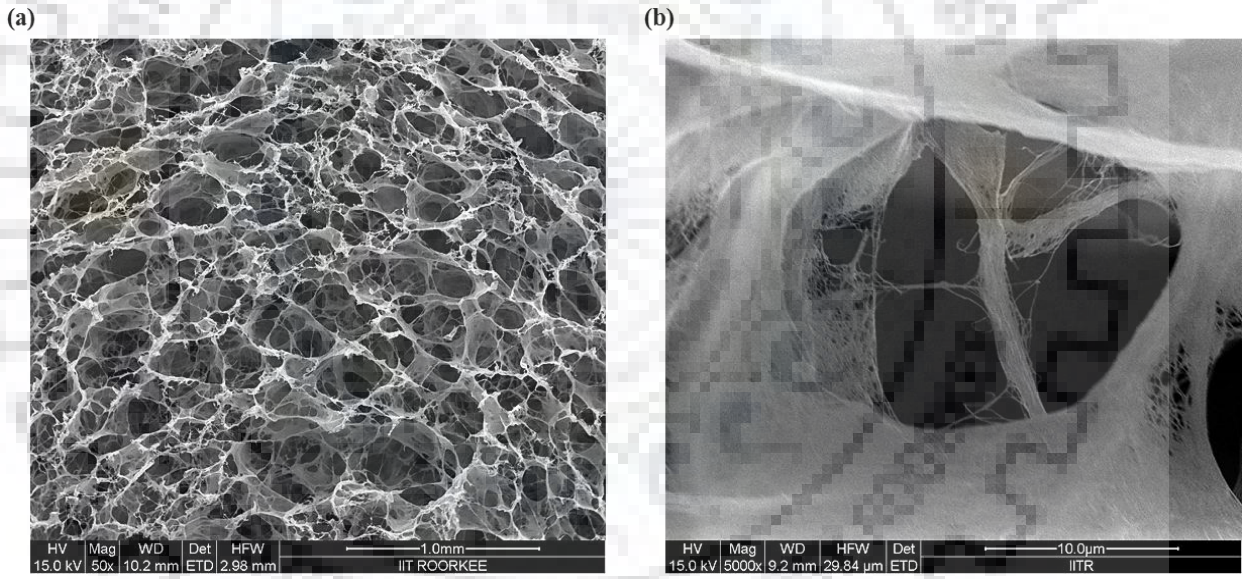

Fig. 6.3 Microscopic morphology of mBNC scaffold at (a) 50 X and (b) 5k X magnifications showing a microporous-nanofibrous architecture

6.3.1.2 FTIR

The FTIR spectrum of mBNC scaffold is depicted in Fig. 6.4; as evident from the spectrum, no chemical changes were found in the cellulose structure after scaffold preparation as the spectrum was similar to that obtained from native BNC membrane except minor shifting and some broadening or increasing in the intensity of the peaks. The characteristic broad and dominating peak appeared ~ 3435 cm^{-1} is attributed to the presence of hydroxyl groups (O-H stretching) (Kiziltas *et al*., 2015). The peak at~ 2920 cm^{-1} represents C-H stretching (Oh *et al*.,

2005), ~ 1640 cm^{-1} shows O-H bending of adsorbed water (Yassine *et al*., 2016), ~ 1427 cm^{-1} signalizes C-H_2 symmetric bending (Oh *et al*., 2005), ~ 1372 cm^{-1} denotes C-H bending (Colom and Carrillo, 2002; Oh *et al*., 2005) and ~ 1321 cm^{-1} indicates C-H_2 wagging (Colom and Carrillo, 2002; Oh *et al*., 2005). The other peaks appeared at ~ 1163 cm^{-1}, 1112 cm^{-1}, 1059 cm^{-1} and 897 cm^{-1} signifies C-O-C asymmetric bridge stretching, C-C ring stretching of cellulose, C-O-C pyranose ring stretching vibration and C-O-C symmetric stretching in plane, respectively (Oh *et al*., 2005; Movasaghi *et al*., 2008; Shao *et al*., 2015; Fan *et al*., 2016).

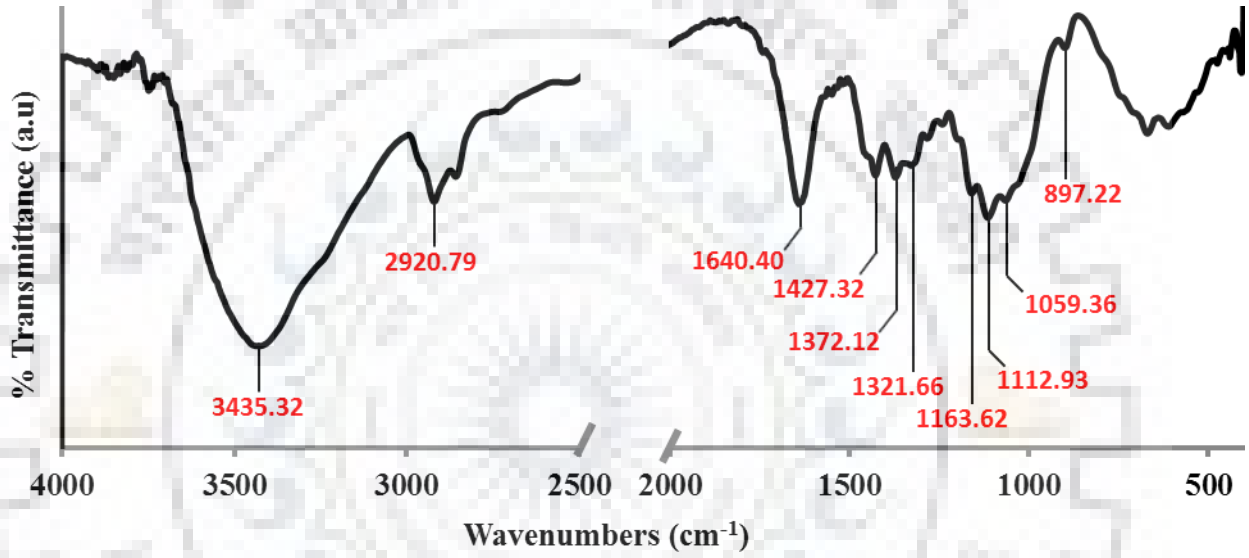

Fig. 6.4 FTIR spectrum of mBNC scaffold

6.3.1.3 XRD

X-ray diffraction analysis of mBNC scaffold had shown similar XRD profile as obtained from native BNC membrane with three characteristic peaks at 2θ = 14.6, 16.2 and 22.2° (Fig. 6.5), corresponding to ($1\bar{1}0$), (110) and (200) crystallographic planes of the cellulose lattice respectively. However, the crystallinity index (CrI) of the cellulose got decreased from 87.7 % (native BNC membrane produced under optimized conditions, Chapter 3, Table 3.4) to 54.66 % after scaffold preparation which could be due to the disruption of cellulose chain assembly during crushing process used for the preparation of scaffold.

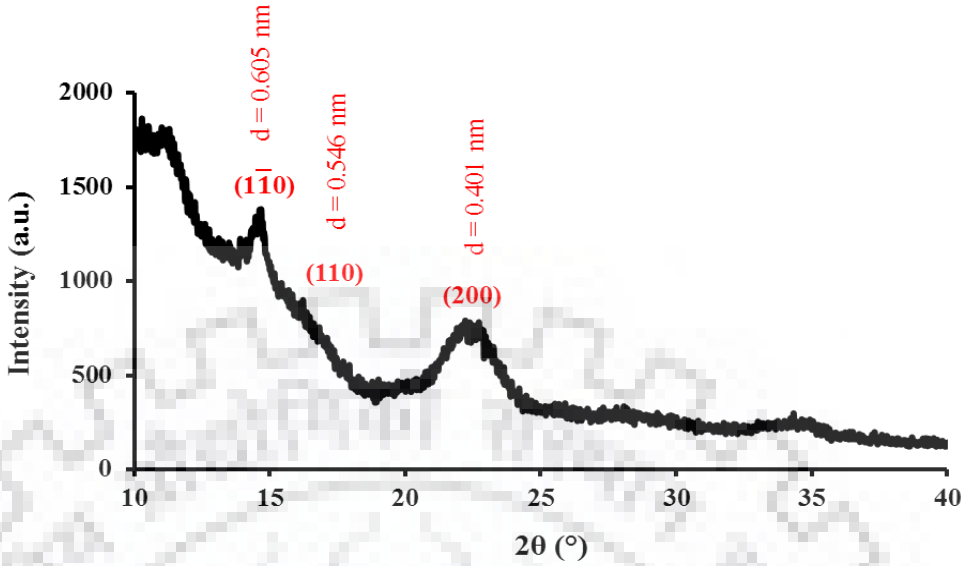

Fig. 6.5 X-ray diffraction profile of mBNC scaffold

6.3.1.4 TGA

Thermogravimetric analysis of mBNC scaffold had also shown the similar TG-DTG profile as obtained with native BNC membrane (Fig. 6.6); however, the degradation of mBNC scaffold started at ~285 °C and 33.19 % mass was remained at 350 °C, while the native BNC membrane produced under optimized conditions in modified HS medium (Chapter 3, Section 3.3.6.3) was stable up to ~295 °C and 43.69 % residual mass was present at 350 °C. The decrease in the thermal stability of mBNC scaffold could be ascribed to its lower crystallinity level.

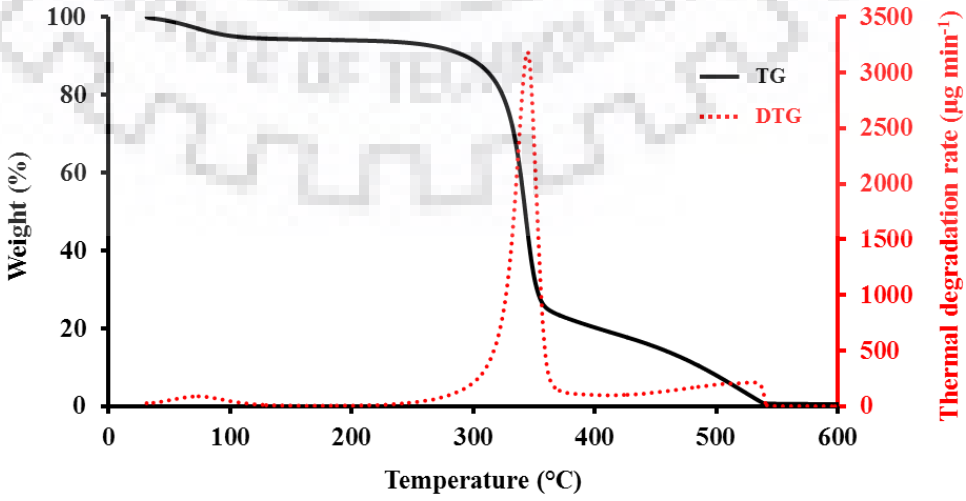

Fig. 6.6 TG-DTG curve of mBNC scaffold

6.3.2 Degradation behavior of the scaffolds

Tissue engineering scaffolds are usually required to either degrade or be reabsorbed by the body after successful tissue regeneration. Thus, mBNC scaffolds were incubated in PBS (pH 7.4) and PBS containing lysozyme (pH 7.4) solutions separately, at 37 °C for 15, 30 and 60 days, to evaluate the weight loss in the scaffolds due to dissolution and degradation. No significant change in the weight of the scaffolds was observed in either of the solutions even after 60 days (Fig. 6.7), which indicated that the time needed for the degradation of the scaffolds may be longer than the observation period. In a study by Martson *et al*. (1999) in a rat model, reported that the cellulose sponges did not fully degrade even after 60 weeks *in vivo*. Though, the cellulose sponges was totally filled up with the connective tissues after 8 weeks of implantation but the appearance of cracks and fissures, and softening of the pore walls of the cellulose sponge were observed after 16 weeks of implantation and hence they regarded it as a slowly degradable implantation material.

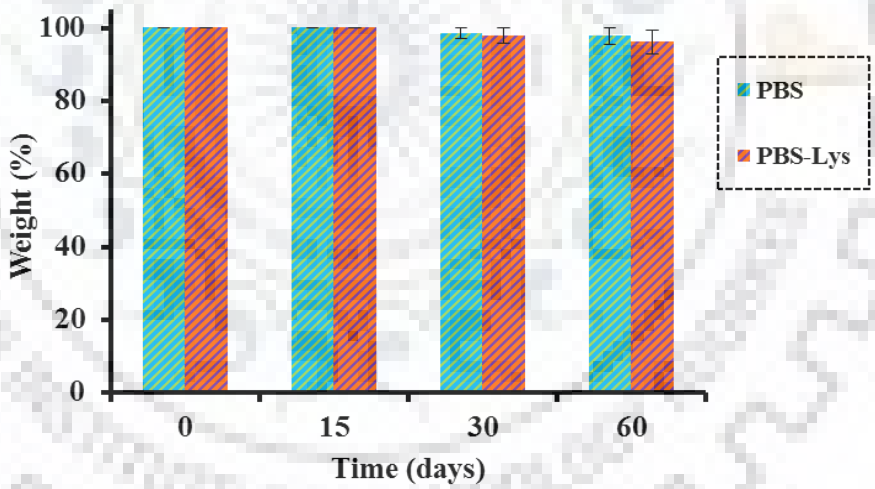

Fig. 6.7 Degradation behavior of mBNC scaffolds as a function of incubation time (15, 30 and 60 days) at 37 °C. Values are represented as mean ± SD (n = 3) (PBS: Phosphate buffered saline; PBS-Lys: Phosphate buffered saline containing lysozyme).

Since, cellulose is generally degraded in nature by the microbial enzymes through hydrolase attack on the β(1–4) linkages and these enzymes are absent in the mammals (Martson *et al*., 1999). In this case, the degradation of the cellulose sponge is probably a combination of chemical, biological and mechanical processes; or in other words, we can say that its degradation depends on the several factors, including the availability of the enzymes that degrade cellulose, its

crystallinity, surface area, aggregation state, and the shape and morphology of the scaffolds (Martson *et al*., 1999; Zaborowska *et al*., 2010). Thus, lowering in the crystallinity of the cellulose after scaffold preparation (as mentioned in above in Section 6.3.1.3) may accelerate its degradation after implantation.

6.3.3 Cell studies

6.3.3.1 Cell attachment

Porosity and pore size play an important role in cell attachment and proliferation in 3-D porous scaffolds. Representative FE-SEM micrographs of cell attachment on mBNC scaffold are shown in Fig. 6.8. The images revealed strong cell adhesion with extended morphology of the cells, on the surface (yellow arrow) as well as inside the pores (cyan arrow) of mBNC scaffold, indicating its potential for tissue in-growth as the pores were large enough to allow cell growth and migration.

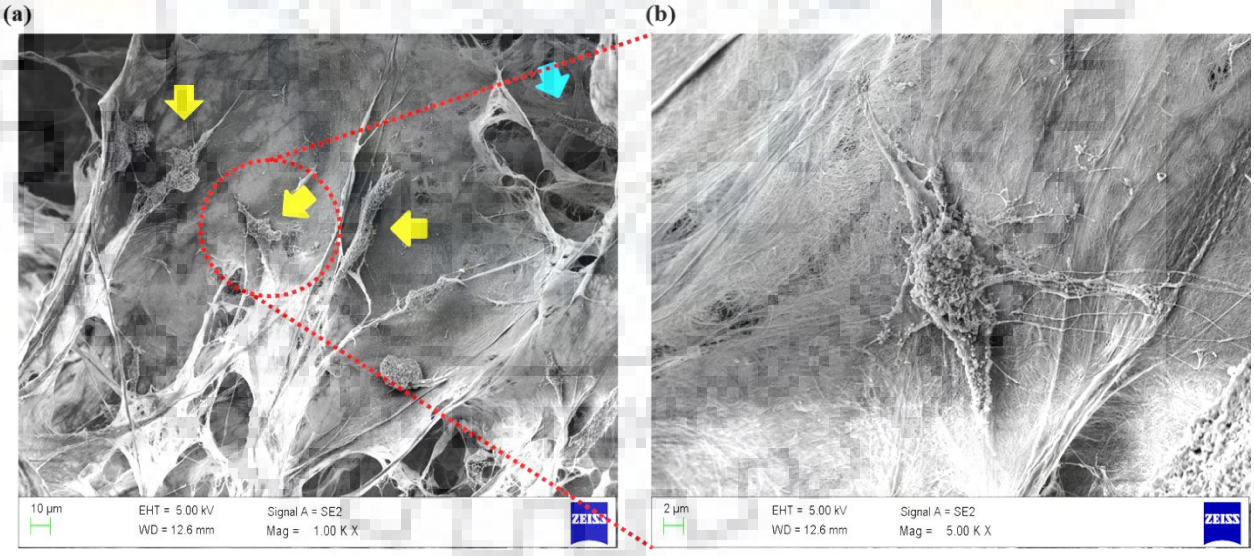

Fig. 6.8 FE-SEM micrographs showing C3H10T1/2 cells attachment on 3-D mBNC scaffold at (a) 1kX and (b) 5kX magnifications

6.3.3.2 Cell viability and proliferation

Cell viability of C3H10T1/2 cells on mBNC scaffold was examined using live/dead cell staining. The flourscence microscopic images of C3H10T1/2 cells cultured for 1, 4 and 7 days on mBNC scaffolds are shown in Fig. 6.9. The scaffolds exhibited very good biocompatibility with hardly any detectable cell death and the cells continued to proliferate as the results indicated an increase in cell number with respect to time.

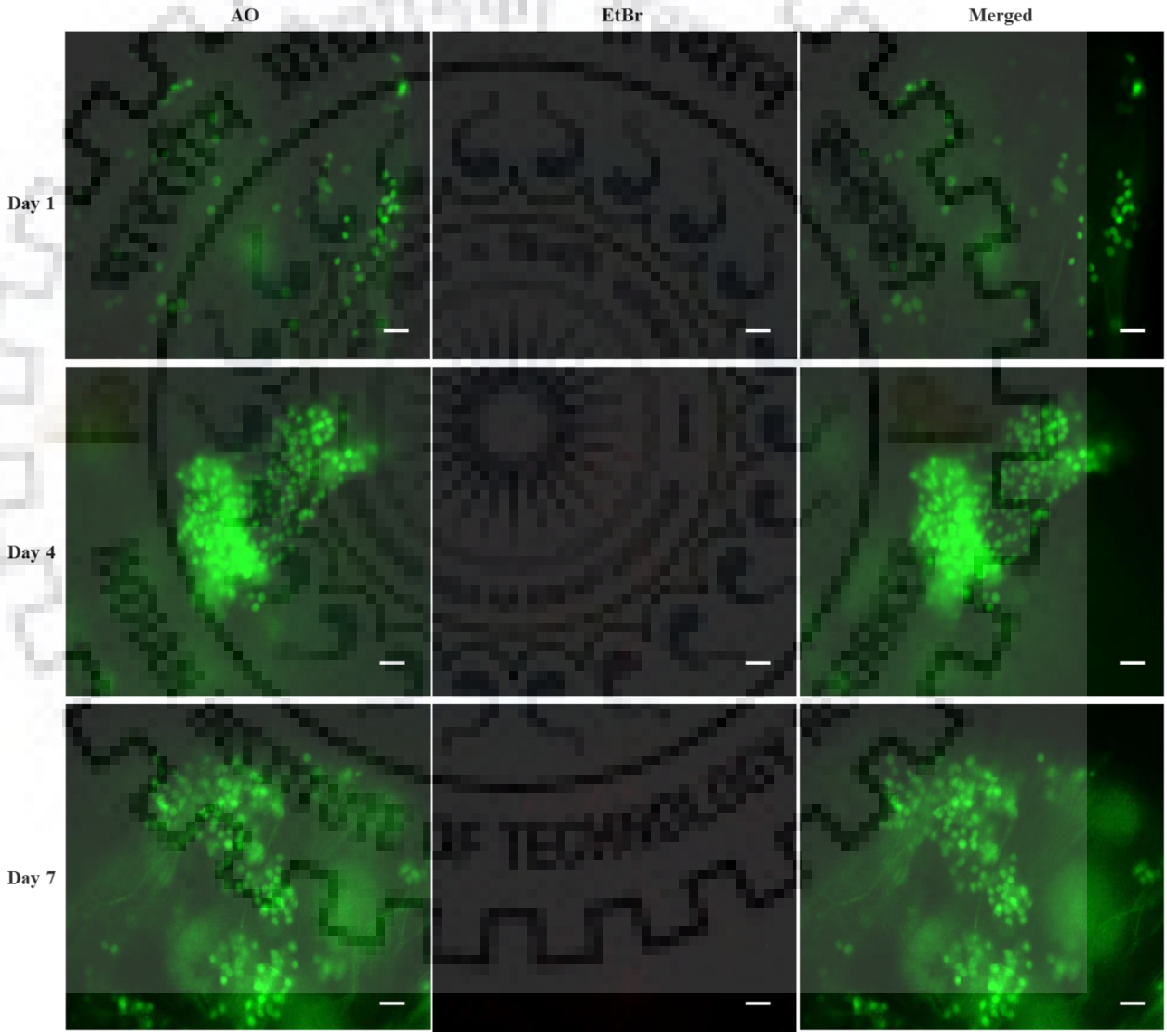

Fig. 6.9 Live/dead cell staining of C3H10T1/2 cells in proliferation medium seeded on mBNC scaffolds at days 1, 4, and 7. Live cells were stained green by acridine orange (AO) and dead cells were stained red by ethidium bromide (EtBr). Scale bar = 50 µm

To further confirm the non-toxicity of mBNC scaffolds, the release of LDH (lactate dehydrogenase) in culture medium was assessed after 1, 4 and 7 days of cell seeding, as the amount of LDH released in the culture medium is proportional to the number of damaged or lysed cells. No significant difference in the LDH activity was observed at the above mentioned time points as depicted in Fig. 6.10, which further confirmed the biocompatibility of the scaffolds.

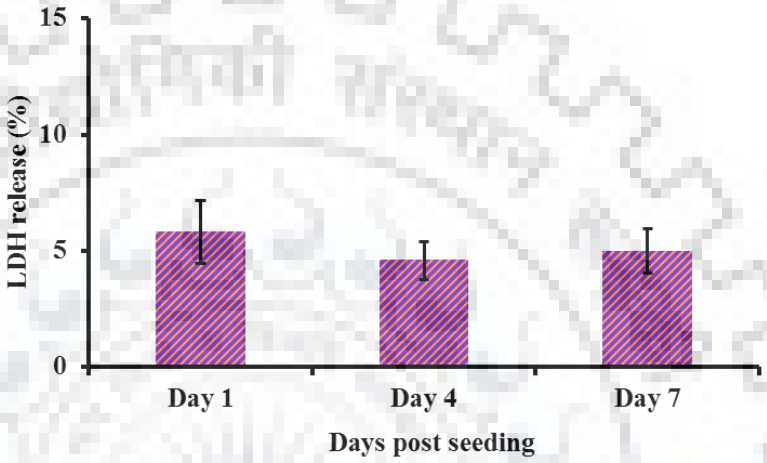

Fig. 6.10 Evaluation of mBNC scaffold cytotoxicity via LDH assay at 1, 4 and 7 days of post seeding (n=6)

To verify the results obtained from live/dead cell staining and LDH assay, the cell viability and proliferation was further assessed by MTT assay. The results showed that cells were metabolically active (Fig. 6.11) and well spread throughout the scaffold during the time. This is attributed to the availability of a larger space for cellular growth and proliferation in the porous and 3-D structure of the scaffolds. Consequently, diffusion and exchange of nutrients and waste throughout the scaffolds were ensured, allowing cells to proliferate and be metabolically active.

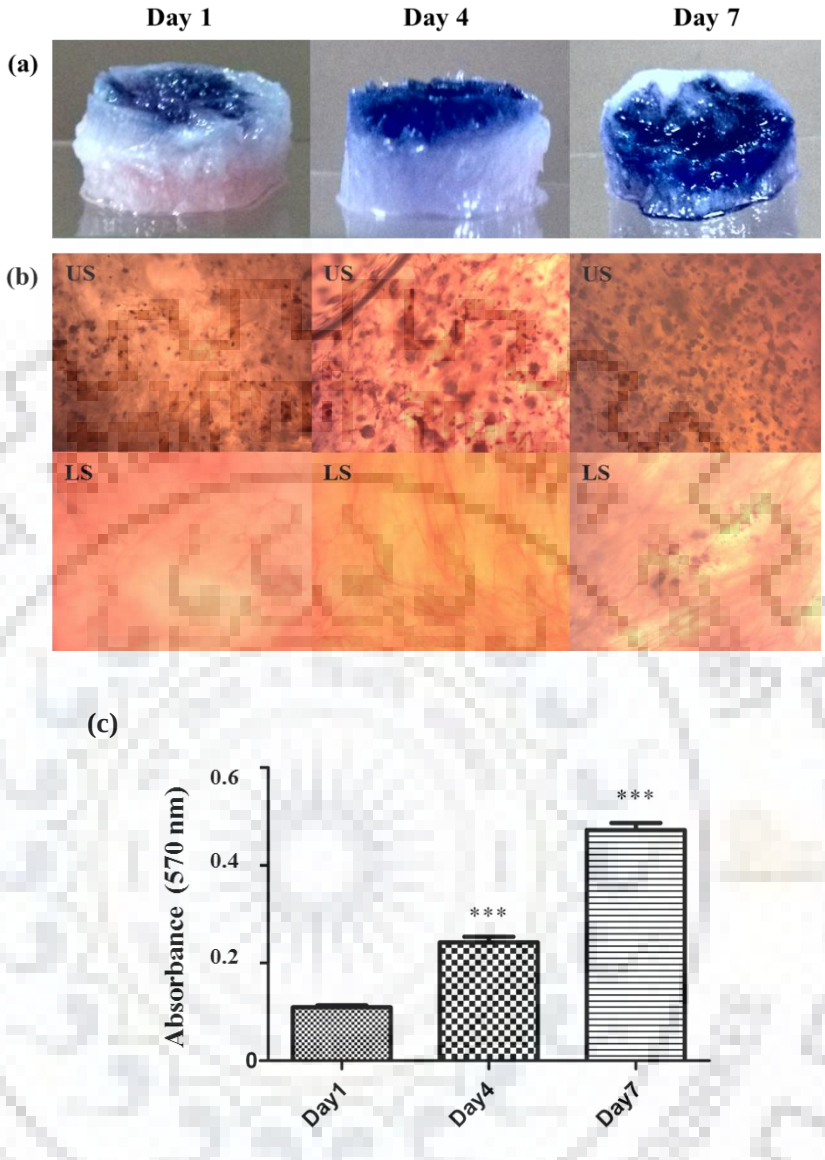

Fig. 6.11 MTT assay of C3H10T1/2 cells seeded on mBNC scaffolds at days 1, 4 and 7: (a) visual aspects of MTT assay showing an increase in purple color intensity during the time due to an increase in metabolically active cells; (b) microscopic aspects of MTT assay showing formazan crystals and (c) the histogram representing quantitative data (n=6; $P < 0.0001$) of MTT assay. (US: Upper Side; LS: Lower Side of the scaffold)

6.3.3.3 Cell infiltration

Cell ingress into mBNC scaffolds was observed by DAPI stained cell nuclei in scaffold cross sections. As delineated in Fig. 6.12, a small portion of cells penetrated into the depth of the scaffold at day 1. However, by day 7, C3H10T1/2 cells had infiltrated and homogeneously distributed throughout the entire depth of scaffold; indicating the potential of mBNC scaffold for tissue in-growth.

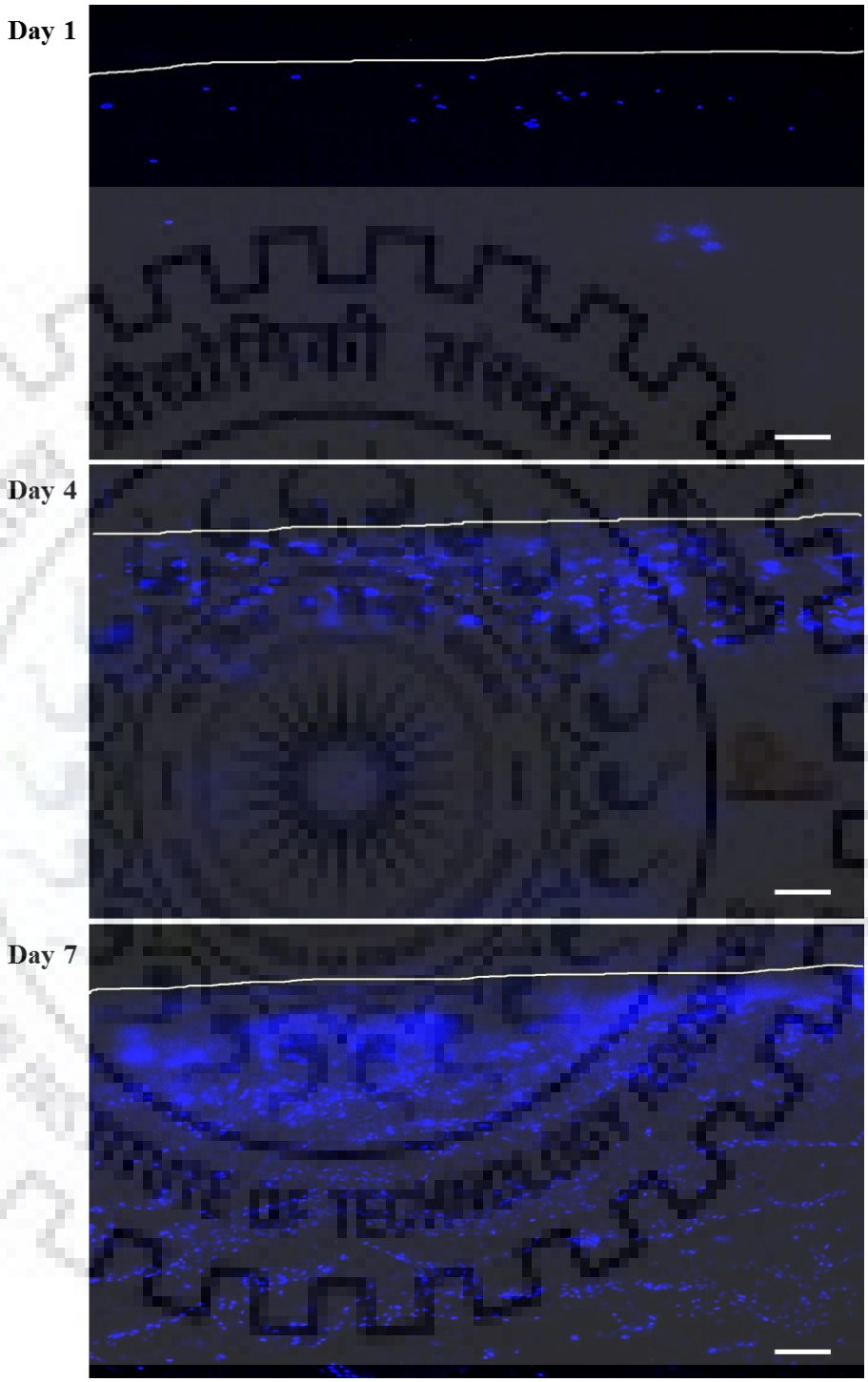

Fig. 6.12 C3H10T1/2 cells infiltration into mBNC scaffolds at days 1, 4 and 7 as shown by fluorescent DAPI staining of cell nuclei in scaffold transverse-sections. White lines are drawn on the fluorescent images to show the outer periphery of each scaffold cross section. Scale bar = 200 µm

6.3.3.4 Cell differentiation/osteogenesis

The mineral deposition is a late stage marker of osteogenic differentiation that can be used to confirm that the cells have entered into the mineralization phase to deposit mineralized ECM which is then followed by bone formation. Hence, the osteogenic potential of cell seeded mBNC scaffolds was examined through alizarin red staining (ARS) where the binding of calcium ions in mineralized ECM forms an ARS-calcium complex through chelation process.

After 7, 14 and 21 days of culturing in proliferation and osteogenic media, the cell seeded scaffolds were stained with alizarin red s to determine calcium mineralization on mBNC scaffolds. Fig. 6.13 shows the optical and microscopic images of the ARS staining for the cell seeded mBNC scaffolds, confirming the variations in stain intensity of the scaffolds with culture media, culturing time and cell preconditioning with bone morphogenetic protein-2 (BMP-2). At day 7, the alizarin red stain showed reddish dots on all the scaffolds either cultured in proliferation media or osteogenic media; however the stain intensity was quite higher in Group OM and OMB. The similar trend was observed at day 14 but the stain intensity was relatively higher in all the groups' *i.e* PM, PMB, OM and OMB. At day 21, the stain intensity was much higher in all the groups and the scaffolds of Group OM and OMB completely turned red. This implies the time dependence of cell mineralization to produce more Ca^{2+} binding sites for ARS.

Further, preconditioning of C3H10T1/2 cells with BMP-2 using 15 min exposure to 50 ng/mL BMP-2 increased the osteogenic differentiation of C3H10T1/2 cells in both proliferation and osteogenic media (Fig. 6.13). However, the discrepancies in the osteogenesis of C3H10T1/2 cells stimulated with BMP-2 in proliferation and osteogenic media might result from the variations in the experimental set-ups especially in terms of osteogenic stimulants present in culture media as it has previously been described that BMP-2 enhances dexamethasone-induced osteogenesis [Lysdahl *et al*., 2014] which justifies the reason of enhanced mineralization in Group OMB.

(a)

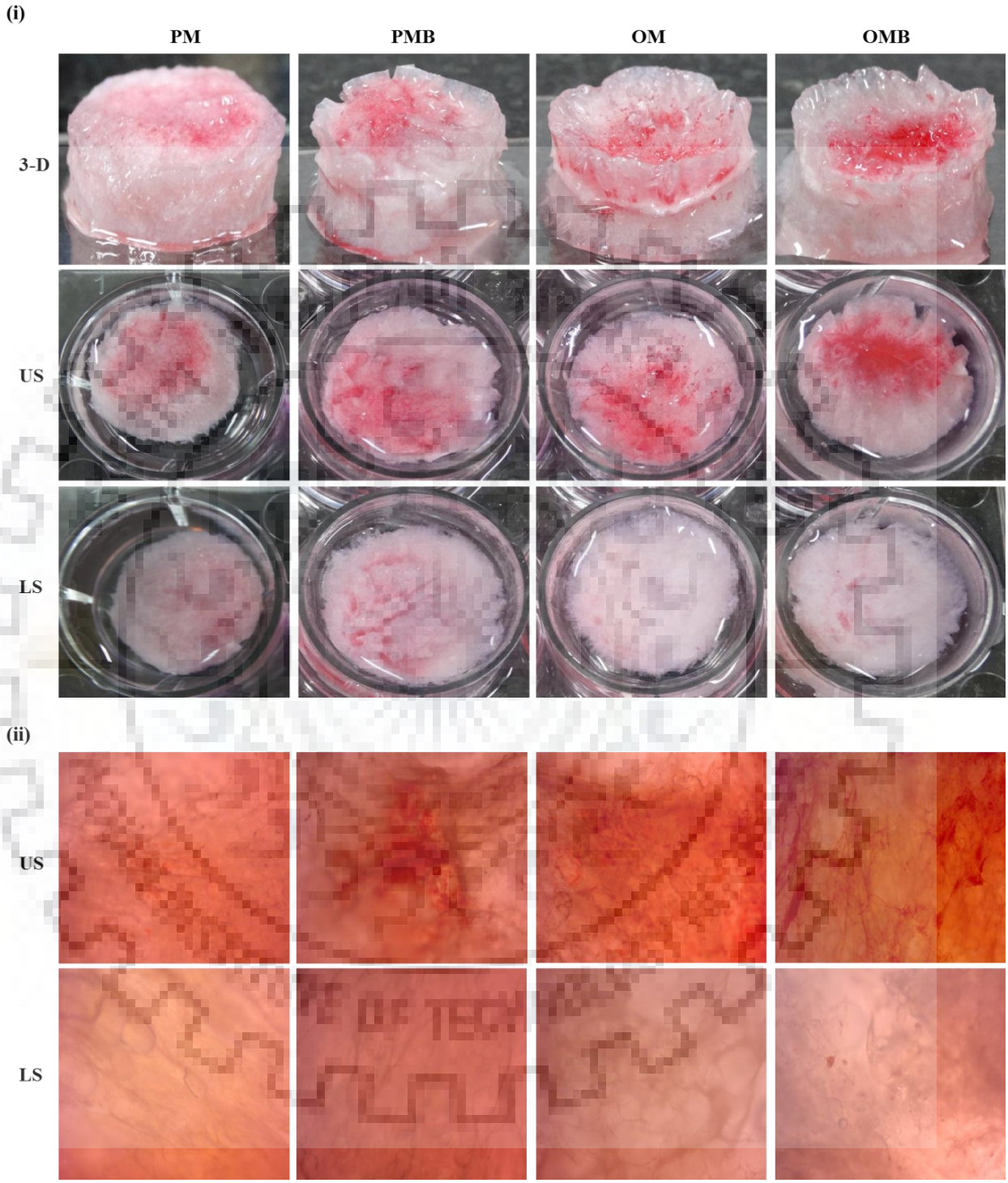

(b)

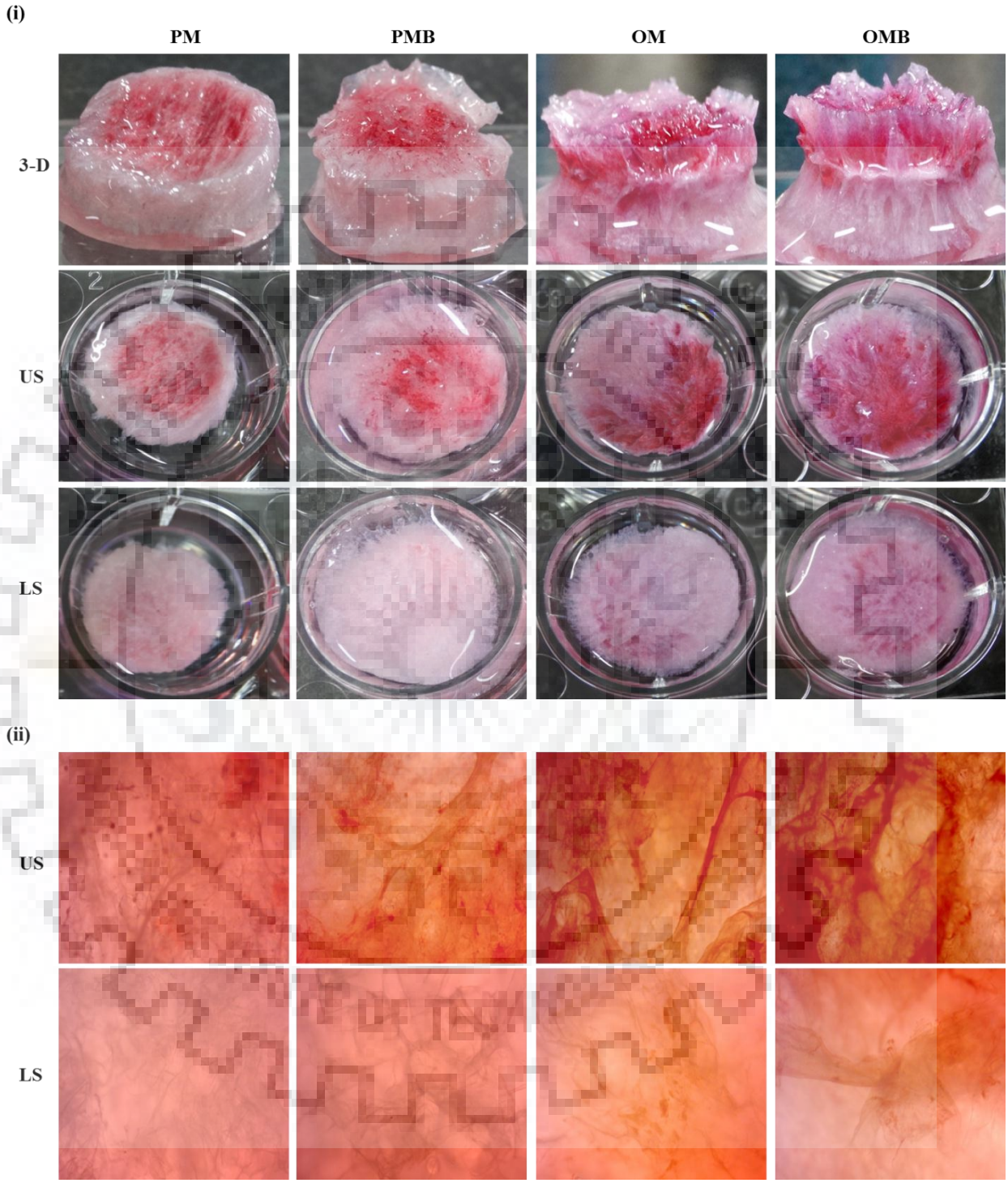

(c)

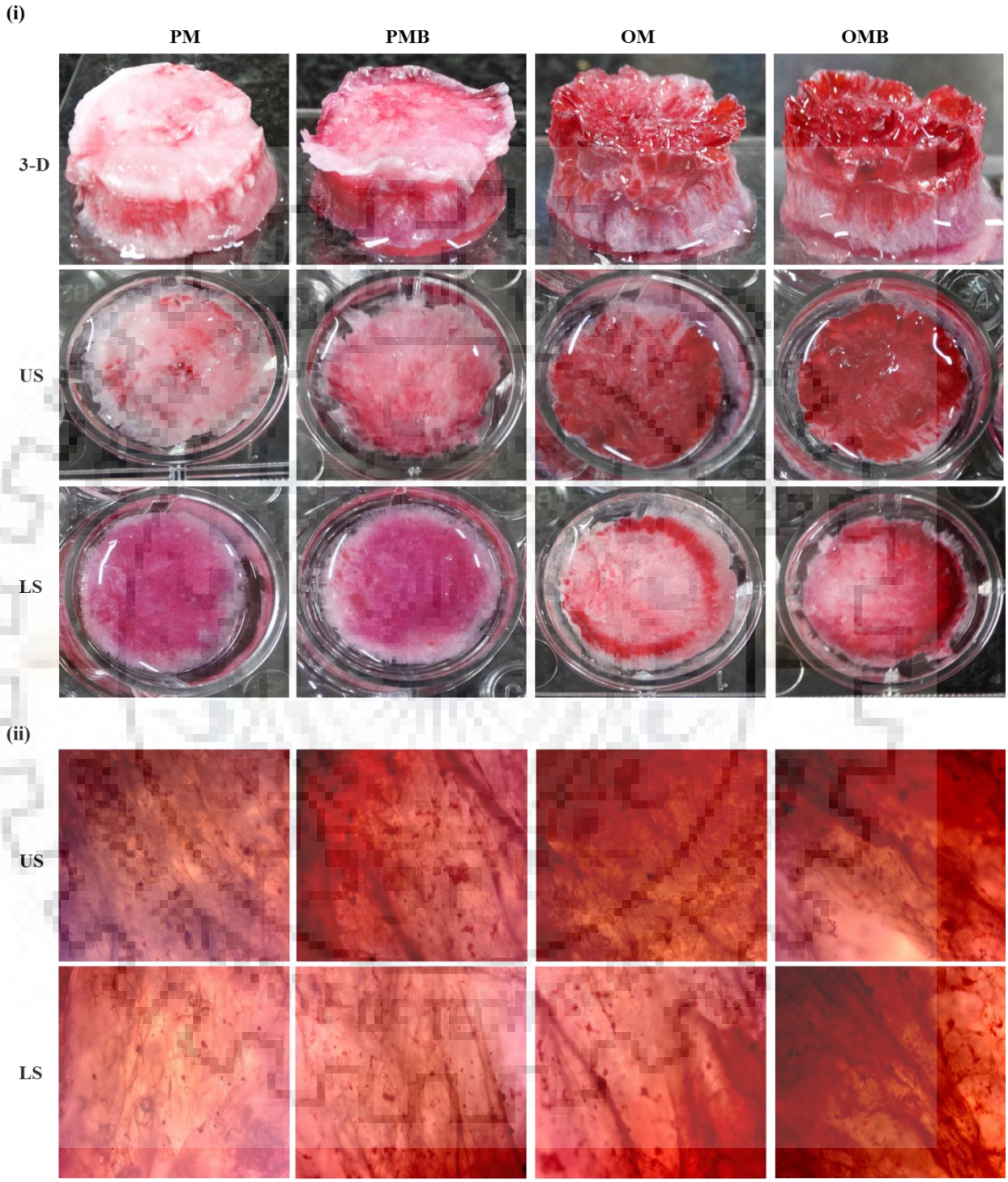

Fig. 6.13 Alizarin red staining of C3H10T1/2 cells seeded mBNC scaffolds at day 7 (a), day 14 (b) and day 21 (c). Panel (i) and (ii) shows the visual and microscopic images of ECM mineralization on the scaffolds, respectively. (3-D: 3-dimensional; US: upper side of the scaffold; LS: lower side of the scaffold)

Mineralization is a process of calcium phosphate deposition on substrate surfaces [Toskas *et al*., 2013; Lai *et al*., 2015] which can be examined by observing the mineral deposition on the cell surface through microscopy or other quantitative assays. A cross confirmation to the mineralization of C3H10T1/2 cells was further done by FE-SEM analysis. Field-emission scanning electron microscopic images of all the four groups were acquired after 21 days of culturing and depicted the same trend as observed from ARS staining (Fig. 6.14). A clear cellular deposition of calcium phosphate pellets was observed for the Group PMB, OM and OMB but the cells cultured in osteogenic media (Fig. 6.14 c, d) was found to have greater extent of mineralization than the cells cultured in proliferation media (Fig. 6.14 a, b).

A quantitative assessment of C3H10T1/2 cells osteo-differentiation from the extent of mineralization was carried out by EDX analysis of the mineralized ECM covering the cells. The EDX mapping and EDX spectra are shown in Fig. 6.14 (ii-vii). EDX mapping had confirmed the presence of calcium and phosphate in the cellular deposition (Fig. 6.14 v, vi) and higher amount of Ca and P content was observed in Group OMB (Fig. 6.14 d (vii)) followed by the Group OM (Fig. 6.14 c (vii)). The results of EDX analysis further demonstrated the potential of mBNC scaffolds for bone tissue engineering applications.

(a)

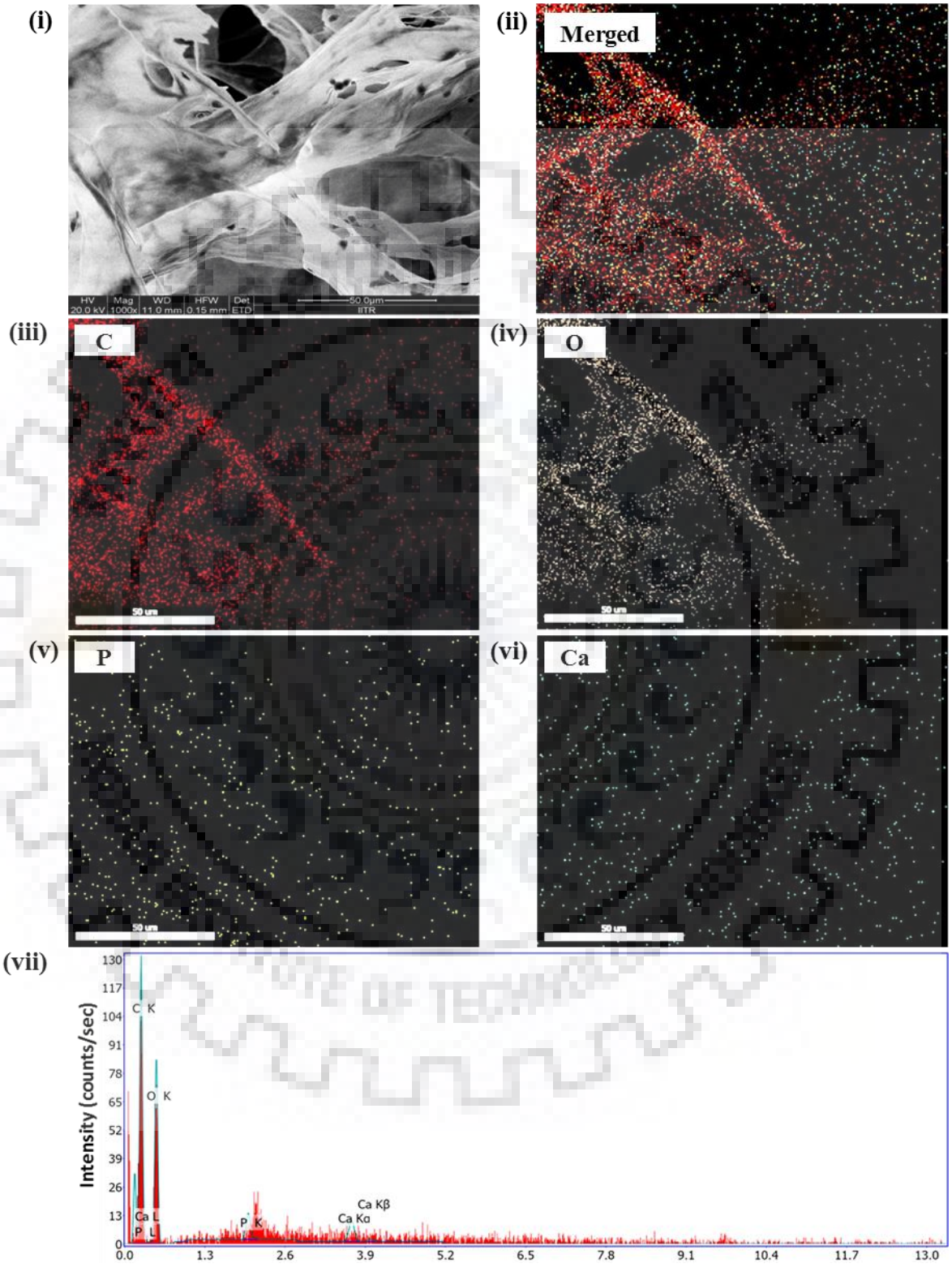
(i)
(ii)
Merged
(iii)
C
(iv)
O
(v)
P
(vi)
Ca
(vii)
Intensity (counts/sec)
C K
O K
Ca L
P L
P K
Ca Kβ
Ca Kα
0.0
1.3
2.6
3.9
5.2
6.5
7.8
9.1
10.4
11.7
13.0

(b)

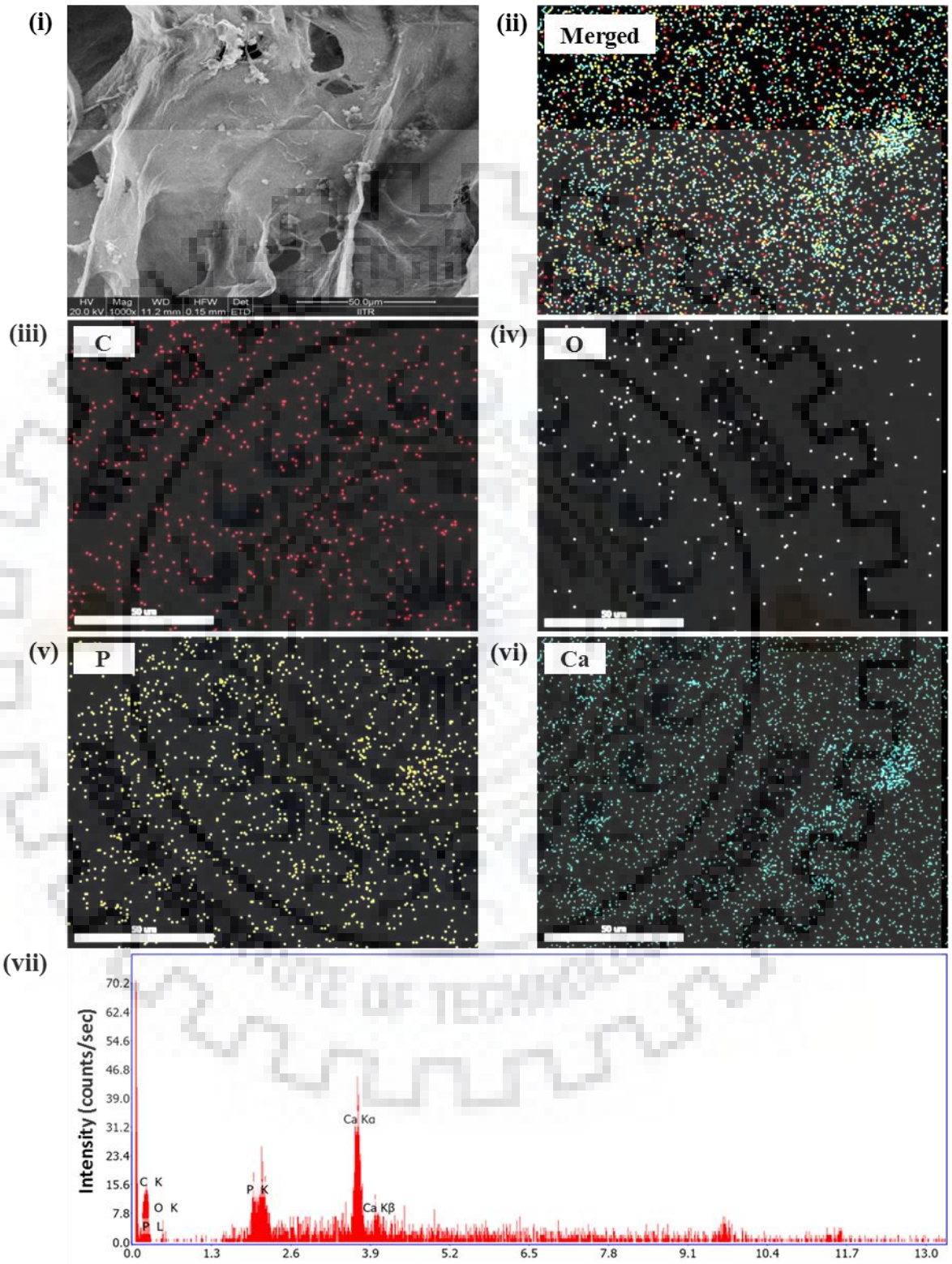
(i)
(ii)
Merged
(iii)
C
(iv)
O
(v)
P
(vi)
Ca
(vii)
Intensity (counts/sec)
70.2
62.4
54.6
46.8
39.0
31.2
23.4
15.6
7.8
0.0
C K
O K
P L
P K
Ca Kα
Ca Kβ
0.0
1.3
2.6
3.9
5.2
6.5
7.8
9.1
10.4
11.7
13.0

(c)

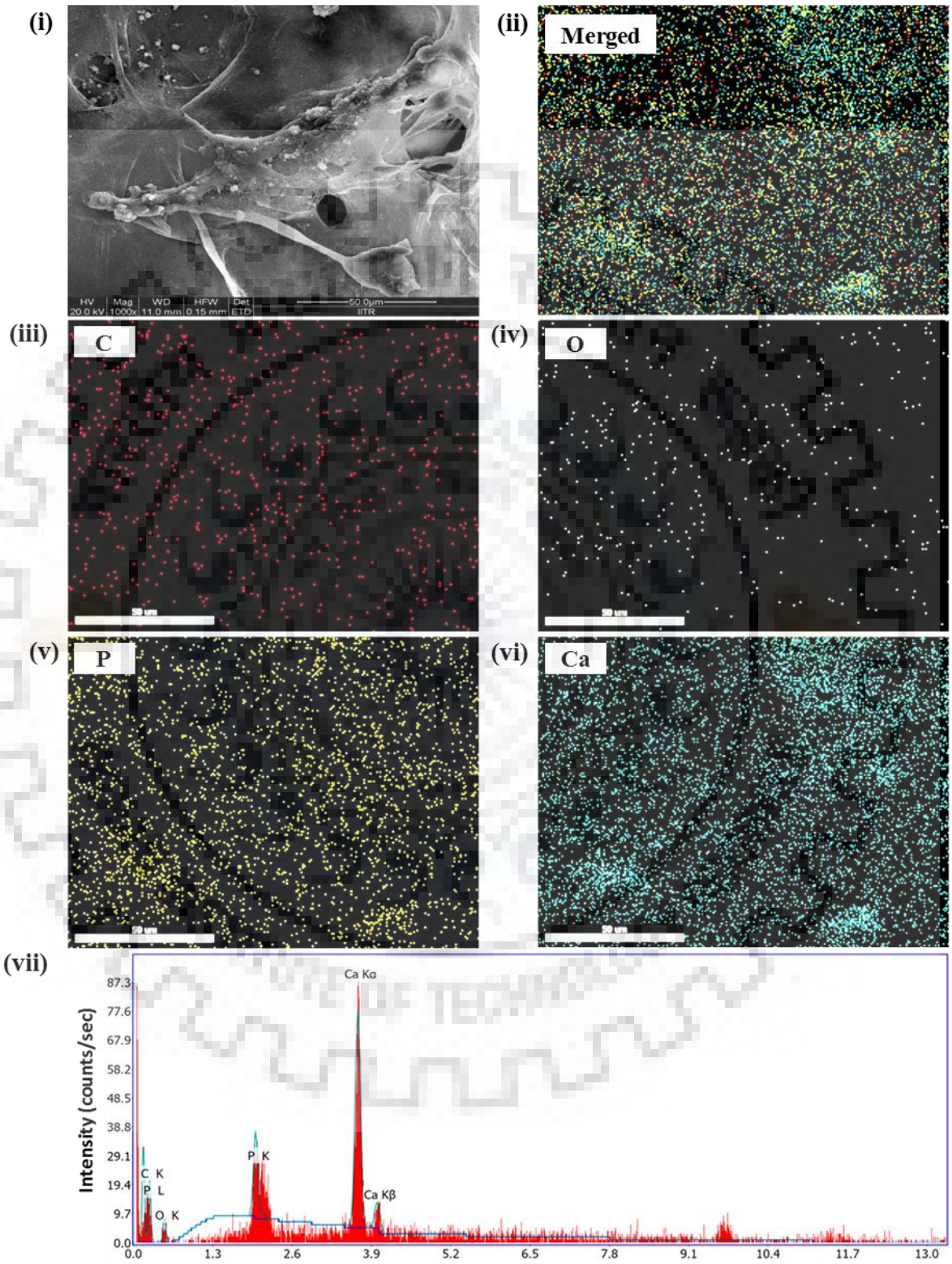
(i)
(ii)
Merged
(iii)
C
(iv)
O
(v)
P
(vi)
Ca
(vii)
Intensity (counts/sec)
87.3
77.6
67.9
58.2
48.5
38.8
29.1
19.4
9.7
0.0
C K
P L
O K
P K
Ca Kα
Ca Kβ
0.0
1.3
2.6
3.9
5.2
6.5
7.8
9.1
10.4
11.7
13.0

(d)

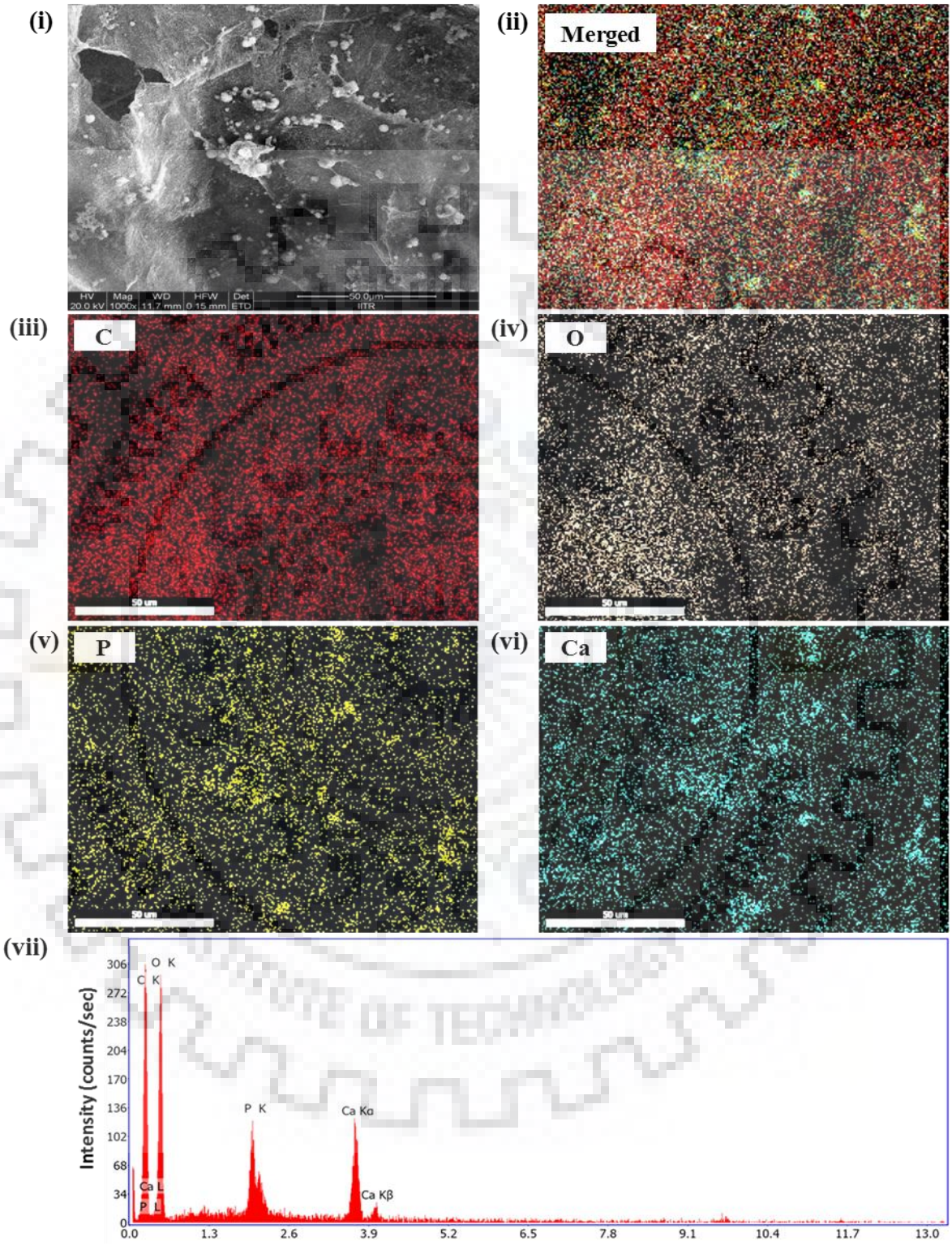

Fig. 6.14 FE-SEM micrograph (i), EDX mapping (ii-vi) and EDX spectra of mineral deposition of C3H10T1/2 cells seeded mBNC scaffolds after 21 days of culturing in PM (a), PMB (b), OM (c) and OMB

6.4 CONCLUSIONS

Highly porous and nanfibrous 3-D BNC scaffolds were fabricated using an easy freeze dry method. The scaffolds had shown an interconnected porous geometry with some reduction in the crystallinity index of cellulose which is ideal for its degradation along with new tissue formation. The cell attachment studies carried out using C3H10T1/2 mesenchymal stem cells indicated strong cell adhesion with extended morphology of the cells on the surface as well as inside the pores of mBNC scaffold. The scaffolds exhibited very good biocompatibility with hardly any detectable cell death and the cells continued to proliferate with respect to time. Moreover, the cells had infiltrated and homogeneously distributed throughout the entire depth of scaffold; indicating its potential of for tissue in-growth. Additionally, alizarin red staining (ARS) and energy-dispersive X-ray spectroscopy (EDS) analyses revealed the osteogenic differentiation and successful mineralization of the cells on the scaffolds.

The viability, growth and infiltration of C3H10T1/2 cells in 3-D mBNC scaffolds are thus the promising aspects for the practical application of these scaffolds for bone tissue regeneration. Furthermore, this study could be extended for developing composite 3-D scaffolds that mimic with the natural histological environment of bone for faster bone regeneration.

Bibliography

1. Akduman, B., Uygun, M., Çoban, E. P., Uygun, D. A., Bıyık, H., Akgöl, S. (2013). Reversible immobilization of urease by using bacterial cellulose nanofibers. *Applied Biochemistry and Biotechnology*, 171(8), 2285-2294.

2. Amin, M. C. I. M., Ahmad, N., Halib, N., Ahmad, I. (2012). Synthesis and characterization of thermo-and pH-responsive bacterial cellulose/acrylic acid hydrogels for drug delivery. *Carbohydrate Polymers*, 88(2), 465-473.

3. Amini, A. R., Laurencin, C. T., Nukavarapu, S. P. (2012). Bone tissue engineering: Recent advances and challenges. *Critical Reviews in Biomedical Engineering*, 40(5), 363–408.

4. Atalla, R. H. & Vanderhart, D. L. (1984). Native cellulose : a composite of two distinct crystalline forms. *Science*, 223(4633), 283-285.

5. Atwa, N. A., El-Diwany, A. I., El-Saied, H., Basta, A. H. (2015). Improvement in bacterial cellulose production using *Gluconacetobacter xylinus* ATCC 10245 and characterization of the cellulose pellicles produced. *Egyptian Pharmaceutical Journal*, 14(2), 123-129.

6. Bäckdahl, H., Helenius, G., Bodin, A., Nannmark, U., Johansson, B. R., Risberg, B., Gatenholm, P. (2006). Mechanical properties of bacterial cellulose and interactions with smooth muscle cells. *Biomaterials*, 27(9), 2141-2149.

7. Baldikova, E., Pospiskova, K., Ladakis, D., Kookos, I. K., Koutinas, A. A., Safarikova, M., Safarik, I. (2017). Magnetically modified bacterial cellulose: A promising carrier for immobilization of affinity ligands, enzymes, and cells. *Materials Science and Engineering C*, 71, 214–221.

8. Barsha, J. & Hibbert, H. (1934). Studies on reactions relating to carbohydrates and polysaccharides: xlvi. Structure of the cellulose synthesized by the action of *Acetobacter xylinus* on fructose and glycerol. *Canadian Journal of Research*, 10(2), 170-179.

9. Barud, H. G., Silva, R. R., Silva Barud, H., Tercjak, A., Gutierrez, J., Lustri, W. R., ..., Ribeiro, S. J. L. (2016). A multipurpose natural and renewable polymer in medical applications: Bacterial cellulose. *Carbohydrate Polymers*, 153, 406-420.

10. Barud, H. S., Ribeiro, S. J. L., Carone, C. L. P., Ligabue, R., Einloft, S., Queiroz, P. V. S., Borges, A.P.B., Jahno, V. D. (2013). Optically transparent membrane based on bacterial Cellulose/Polycaprolactone. *Polímeros*, 23(1), 135-138.

11. Bilgi, E., Bayir, E., Sendemir-Urkmez, A., Hames, E. E. (2016). Optimization of bacterial cellulose production by *Gluconacetobacter xylinus* using carob and haricot bean. *International Journal of Biological Macromolecules*, 90, 2-10.

12. Bodhibukkana, C., Srichana, T., Kaewnopparat, S., Tangthong, N., Bouking, P., Martin, G. P., Suedee, R. (2006). Composite membrane of bacterially-derived cellulose and

molecularly imprinted polymer for use as a transdermal enantioselective controlled-release system of racemic propranolol. *Journal of Controlled Release*, 113(1), 43-56.

13. Bodin, A., Bharadwaj, S., Wu, S., Gatenholm, P., Atala, A., Zhang, Y. (2010). Tissue-engineered conduit using urine-derived stem cells seeded bacterial cellulose polymer in urinary reconstruction and diversion. *Biomaterials*, 31(34), 8889-8901.

14. Bodin, A., Concaro, S., Brittberg, M., Gatenholm, P. (2007). Bacterial cellulose as a potential meniscus implant. *Journal of tissue engineering and regenerative medicine*, 1(5), 406-408.

15. Brien, F. J. O. (2011). Biomaterials & scaffolds for tissue engineering. *Materials Today*, 14(3), 88–95.

16. Brown, A. J. (1886). XLIII.—On an acetic ferment which forms cellulose. *Journal of the Chemical Society, Transactions*, 49, 432-439.

17. Brown, R.M. (1996). The biosynthesis of cellulose. *Journal of Macromolecular Science, Part A Pure and Applied Chemistry*, 33 (10), 1345-1373.

18. Cacicedo, M.L., Castro, M.C., Servetas, I., Bosnea, L., Boura, K., Tsafrakidou , P., Dima, A., Terpou, A., Koutinas, A., Castro, G.R. (2016). Progress in bacterial cellulose matrices for biotechnological applications. *Bioresource Technology*, 213, 172-180.

19. Carreira, P., Mendes J.A.S., Trovatti, E., Serafim, L.S., Freire, C.S.R., Silvestre, A.J.D., Neto, C.P. (2011). Utilization of residues from agro-forest industries in the production of high value bacterial cellulose. *Bioresource Technology*, 102, 7354-7360.

20. Castro, C., Zuluaga, R., Álvarez, C., Putaux, J.-L., Caro, G., Rojas, O. J., Mondragon, I., Ganan, P. (2012). Bacterial cellulose produced by a new acid-resistant strain of *Gluconacetobacter* genus. *Carbohydrate Polymers*, 89, 1033-1037.

21. Castro, C., Zuluaga, R., Putaux, J.L., Caro, G., Mondragon, I., Ganan, P. (2011). Structural characterization of bacterial cellulose produced by *Gluconacetobacter swingsii* sp. from Colombian agroindustrial wastes. *Carbohydrate Polymers*, 84, 96-102.

22. Cavicchioli, M., Corso, C. T., Coelho, F., Mendes, L., Saska, S., Soares, C. P., ..., Ribeiro, S. J. L. (2015). Characterization and cytotoxic, genotoxic and mutagenic evaluations of bacterial cellulose membranes incorporated with ciprofloxacin: A potential material for use as therapeutic contact lens. *World Journal of Pharmacy and Pharmaceutical Sciences*, 4(7), 1626-1647.

23. Cavka, A., Guo, X., Tang, S. J., Winestrand, S., Jönsson, L. J., Hong, F. (2013). Production of bacterial cellulose and enzyme from waste fiber sludge. *Biotechnology for Biofuels*, 6(1), 25.

24. Chawla, P. R., Bajaj, I. B., Survase, S. A. Singhal, R. S. (2009). Microbial Cellulose : Fermentative production and applications. *Food Technology and Biotechnology*, 47(2), 107-124.

25. Chen, L., Hong, F., Yang, X.-X., & Han, S.-F. (2013). Biotransformation of wheat straw to bacterial cellulose and its mechanism. *Bioresource Technology*, 135, 464–468.

26. Cheng, Z., Yang, R., Liu, X., Liu, X., Chen, H. (2017). Green synthesis of bacterial cellulose via acetic acid pre-hydrolysis liquor of agricultural corn stalk used as carbon source. *Bioresource Technology*, 234, 8-14.

27. Colom, X. & Carrillo, F. (2002). Crystallinity changes in lyocell and viscose-type fibres by caustic treatment. *European Polymer Journal*, 38, 2225-2230.

28. Czaja, W., Krystynowicz, A., Bielecki, S., Brown, R. M. (2006). Microbial cellulose—the natural power to heal wounds. *Biomaterials*, 27(2), 145-151.

29. Deinema, M. H., Zevenhuizen, L. P. T. M. (1971). Formation of cellulose fibrils by gram-negative bacteria and their role in bacterial flocculation. *Archives of Microbiology*, 78(1), 42-57.

30. Dubey, S., Saroj, S., Agarwal, P., Singh, R. P. (2015). Bacterial cellulose: An innovative nanobiopolymer for drug delivery. In B. Singh, K. K. Singh, & G. S. Rekhi (Eds.), *NanoBioMedicine Vol. 2: Nanopharmaceuticals*. Studium Press LLC, Houston, USA, pp. 185-200.

31. Dubey, S., Sharma, R.K., Agarwal, P., Singh, J., Sinha, N., Singh, R.P. (2017). From rotten grapes to industrial exploitation: *Komagataeibacter europaeus* SGP37, a micro-factory for macroscale production of bacterial nanocellulose. *International Journal of Biological Macromolecules*, 96, 52-60.

32. Eckert, C. A. & Trinh, C. T. (2016). Biotechnology for biofuel production and optimization. (C. A. Eckert & C. T. Trinh, Eds.). *Elsevier, Amsterdam, Netherlands*, Chapter 1.

33. El-Saied, H., El-Diwany, A. I., Basta, A. H., Atwa, N. A., EI-Ghwas, D. E. (2008). Production and characterization of economical bacterial cellulose. *BioResources*, 3(4), 1196-1217.

34. Fan, X., Gao, Y., He, W., Hu, H., Tian, M., Wang, K., Pan, S. (2016). Production of nano bacterial cellulose from beverage industrial waste of citrus peel and pomace using *Komagataeibacter xylinus*. *Carbohydrate Polymers*, 151, 1068-1072.

35. FAO. (2016). Citrus Fruit Statistics (2015). *Food and Agriculture Organization of the United Nations,* Rome, Italy (http://www.fao.org/3/a-i5558e).

36. FAO. (2017). Banana market review (2015-2016). *Food and Agriculture Organization of the United Nations,* Rome, Italy (http://www.fao.org/3/a-i7410e)

37. Fontana, J. D., De Souza, A. M., Fontana, C. K., Torriani, I. L., Moreschi, J. C., Gallotti, B. J., ..., Farah, L. F. (1990). *Acetobacter* cellulose pellicle as a temporary skin substitute. *Applied Biochemistry and Biotechnology*, 24(1), 253-264.

38. Fu, L., Zhang, J., Yang, G. (2013). Present status and applications of bacterial cellulose-based materials for skin tissue repair. *Carbohydrate Polymers*, 92(2), 1432-1442.

39. Gao, C., Wan, Y., Yang, C., Dai, K., Tang, T., Luo, H., Wang, J. (2011). Preparation and characterization of bacterial cellulose sponge with hierarchical pore structure as tissue engineering scaffold. *Journal of Porous Materials*, 18, 139-145.

40. Gea, S., Reynolds, C.T., Roohpour, N., Wirjosentono, B., Soykeabkaew, N., Bilotti, E., Peijs, T. (2011). Investigation into the structural, morphological, mechanical and thermal behavior of bacterial cellulose after a two-step purification process. *Bioresource Technology*, 102, 9105-9110.

41. George, J., Ramana, K. V., Sabapathy, S. N., Bawa, A. S. (2005). Physico-mechanical properties of chemically treated bacterial (*Acetobacter xylinum*) cellulose membrane. *World Journal of Microbiology and Biotechnology*, 21(8), 1323-1327.

42. Goelzer, F.D.E., Faria-Tischer, P.C.S., Vitorino, J.C., Sierakowski, M.R., Tischer, C.A. (2009). Production and characterization of nanospheres of bacterial cellulose from *Acetobacter xylinum* from processed rice bark. Materials Science and Engineering C, 29, 546-551.

43. Gomes, F.P., Silva, N.H.C.S., Trovatti, E., Serafim, L.S., Duarte, M.F., Silvestre, A.J.D., Neto, C.P., Freire, C.S.R. (2013). Production of bacterial cellulose by *Gluconacetobacter sacchari* using dry olive mill residue. *Biomass Bioenergy*, 55, 205-211.

44. Grande, C. J., Torres, F. G., Gomez, C. M., Carmen Bañó, M. (2009). Nanocomposites of bacterial cellulose/hydroxyapatite for biomedical applications. *Acta Biomaterialia*, 5(5), 1605–1615.

45. Gu, J., Catchmark, J.M., (2012). Impact of hemicelluloses and pectin on sphere-like bacterial cellulose assembly. *Carbohydrate Polymers*, 88, 547-557.

46. Helbert, W., Cavaille, J. Y., Dufresne, A. (1996). Thermoplastic nanocomposites filled with wheat straw cellulose whiskers. Part I: Processing and mechanical behavior. *Polymer Composites*, 17(4), 604-611.

47. Hestrin, S. & Schramm, M. (1954). Synthesis of cellulose by *Acetobacter xylinum*. *Biochemical Journal*, 58(2), 345-352.

48. Hong, F. & Qiu, K. (2008). An alternative carbon source from konjac powder for enhancing production of bacterial cellulose in static cultures by a model strain *Acetobacter aceti* subsp. *xylinus* ATCC 23770. *Carbohydrate Polymers*, 72(3), 545-549.

49. Hong, L., Wang, Y.L., Jia, S.R., Huang, Y., Gao, C., Wan, Y.Z. (2006). Hydroxyapatite/bacterial cellulose composites synthesized via a biomimetic route. *Materials Letters*, 60, 1710-1713.

50. Horii, F., Yamamoto, H., Hirai, A. (1997). Microstructural analysis of microfibrils of bacterial cellulose. *Macromolecular Symposia*, 120, 197-205.

51. Hornung, M., Ludwig, M., Gerrard, A.M., Schmauder, H.P. (2006). Optimizing the production of bacterial cellulose in surface culture: Evaluation of substrate mass transfer influences on the bioreaction (Part 1). *Engineering in Life Sciences*, 6, 537-545.

52. Hornung, M., Ludwig, M., Schmauder, H. P. (2007). Optimizing the production of bacterial cellulose in surface culture: A novel aerosol bioreactor working on a fed batch principle (Part 3). *Engineering in Life Sciences*, 7(1), 35-41.

53. Hsieh, J.T., Wang, M.J., Lai, J.T., Liu, H.S. (2016). A novel static cultivation of bacterial cellulose production by intermittent feeding strategy. *Journal of the Taiwan Institute of Chemical Engineers*, 63, 46-51.

54. Huang, C., Guo, H. J., Xiong, L., Wang, B., Shi, S. L., Chen, X. F., ..., Chen, X. D. (2016). Using wastewater after lipid fermentation as substrate for bacterial cellulose production by *Gluconacetobacter xylinus*. *Carbohydrate Polymers*, 136, 198-202.

55. Huang, C., Yang, X. Y., Xiong, L., Guo, H. J., Luo, J., Wang, B., ..., Chen, X. D. (2015a). Utilization of corncob acid hydrolysate for bacterial cellulose production by *Gluconacetobacter xylinus*. *Applied Biochemistry and Biotechnology*, 175(3), 1678-1688.

56. Huang, C., Yang, X.-Y., Xiong, L., Guo, H.-J., Luo, J., Wang, B., Zhang, H.-R., Lin, X.-Q., Chen, X.-D. (2015c). Evaluating the possibility of using acetone-butanol-ethanol (ABE) fermentation wastewater for bacterial cellulose production by *Gluconacetobacter xylinus*. *Letters in Applied Microbiology*, 60, 491-496.

57. Huang, J. W., Lv, X. G., Li, Z., Song, L. J., Feng, C., Xie, M. K., ..., Xu, Y. M. (2015b). Urethral reconstruction with a 3D porous bacterial cellulose scaffold seeded with lingual keratinocytes in a rabbit model. *Biomedical Materials*, 10(5), 055005.

58. Huang, L., Chen, X., Nguyen, T. X., Tang, H., Zhang, L., Yang, G. (2013). Nano-cellulose 3D-networks as controlled-release drug carriers. *Journal of Materials Chemistry B*, 1(23), 2976-2984.

59. Huang, Y., Wang, J., Yang, F., Shao, Y., Zhang, X., Dai, K. (2017). Modification and evaluation of micro-nano structured porous bacterial cellulose scaffold for bone tissue engineering. *Materials Science and Engineering: C*, 75, 1034-1041.

60. Huang, Y., Zhu, C., Yang, J., Nie, Y., Chen, C., Sun, D. (2014). Recent advances in bacterial cellulose. *Cellulose*, 21(1), 1–30.

61. Hui, Jiya., Jia, Y., Wang, J., Hu, Y., Zhang, Y., Jia, S. (2009). Potentiality of bacterial cellulose as the scaffold of tissue engineering of cornea. *Biomedical Engineering and Informatics, 2009. BMEI'09. 2nd International Conference*, 1-5.

62. Hungund, B., Prabhu, S., Shetty, C., Acharya, S., Prabhu, V., Gupta, S. G. (2013). Production of bacterial cellulose from *Gluconacetobacter persimmonis* GH-2 using dual

and cheaper carbon sources. *Journal of Microbial & Biochemical Technology*, 5(2), 31–33.

63. Hutmacher, D. W. (2000). Scaffolds in tissue engineering bone and cartilage. *Biomaterials*, 21(24), 2529-2543.

64. Hyun, J. Y., Mahanty, B., Kim, C. G. (2014). Utilization of Makgeolli Sludge Filtrate (MSF) as low-cost substrate for bacterial cellulose production by *Gluconacetobacter xylinus*. *Applied Biochemistry and Biotechnology*, 172, 3748-3760.

65. Iguchi, M., Yamanaka, S. Budhiono, A. (2000). Bacterial cellulose-a masterpiece of nature's arts. *Journal of Materials Science*, 35(2), 261-270.

66. Jahan, F., Kumar, V., Rawat, G., Saxena, R. K. (2012). Production of microbial cellulose by a bacterium isolated from fruit. *Applied Biochemistry and Biotechnology*, 167(5), 1157-1171.

67. Joshi, C. & Khare, S.K. (2011). Utilization of deoiled Jatropha curcas seed cake for production of xylanase from thermophilic *Scytalidium thermophilum*. *Bioresource Technology*, 102, 1722-1726.

68. Joshi, C. & Khare, S.K. (2013). Purification and characterization of *Pseudomonas aeruginosa* lipase produced by SSF of deoiled Jatropha seed cake. *Biocatalysis and Agricultural Biotechnology*, 2, 32-37.

69. Jozala, A. F., Lencastre-Novaes, L. C., Lopes, A. M., Santos-Ebinuma, V. C., Mazzola, P. G., Pessoa-Jr, A., Grotto, D., Gerenutti, M., Chaud, M. V. (2016). Bacterial nanocellulose production and application: a 10-year overview. *Applied Microbiology and Biotechnology*, 100, 2063-2072.

70. Jung, H. I., Jeong, J. H., Lee, O. M., Park, G. T., Kim, K. K., Park, H. C., ..., Son, H. J. (2010). Influence of glycerol on production and structural–physical properties of cellulose from *Acetobacter* sp. V6 cultured in shake flasks. *Bioresource Technology*, 101(10), 3602-3608.

71. Jung, J. Y., Park, J. K., Chang, H. N. (2005). Bacterial cellulose production by *Gluconacetobacter hansenii* in an agitated culture without living non-cellulose producing cells. *Enzyme and Microbial Technology*, 37(3), 347-354.

72. Katti, K. S. (2004). Biomaterials in total joint replacement. *Colloids and Surfaces B: Biointerfaces*, 39(3), 133-142.

73. Keshk, S. & Sameshima, K. (2006a). Influence of lignosulfonate on crystal structure and productivity of bacterial cellulose in a static culture. *Enzyme and Microbial Technology*, 40, 4-8.

74. Keshk, S. & Sameshima, K. (2006b). The utilization of sugar cane molasses with/without the presence of lignosulfonate for the production of bacterial cellulose. *Applied Microbiology and Biotechnology*, 72(2), 291-296.

75. Keshk, S. M. A. S. (2014). Vitamin C enhances bacterial cellulose production in *Gluconacetobacter xylinus*. *Carbohydrate Polymers*, 99, 98-100.

76. Keshk, S. M. A. S., Razek, T. M. A., Sameshima, K. (2006). Bacterial cellulose production from beet molasses. *African Journal of Biotechnology*, 5(17), 1519-1523.

77. Keskin, Z., Urkmez, A.S., Hames, E.E. (2017). Novel keratin modified bacterial cellulose nanocomposite production and characterization for skin tissue engineering. *Materials Science and Engineering C*, 75, 1144-1153.

78. Khawas, P., Das, A. J., Deka S. C. (2016). Production of renewable cellulose nanopaper from culinary banana (*Musa* ABB) peel and its characterization. *Industrial Crops and Products*, 86, 102-112.

79. Kim, Y.-J., Kim, J.-N., Wee, Y.-J., Park, D.-H., Ryu, H.-W. (2007). Bacterial cellulose production by *Gluconacetobacter* sp. PKY5 in a rotary biofilm contactor. *Applied Biochemistry and Biotechnology*, 137-140, 529–537.

80. Kiziltas, E.E., Kiziltas, A., Gardner, D.J. (2015). Synthesis of bacterial cellulose using hot water extracted wood sugars. *Carbohydrate Polymers*, 124, 131-138.

81. Klemm, D., Schumann, D., Udhardt, U., Marsch, S. (2001). Bacterial synthesized cellulose—artificial blood vessels for microsurgery. *Progress in Polymer Science*, 26(9), 1561-1603.

82. Kobayashi, S., Kashiwa, K., Shimada, J., Kawasaki, T., Shoda, S. I. (1992). Enzymatic polymerization: The first *in vitro* synthesis of cellulose *via* nonbiosynthetic path catalyzed by cellulase. *Macromolecular Symposia*, 54-55(1), 509–518.

83. Kowalska-Ludwicka, K., Cala, J., Grobelski, B., Sygut, D., Jesionek-Kupnicka, D., Kolodziejczyk, M., ..., Pasieka, Z. (2013). Modified bacterial cellulose tubes for regeneration of damaged peripheral nerves. *Archives of Medical Science*, 9(3), 527-534.

84. Krystynowicz, A., Czaja, W., Wiktorowska-Jezierska, A., Goncalves-Miskiewicz, M., Turkiewicz, M., Bielecki, S. (2002). Factors affecting the yield and properties of bacterial cellulose. *Journal of Industrial Microbiology & Biotechnology*, 29, 189-195.

85. Kumar, V., Chhabra, D., Shukla, P. (2017). Xylanase production from *Thermomyces lanuginosus* VAPS-24 using low cost agro-industrial residues via hybrid optimization tools and its potential use for saccharification. *Bioresource Technology*, 243, 1009-1019.

86. Kumbhar, J.V., Rajwade, J.M., Paknikar, K.M. (2015). Fruit peels support higher yield and superior quality bacterial cellulose production. *Applied Microbiology and Biotechnology*, 99, 6677-6691.

87. Kuo, C. H., Chen, J. H., Liou, B. K., Lee, C. K. (2016). Utilization of acetate buffer to improve bacterial cellulose production by *Gluconacetobacter xylinus*. *Food Hydrocolloids*, 53, 98-103.

88. Lai, G. J., Shalumon, K. T., & Chen, J. P. (2015). Response of human mesenchymal stem cells to intrafibrillar nanohydroxyapatite content and extrafibrillar nanohydroxyapatite in biomimetic chitosan/silk fibroin/nanohydroxyapatite nanofibrous membrane scaffolds. *International journal of nanomedicine*, 10, 567-584.

89. Lee, J. M., Kim, J. H., Lee, O. J., Park, C. H. (2013). The fixation effect of a silk fibroin–bacterial cellulose composite plate in segmental defects of the Zygomatic Arch: An experimental study. *JAMA Otolaryngology–Head & Neck Surgery*, 139(6), 629-635.

90. Lee, K. Y., Buldum, G., Mantalaris, A., & Bismarck, A. (2014). More than meets the eye in bacterial cellulose: Biosynthesis, bioprocessing, and applications in advanced fiber composites. *Macromolecular Bioscience*, 14, 10-32.

91. Lee, S. Y. & Kim, H. U. (2015). Systems strategies for developing industrial microbial strains. *Nature Biotechnology*, 33(10), 1061-1072.

92. Leitão, A. F., Faria, M. A., Faustino, A. M. R., Moreira, R., Mela, P., Loureiro, L., ..., Gama, M. (2016). A novel small-caliber bacterial cellulose vascular prosthesis: Production, characterization, and preliminary *In Vivo* testing. *Macromolecular Bioscience*, 16(1), 139-150.

93. Li, C., Vepari, C., Jin, H. J., Kim, H. J., Kaplan, D. L. (2006). Electrospun silk-BMP-2 scaffolds for bone tissue engineering. *Biomaterials*, 27(16), 3115-3124.

94. Li, H. X., Kim, S. J., Lee, Y. W., Kee, C. D., Oh, II. K. (2011). Determination of the stoichiometry and critical oxygen tension in the production culture of bacterial cellulose using saccharified food wastes. *Korean Journal of Chemical Engineering*, *28*(12), 2306-2311.

95. Li, Y., Tian, C., Tian, H., Zhang, J., He, X., Ping, W., Lei, H. (2012). Improvement of bacterial cellulose production by manipulating the metabolic pathways in which ethanol and sodium citrate involved. *Applied Microbiology and Biotechnology*, 96, 1479-1487.

96. Li, Z., Wang, L., Hua, J., Jia, S., Zhang, J., Liu, H. (2015). Production of nano bacterial cellulose from waste water of candied jujube-processing industry using *Acetobacter xylinum*. *Carbohydrate Polymers*, 120, 115-119.

97. Lin, D., Lopez-Sanchez, P., Li, R., Li, Z. (2014). Production of bacterial cellulose by *Gluconacetobacter hansenii* CGMCC 3917 using only waste beer yeast as nutrient source. *Bioresource Technology*, 151, 113-119.

98. Lin, S.-P., Calvar, I. L., Catchmark, J. M., Liu, J.-R., Demirci, A. Cheng, K.-C. (2013). Biosynthesis, production and applications of bacterial cellulose. *Cellulose*, 20(5), 2191-2219.

99. Lin, Y. K., Chen, K. H., Ou, K. L., Liu, M. (2011). Effects of different extracellular matrices and growth factor immobilization on biodegradability and biocompatibility of

macroporous bacterial cellulose. *Journal of Bioactive and Compatible Polymers*, 26(5), 508-518.

100. Liuzhenlin, Liuxiˇaozhi, Liang Zhongmˇin, Zhangchaozheng, (2011). Preparation method of artificial endocranium. *CN Patent*, 102000357A.

101. Lojewska, J., Miskowiec, P., Lojewski, T., Proniewicz, L. M. (2005). Cellulose oxidative and hydrolytic degradation: In situ FTIR approach. *Polymer Degradation and Stability*, 88, 512-520.

102. Lysdahl, H., Baatrup, A., Foldager, C. B., & Bünger, C. (2014). Preconditioning human mesenchymal stem cells with a low concentration of BMP2 stimulates proliferation and osteogenic differentiation *in vitro*. *BioResearch Open Access*, 3(6), 278-285.

103. Märtson, M., Viljanto, J., Hurme, T., Laippala, P., & Saukko, P. (1999). Is cellulose sponge degradable or stable as implantation material? An *in vivo* subcutaneous study in the rat. *Biomaterials*, 20(21), 1989-1995.

104. Masuko, T., Minami, A., Iwasaki, N., Majima, T., Nishimura, S.I., Lee, Y.C. (2005). Carbohydrate analysis by a phenol-sulfuric acid method in microplate format. *Analytical Biochemistry*, 339, 69-72.

105. McKenna, B. A., Mikkelsen, D., Wehr, J. B., Gidley, M. J., Menzies, N. W. (2009). Mechanical and structural properties of native and alkali-treated bacterial cellulose produced by *Gluconacetobacter xylinus* strain ATCC 53524. *Cellulose*, 16(6), 1047-1055.

106. Messaddeq, Y., Ribeiro, S. J. L., Thomazini, W. (2008). Trigger, Pesquisa & Desenvolvimentos Biotecnologicos Ltda. (TRIG-Non-standard), assignee. Contact lens for therapy, method and apparatus for their production and use. *Brazil patent BR*, PI0603704-6.

107. Mikkelsen, D., Flanagan, B. M., Dykes, G. A., Gidley, M. J. (2009). Influence of different carbon sources on bacterial cellulose production by *Gluconacetobacter xylinus* strain ATCC 53524. *Journal of Applied Microbiology*, 107, 576-583.

108. Miller, G. L. (1959). Use of dinitrosalicylic acid reagent for determination of reducing sugar. *Analytical Chemistry*, 31(3), 426-428.

109. Mohammadkazemi, F., Azin, M., Ashori, A. (2015). Production of bacterial cellulose using different carbon sources and culture media. *Carbohydrate Polymers*, 117, 518-523.

110. Mohite, B. V. & Patil, S. V. (2014a). A novel biomaterial: bacterial cellulose and its new era applications. *Biotechnology and Applied Biochemistry*, 61 (2), 101-110.

111. Mohite, B. V. & Patil, S. V. (2014b). Physical, structural, mechanical and thermal characterization of bacterial cellulose by *G. hansenii* NCIM 2529. *Carbohydrate Polymers*, 106, 132-141.

112. Moniri, M., Boroumand Moghaddam, A., Azizi, S., Abdul Rahim, R., Bin Ariff, A., Zuhainis Saad, W., ..., Mohamad, R. (2017). Production and status of bacterial cellulose in biomedical engineering. *Nanomaterials*, 7(9), 257.

113. Mori, R., Nakai, T., Enomoto, K., Uchio, Y., Yoshino, K. (2011). Increased antibiotic release from a bone cement containing bacterial cellulose. *Clinical Orthopaedics and Related Research*, 469(2), 600-606.

114. Motamedian, S. R., Hosseinpour, S., Ahsaie, M. G., Khojasteh, A. (2015). Smart scaffolds in bone tissue engineering: A systematic review of literature. *World Journal of Stem Cells*, 7(3), 657-668.

115. Movasaghi, Z., Rehman, S., Rehman, I. U. (2008). Fourier transform infrared (FTIR) spectroscopy of biological tissues. *Applied Spectroscopy Reviews*, 43, 134-179.

116. Nakatsubo, F., Kamitakahara, H., Hori, M. (1996). Cationic ring-opening polymerization of 3, 6-di-O-benzyl-α-D-glucose 1, 2, 4-orthopivalate and the first chemical synthesis of cellulose. *Journal of the American Chemical Society*, 118(7), 1677-1681.

117. Napoli, C., Dazzo, F., Hubbell, D. (1975). Production of cellulose microfibrils by *Rhizobium*. *Applied Microbiology*, 30(1), 123-131.

118. Nguyen, V. T., Flanagan, B., Mikkelsen, D., Ramirez, S., Rivas, L., Gidley, M. J., Dykes, G. A. (2010). Spontaneous mutation results in lower cellulose production by a *Gluconacetobacter xylinus* strain from Kombucha. *Carbohydrate Polymers*, 80(2), 337-343.

119. Nguyen, V.T., Flanagan, B., Gidley, M.J., Dykes, G.A. (2008). Characterization of cellulose production by a *Gluconacetobacter xylinus* strain from Kombucha. *Current Microbiology*, 57, 449-453.

120. Oh, S.Y., Yoo, D.I., Shin, Y., Kim, H.C., Kim, H.Y., Chung, Y.S., Park, W.H., Youk, J.H. (2005). Crystalline structure analysis of cellulose treated with sodium hydroxide and carbon dioxide by means of X-ray diffraction and FTIR spectroscopy. *Carbohydrate Research*, 340, 2376-2391.

121. Pacheco, G., Nogueira, C. R., Meneguin, A. B., Trovatti, E., Silva, M. C. C., Machado, R. T. A., Ribeiro, S. J. L., Filho, E. C. S., Barud, H. S. (2017). Development and characterization of bacterial cellulose produced by cashew tree residues as alternative carbon source. *Industrial Crops and Products*, 107, 13-19.

122. Park, S., Baker, J. O., Himmel, M. E., Parilla, P. A., Johnson, D. K. (2010). Cellulose crystallinity index : measurement techniques and their impact on interpreting cellulase performance. *Biotechnology for Biofuels*, 3: 10.

123. Parola, E. C. (1970). Biology of the sugar-fermenting *Sarcinae*. *Bacteriological Reviews*, 34(1), 82-97.

124. Payen, A. (1838). "Mémoire sur la composition du tissu propre des plantes et du ligneux" (Memory on the composition of the clean tissue of plants and ligneous. *Comptes rendus*, 7, 1052-1056.

125. Petersen, N. & Gatenholm, P. (2011). Bacterial cellulose-based materials and medical devices: Current state and perspectives. *Applied Microbiology and Biotechnology*, 91(5), 1277-1286.

126. Picheth, G. F., Pirich, C. L., Sierakowski, M. R., Woehl, M. A., Sakakibara, C. N., Souza, C. F., Martin, A. A., Silva, R., Freitas, R. A. (2017). Bacterial cellulose in biomedical applications: A review. *International Journal of Biological Macromolecules*, 104, 97-106.

127. Pigossi, S. C., de Oliveira, G. J., Finoti, L. S., Nepomuceno, R., Spolidorio, L. C., Rossa, C., ..., Scarel-Caminaga, R. M. (2015). Bacterial cellulose-hydroxyapatite composites with osteogenic growth peptide (OGP) or pentapeptide OGP on bone regeneration in critical-size calvarial defect model. *Journal of Biomedical Materials Research Part A*, 103(10), 3397-3406.

128. Rajwade, J. M., Paknikar, K. M., Kumbhar, J. V. (2015). Applications of bacterial cellulose and its composites in biomedicine. *Applied Microbiology and Biotechnology*, 99, 2491-2511.

129. Rane, A. N., Baikar, V. V., Kumar, V. R., Deopurkar, R. L. (2017). Agro-Industrial wastes for production of biosurfactant by *Bacillus subtilis* ANR 88 and its application in synthesis of silver and gold nanoparticles. *Frontiers in Microbiology*, 8, 492.

130. Rattanavichai, W. & Cheng, W. (2014). Effects of hot-water extract of banana (*Musa acuminata*) fruit's peel on the antibacterial activity, and anti-hypothermal stress, immune responses and disease resistance of the giant freshwater prawn, *Macrobrachium rosenbegii*. *Fish and Shellfish Immunology*, 39, 326-335.

131. Reiniati, I., Hrymak, A. N., Margaritis, A. (2017a). Kinetics of cell growth and crystalline nanocellulose production by *Komagataeibacter xylinus*. *Biochemical Engineering Journal*, 127, 21-31.

132. Reiniati, I., Hrymak, A. N., Margaritis, A. (2017b). Recent developments in the production and applications of bacterial cellulose fibers and nanocrystals. *Critical Reviews in Biotechnology*, 37(4), 510-524.

133. Ross, P., Mayer, R., Benziman, M. (1991). Cellulose biosynthesis and function in bacteria. *Microbiological Reviews*, 55(1), 35-58.

134. Sadaf, A. & Khare, S. K. (2014). Production of *Sporotrichum thermophile* xylanase by solid state fermentation utilizing deoiled *Jatropha curcas* seed cake and its application in xylooligosachharide synthesis. *Bioresource Technology*, 153, 126-130.

135. Sakairi, N., Asano, H., Ogawa, M., Nishi, N., Tokura, S. (1998). A method for direct harvest of bacterial cellulose filaments during continuous cultivation of *Acetobacter xylinum*. *Carbohydrate Polymers*, 35, 233-237.

136. Salgado, A. J., Coutinho, O. P., Reis, R. L. (2004). Bone tissue engineering: state of the art and future trends. *Macromolecular bioscience*, 4(8), 743-765.

137. Samir, M. A. S. A., Alloin, F., Dufresne, A. (2005). Review of Recent Research into cellulosic whiskers, their properties and their application in nanocomposite field. *Biomacromolecules*, 6(2), 612-626.

138. Santos, S. M., Carbajo, J. M., Quintana, E., Ibarra, D., Gomez, N., Ladero, M., ..., Villar, J. C. (2015). Characterization of purified bacterial cellulose focused on its use on paper restoration. *Carbohydrate Polymers*, 116, 173-181.

139. Saska, S., Barud, H. S., Gaspar, A. M. M., Marchetto, R., Ribeiro, S. J. L., Messaddeq, Y. (2011). Bacterial cellulose-hydroxyapatite nanocomposites for bone regeneration. *International Journal of Biomaterials*, 2011, 175362.

140. Schramm, M. & Hestrin, S. (1954). Factors affecting production of cellulose at the air/ liquid interface of a culture of *Acetobacter xylinum*. *Journal of General Microbiology*, 11(1), 123-129.

141. Schumann, D. A., Wippermann, J., Klemm, D. O., Kramer, F., Koth, D., Kosmehl, H., ..., Salehi-Gelani, S. (2009). Artificial vascular implants from bacterial cellulose: Preliminary results of small arterial substitutes. *Cellulose*, 16(5), 877-885.

142. Segal, L., Creely, J. J., Martin Jr, A. E., Conrad, C. M. (1959). An Empirical method for estimating the degree of crystallinity of native cellulose using the X-Ray diffractometer. *Textile Research Journal*, 29(10), 786-794.

143. Seto, A., Saito, Y., Matsushige, M., Kobayashi, H., Sasaki, Y., Tonouchi, N., Yoshinaga, F., Ueda, K., Beppu, T. (2006). Effective cellulose production by a coculture of *Gluconacetobacter xylinus* and *Lactobacillus mali*. *Applied Microbiology and Biotechnology*, 73(4), 915-921.

144. Shao, W., Liu, H., Liu, X., Wang, S., Zhang, R. (2015). Anti-bacterial performances and biocompatibility of bacterial cellulose/graphene oxide composites. *RSC Advances*, 5, 4795-4803.

145. Sharma, K., Mahato, N., Cho, M. H., Lee, Y. R. (2017). Converting citrus wastes into value-added products: Economic and environmentally friendly approaches. *Nutrition*. 34, 29-46.

146. Sheykhnazari, S., Tabarsa, T., Ashori, A., Shakeri, A., Golalipour, M. (2011). Bacterial synthesized cellulose nanofibers; Effects of growth times and culture mediums on the structural characteristics. *Carbohydrate Polymers*, 86, 1187-1191.

147. Shezad, O., Khan, S., Khan, T., Park, J.K. (2010). Physicochemical and mechanical characterization of bacterial cellulose produced with an excellent productivity in static conditions using a simple fed-batch cultivation strategy. *Carbohydrate Polymers*, 82, 173-180.

148. Shi, Z., Zhang, Y., Phillips, G. O., Yang G. (2014). Utilization of bacterial cellulose in food. *Food Hydrocolloids*, 35, 539-545.

149. Shibazaki, H., Kuga, S., Okano, T. (1997). Mercerization and acid hydrolysis of bacterial cellulose. *Cellulose*, 4(2), 75-87.

150. Shoda, M. & Sugano, Y. (2005). Recent advances in bacterial cellulose production. *Biotechnology and Bioprocess Engineering*, 10, 1-8.

151. Singh, V., Haque, S., Niwas, R., Srivastava, A., Pasupuleti, M., Tripathi, C. K. M. (2017). Strategies for fermentation medium optimization: An in-depth review. *Frontiers in Microbiology*, 7, 2087. doi: 10.3389/fmicb.2016.02087.

152. Soykeabkaew, N., Sian, C., Gea, S., Nishino, T., Peijs, T. (2009). All-cellulose nanocomposites by surface selective dissolution of bacterial cellulose. *Cellulose*, 16(3), 435-444.

153. Sukan, A., Roy, I., Keshavarz, T. (2014). Agro-Industrial waste materials as substrates for the production of Poly(3-Hydroxybutyric Acid). *Journal of Biomaterials and Nanobiotechnology*, 5(4), 229-240.

154. Sulaeva, I., Henniges, U., Rosenau, T., Potthast, A. (2015). Bacterial cellulose as a material for wound treatment: Properties and modifications. A review. *Biotechnology Advances*, 33(8), 1547-1571.

155. Sun, D., Zhou, L., Wu, Q., Yang, S. (2007). Preliminary research on structure and properties of nano-cellulose. *Journal of Wuhan University of Technology-Mater. Sci. Ed.*, 22(4), 677-680.

156. Svensson, A., Nicklasson, E., Harrah, T., Panilaitis, B., Kaplan, D. L., Brittberg, M., Gatenholm, P. (2005). Bacterial cellulose as a potential scaffold for tissue engineering of cartilage. *Biomaterials*, 26, 419-431.

157. Tamura, K., Stecher, G., Peterson, D., Filipski, A., Kumar, S. (2013). MEGA6 : Molecular Evolutionary Genetics Analysis Version 6 . 0. *Molecular Biology and Evolution*, 30(12), 2725-2729.

158. Tang, W., Jia, S., Jia, Y., Yang, H. (2010). The influence of fermentation conditions and post-treatment methods on porosity of bacterial cellulose membrane. *World Journal of Microbiology and Biotechnology*, 26, 125-131.

159. Tanskul, S., Amornthatree, K., Jaturonlak, N. (2013). A new cellulose-producing bacterium, *Rhodococcus* sp. MI 2: Screening and optimization of culture conditions. *Carbohydrate Polymers*, 92(1), 421-428.

160. Tazi, N., Zhang, Z., Messaddeq, Y., Almeida-Lopes, L., Zanardi, L. M., Levinson, D., Rouabhia, M. (2012). Hydroxyapatite bioactivated bacterial cellulose promotes osteoblast growth and the formation of bone nodules. *Amb Express*, 2(1), 61.

161. Toskas, G., Cherif, C., Hund, R. D., Laourine, E., Mahltig, B., Fahmi, A., ... Hanke, T. (2013). Chitosan (PEO)/silica hybrid nanofibers as a potential biomaterial for bone regeneration. *Carbohydrate polymers*, 94(2), 713-722.

162. Trovatti, E., Freire, C. S. R., Pinto, P. C., Almeida, I. F., Costa, P., Silvestre, A. J., ..., Rosado, C. (2012). Bacterial cellulose membranes applied in topical and transdermal delivery of lidocaine hydrochloride and ibuprofen: *In vitro* diffusion studies. *International Journal of Pharmaceutics*, 435(1), 83-87.

163. Trovatti, E., Serafim, L. S., Freire, C. S. R, Silvestre, A. J. D, Neto, C. P. (2011). *Gluconacetobacter sacchari*: An efficient bacterial cellulose cell-factory. *Carbohydrate Polymers*, 86(3), 1417-1420.

164. Tsouko, E., Kourmentza, C., Ladakis, D., Kopsahelis, N., Mandala, I., Papanikolaou, S., Paloukis, F., Alves, V., Koutinas, A. (2015). Bacterial cellulose production from industrial waste and by-product streams. *International Journal of Molecular Sciences*, 16, 14832-14849.

165. Tyagi, N. & Suresh, S. (2013). Isolation and characterization of cellulose producing bacterial strain from orange pulp. *Advanced Materials Research*, 626, 475-479.

166. Tyagi, N. & Suresh, S. (2016). Production of cellulose from sugarcane molasses using *Gluconacetobacter intermedius* SNT-1 : optimization & characterization. *Journal of Cleaner Production*, 112, 71-80.

167. Ul-Islam, M., Ha, J. H., Khan, T., Park, J. K. (2013). Effects of glucuronic acid oligomers on the production, structure and properties of bacterial cellulose. *Carbohydrate Polymers*, 92, 360-366.

168. Ul-Islam, M., Khan, T., Park, J. K. (2012). Water holding and release properties of bacterial cellulose obtained by *in situ* and *ex situ* modification. *Carbohydrate Polymers*, 88, 596-603.

169. Ul-Islam, M., Ullah, M. W., Khan, S., Shah, N., Park, J. K. (2017). Strategies for cost-effective and enhanced production of bacterial cellulose. *International Journal of Biological Macromolecules*, 102, 1166–1173.

170. Ullah, H., Wahid, F., Santos, H. A., Khan, T. (2016). Advances in biomedical and pharmaceutical applications of functional bacterial cellulose-based nanocomposites. *Carbohydrate Polymers*, 150, 330–352.

171. Vazquez, A., Foresti, M.L., Cerrutti, P., Galvagno, M. (2013). Bacterial cellulose from simple and low cost production media by *Gluconacetobacter xylinus*. *Journal of Polymers and the Environment*, 21, 545-554.

172. Velasco-Bedran, H. & Lopez-Isunza, F. (2007). The unified metabolism of *Gluconacetobacter entanii* in continuous and batch processes. *Process Biochemistry*, 42, 1180-1190.

173. Wada, M., Chanzy, H., Nishiyama, Y., Langan, P. (2004). Cellulose III_I crystal structure and hydrogen bonding by synchrotron X-ray and neutron fiber diffraction. *Macromolecules*, 37(23), 8548-8555.

174. Wada, M., Okano, T., Sugiyama, J. (2001). Allomorphs of native crystalline cellulose I evaluated by two equatorial d-spacings. *Journal of Wood Science*, 47(2), 124-128.

175. Waghmare, A. G. & Arya, S. S. (2016). Utilization of unripe banana peel waste as feedstock for ethanol production. *Bioethanol*, 2, 146-156.

176. Wang, H., Bian, L., Zhou, P., Tang, J., Tang, W. (2013). Core–sheath structured bacterial cellulose/polypyrrole nanocomposites with excellent conductivity as supercapacitors. *Journal of Materials Chemistry A*, 1(3), 578-584.

177. Wang, X., Kong, D., Zhang, Y., Wang, B., Li, X., Qiu, T., Song, Q., Ning, J., Song, Y., Zhi, L. (2016). All-biomaterial supercapacitor derived from bacterial cellulose. *Nanoscale*, 8, 9146-9150.

178. Weinhouse, H., Sapir, S., Amikam, D., Shilo, Y., Volman, G., Ohana, P., & Benziman, M. (1997). C-di-GMP-binding protein, a new factor regulating cellulose synthesis in *Acetobacter xylinum*. *FEBS Letters*, 416, 207-211.

179. Wippermann, J., Schumann, D., Klemm, D., Kosmehl, H., Salehi-Gelani, S., Wahlers, T. (2009). Preliminary results of small arterial substitute performed with a new cylindrical biomaterial composed of bacterial cellulose. *European Journal of Vascular and Endovascular Surgery*, *37*(5), 592-596.

180. Wu, J. M. & Liu, R. H. (2013). Cost-effective production of bacterial cellulose in static cultures using distillery waste water. *Journal of Bioscience and Bioengineering*, 115, 284-290.

181. Wu, J.M. & Liu, R.H. (2012). Thin stillage supplementation greatly enhances bacterial cellulose production by *Gluconacetobacter xylinus*. *Carbohydrate Polymers*, 90, 116-121.

182. Xiong, G., Luo, H., Zhu, Y., Raman, S., & Wan, Y. (2014). Creation of macropores in three-dimensional bacterial cellulose scaffold for potential cancer cell culture. *Carbohydrate polymers*, 114, 553-557.

183. Yamada, Y. (2014). Transfer of *Gluconacetobacter kakiaceti*, *Gluconacetobacter medellinensis* and *Gluconacetobacter maltaceti* to the genus *Komagataeibacter* as *Komagataeibacter kakiaceti* comb. nov., *Komagataeibacter medellinensis* comb. nov. and *Komagataeibacter maltaceti* comb. nov. *International Journal of Systematic and Evolutionary Microbiology*, 64(5), 1670-1672.

184. Yamazawa, A., Iikura, T., Shino, A., Date, Y., Kikuchi, J. (2013). Solid-, solution-, and gas-state NMR monitoring of 13C-Cellulose degradation in an anaerobic microbial ecosystem. *Molecules*, 18(8), 9021-9033.

185. Yang, Y., Jia, J., Xing, J., Chen, J., Lu, S. (2013). Isolation and characteristics analysis of a novel high bacterial cellulose producing strain *Gluconacetobacter intermedius* CIs26. *Carbohydrate Polymers*, 92(2), 2012-2017.

186. Yassine, F., Bassil, N., Flouty, R., Chokr, A., Samrani, A. E., Boiteux, G., Tahchi, M. E. (2016). Culture medium pH influence on *Gluconacetobacter* physiology: Cellulose production rate and yield enhancement in presence of multiple carbon sources. *Carbohydrate Polymers*, 146, 282-291.

187. Yoshino, T., Asakura, T., Toda, K. (1996). Cellulose production by *Acetobacter pasteurianus* on silicone membrane. *Journal of fermentation and Bioengineering*, 81(1), 32-36.

188. Zaborowska, M., Bodin, A., Bäckdahl, H., Popp, J., Goldstein, A., Gatenholm, P. (2010). Microporous bacterial cellulose as a potential scaffold for bone regeneration. *Acta Biomaterialia*, 6, 2540-2547.

189. Zang, S., Zhang, R., Chen, H., Lu, Y., Zhou, J., Chang, X., Qiu, G., Wu, Z., Yang, G. (2015). Investigation on artificial blood vessels prepared from bacterial cellulose. *Materials Science and Engineering C*, 46, 111-117.

190. Zhang, M., Shukla, P., Ayyachamy, M., Permaul, K., Singh, S. (2010). Improved bioethanol production through simultaneous saccharification and fermentation of lignocellulosic agricultural wastes by *Kluyveromyces marxianus* 6556. *World Journal of Microbiology and Biotechnology*, 26, 1041-1046.

191. Zhang, S., Winestrand, S., Chen, L., Li, D., Jönsson, L. J., Hong, F. (2014a). Tolerance of the nanocellulose-producing bacterium *Gluconacetobacter xylinus* to lignocellulose-derived acids and aldehydes. *Journal of Agricultural and Food Chemistry*, 62, 9792-9799.

192. Zhang, S., Winestrand, S., Guo, X., Chen, L., Hong, F., Jönsson, L. J. (2014b). Effects of aromatic compounds on the production of bacterial nanocellulose by *Gluconacetobacter xylinus*. *Microbial Cell Factories*, 13:62. DOI:10.1186/1475-2859-13-62.

193. Zhou, L. L., Sun, D. P., Hu, L. Y., Li, Y. W., Yang, J. Z. (2007). Effect of addition of sodium alginate on bacterial cellulose production by *Acetobacter xylinum*. *Journal of Industrial Microbiology & Biotechnology*, 34(7), 483-489.

194. Zogaj, X., Nimtz, M., Rohde, M., Bokranz, W., Römling, U. (2001). The multicellular morphotypes of *Salmonella typhimurium* and *Escherichia coli* produce cellulose as the second component of the extracellular matrix. *Molecular Microbiology*, 39(6), 1452-1463.

Research Publications

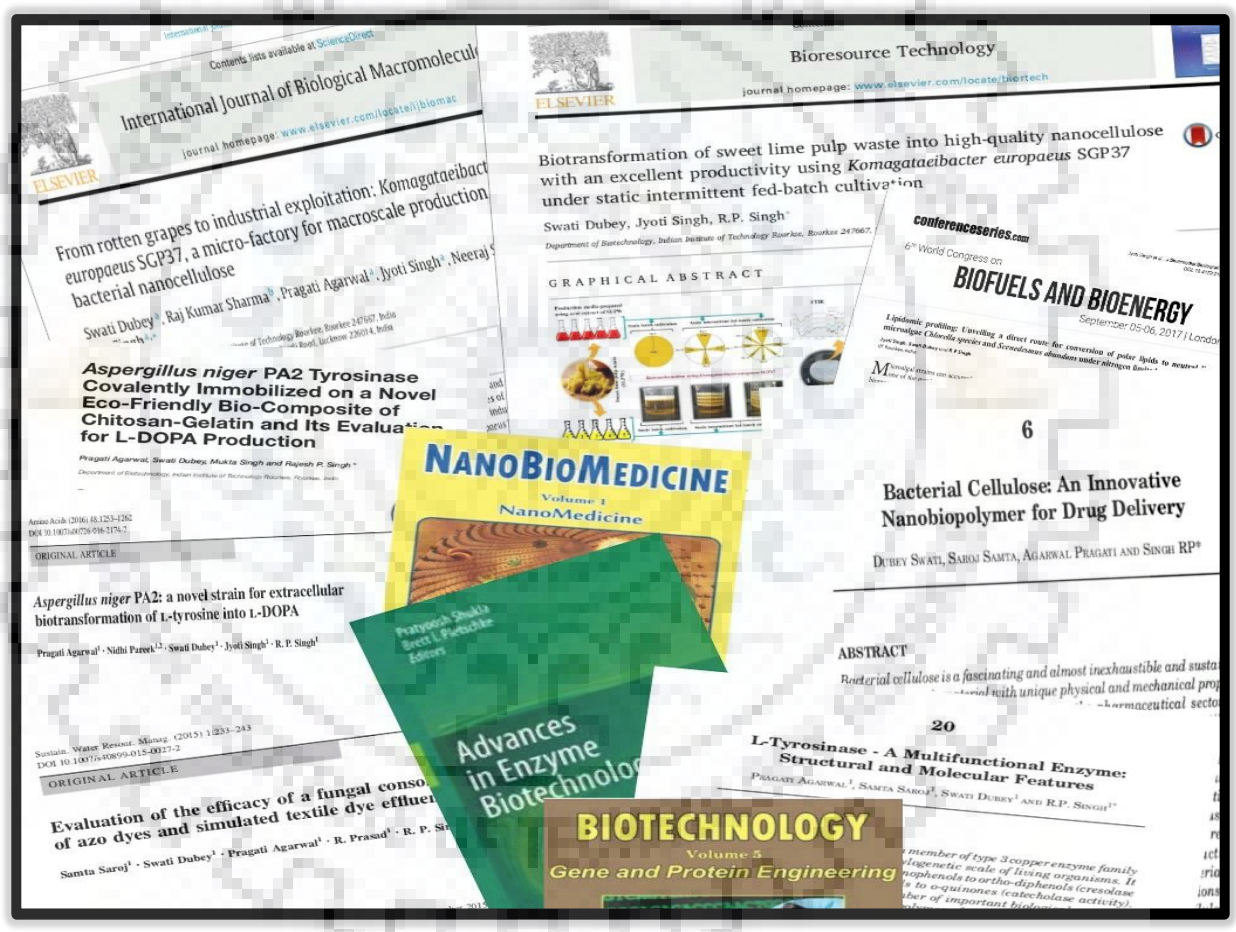

PUBLICATIONS IN PEER REVIEWED JOURNALS

1. **Dubey S**., Singh J. and Singh R. P. (2018). Biotransformation of sweet lime pulp waste into high-quality nanocellulose with an excellent productivity using *Komagataeibacter europaeus* SGP37 under static intermittent fed-batch cultivation. *Bioresource Technology*, 247, 73–80. **(IF: 5.65)**

2. **Dubey S**., Sharma R. K., Agarwal P., Singh J., Sinha N. and Singh R. P. (2017). From rotten grapes to industrial exploitation: *Komagataeibacter europaeus* SGP37, a micro-factory for macroscale production of bacterial nanocellulose. *International Journal of Biological Macromolecules*, 96, 52–60. **(IF: 3.67)**

3. Agarwal P.,Pareek N., **Dubey S**. and Singh R. P. (2016). *Aspergillus niger* PA2: a novel strain for extracellular biotransformation of L-tyrosine into L-DOPA. *Amino Acids*, 48: 1253-1262. **(IF: 3.17)**

4. Agarwal P., **Dubey S**., Singh M. and Singh R. P. (2016). Aspergillus niger PA2 Tyrosinase Covalently Immobilized on a Novel Eco-Friendly Bio-Composite of Chitosan-Gelatin and Its Evaluation for L-DOPA Production. F*rontiers in Microbiology, doi: 10.3389/fmicb.2016.02088* **(IF: 4.07)**

5. Saroj S., **Dubey S.**, Agarwal P., Prasad R. and Singh R. P. (2015). Evaluation of the efficacy of a fungal consortium for degradation of azo dyes and simulated textile dye effluents. *Sustainable Water Resources Management*, 1, 3: 233-243.

MANUSCRIPTS IN COMMUNICATION / PREPARATION

1. **Dubey S**., Agarwal, P. Chakravarty N. and Singh R. P. Bio-valorization of banana peel waste into high-quality nanocellulose (*Communicated*).

2. **Dubey S**., Mishra R., Roy P. and Singh R. P. Osteogenic differentiation of murine mesenchymal stem cells in 3-D microporous nanocellulose-based scaffold for bone tissue engineering (*Manuscript in preparation*).

3. Bhardwaj S., **Dubey S**., Maurya N., Singh R. P. and Singh A. K. Potent "Turn Off" fluorescence sensor based on AIE organic nanoparticles for Hg2+ recognition in aqueous solutions (*Communicated*).

4. Singh J., **Dubey S**., Singh M., Agarwal P. and Singh, R. P. Lipidome profiling: Unravelling TAG biosynthesis in *Chlorella* sp. BTA3008 under nitrogen limited condition for biofuel production (*Communicated*).

BOOK CHAPTERS

1. **Dubey S.,** Saroj S., Agarwal P. and Singh R. P. (2014). Bacterial Cellulose: An innovative nanobiopolymer for drug delivery. Nanobiomedicine Vol. 2: *Nanopharmaceuticals,* Studium Publishers LLC, Houston, USA, 185-200.

2. Agarwal P., Saroj S., **Dubey S.** and Singh R. P. (2013). Structural and molecular features of a multifunctional enzyme L-Tyrosinase. Biotechnology Vol. 5: *Gene and Protein Engineering,* Studium Publishers LLC, Houston, USA, 425-445.

3. Saroj S., Agarwal P., **Dubey S.** and Singh R. P. (2012). Manganese Peroxidases: molecular diversity, heterologous expression and applications. *Advances in Enzyme Biotechnol,* Springer Publ., 67-87.

PROCEEDINGS IN NATIONAL AND INTERNATIONAL CONFERENCES

1. **Dubey S**., Singh J., Singh M., Bhargava A. and Singh R. P. (2014). Bacterial cellulose as a potential scaffold for bone tissue engineering: production and physicostructural characterization. *International Conference on Molecular Signaling: Recent Trends in Biomedical and Translational Research,* IIT Roorkee, Roorkee India, 17-19 Dec, 2014.

2. **Dubey S**., Agarwal P. and Singh R. P. (2014). Biological synthesis of cellulose scaffold: a promising nanobiomaterial for tissue engineering. *International Conference on Recent Advances in Nanoscience and Nanotechnology,* JNU Delhi, India, 15-16 Dec, 2014.

3. **Dubey S**., Saroj S., Agarwal P. and Singh R. P. (2014). Bacterial Cellulose: an innovative nanobiopolymer for tissue engineering and drug delivery. *International Conference on Emerging Trends in Biotechnology,* JNU Delhi, India, 06-09 Nov, 2014.

4. Singh J., **Dubey S**. and Singh R. P. (2017). Lipidomic profiling: Unveiling a direct route for conversion of polar lipids to neutral lipids in microalgae *Chlorella* species and *Scenedesmus abundans* under nitrogen limited condition. *6th World Congress on Biofuels and Bioenergy,* London, UK, 5-6 Sep, 2017.

5. Singh M., **Dubey S**., Singh J. and Singh R. P. (2017). Curcumin loaded PHEMA nanoparticles modified with chitosan for enhanced and prolonged drug delivery. *ICN:3I-2017,* IIT Roorkee, Roorkee, India, 06-08 Dec, 2017.

6. Agarwal P., **Dubey S.** and Singh R. P. (2014). L-Tyorsinase from *Aspergillus niger* PA2 and evaluation of its role for bioremediation of phenols. *International Conference on Molecular Signaling: Recent Trends in Biomedical and Translational Research,* IIT Roorkee, Roorkee India, 17-19 Dec, 2014.

7. Bhargava A., **Dubey S**., Agarwal P. and Singh R.P (2014). Alteration of an aspartate enhances thermostability of L-asparaginase: a novel anti leukemic agent. *Recent Trends in Biomedical and Translational Research,* IIT Roorkee, Roorkee India, 17-19 Dec, 2014.

8. Kishore H. A. S., **Dubey S**. and Singh R. P. (2014). Bovine Serum Albumin Nanoparticles: a potential agent for drug delivery. *International Conference on Recent Advances in Nanoscience and Nanotechnology*, JNU Delhi, India, 15-16 Dec, 2014.

9. Agarwal P., **Dubey S**., Amra P. and Singh R. P. (2014). Gefitinib loaded chitosan nanoparticles for potential application in lung cancer: Preparation and Characterization *International Conference on Recent Advances in Nanoscience and Nanotechnology*, JNU Delhi, India, 15-16 Dec, 2014.

10. Agarwal P., Saroj S., **Dubey S**. and Singh R. P. (2014). Production of microbial L-Tyorsinase: An enzyme with potential therapeutic applications. *International Conference on Emerging Trends in Biotechnology*, JNU Delhi, India, 06-09 Nov, 2014.

11. Bhargava A., **Dubey S**., Agarwal P. and Singh R.P (2014). Engineering thermostability of L-asparaginase by Site directed mutagenesis. *International Conference on Emerging Trends in Biotechnology*, JNU Delhi, India, 06-09 Nov, 2014.

12. Saroj S., **Dubey S.**, Agarwal P. and Singh R. P. (2013). Molecular response regulating azo dye AR183 degradation by *Penicillium oxalicum* SAR-3. *Asian Congress on Biotechnology*, IIT Delhi, India, 15-19 Dec, 2013.

13. Saroj S., **Dubey S**., Bhargava A. and Singh R. P. (2013). Functional expression of L-Asparaginase II an antileukemic agent from *E. coli* MTCC 739. *Asian Congress on Biotechnology*, IIT Delhi, India, 15-19 Dec, 2013.

NUCLEOTIDE SEQUENCES SUBMITTED IN NCBI

1. **Dubey S**., Saroj S. and Singh R. P. (2014) *Komagataeibacter europaeus* strain SGP 16S ribosomal RNA gene, partial sequence. *GenBank Accession No. KJ025079*

2. **Dubey S**. and Singh R. P. (2014) *Komagataeibacter europaeus* strain SGP37 16S ribosomal RNA gene, partial sequence. *GenBank Accession No. KJ101597*